CHARACTERIZATION AND EVALUATION OF THE BARRIER PROPERTIES OF DIFFERENT SKIN MODELS AS AN ALTERNATIVE MODEL FOR HUMAN SKIN

Dissertation
zur Erlangung des akademischen Grades doctor rerum naturalium
(Dr. rer. nat.)

vorgelegt dem Rat der Biologisch-Pharmazeutischen Fakultät
der Friedrich-Schiller- Universität Jena

von Khaled Ahmed
geboren am 03.01.1972 in El-Dakahlia, Ägypten

Gutachter:

Prof. Dr. Alfred Fahr

Prof. Dr. Dagmar Fischer

Prof. Dr. Heike Bunjes (TU Branschweig)

Date of defense: 3rd March 2011

To the spirit of my father and to my family

Acknowledgements

The achievement of this thesis would not have been possible without many people's support. First and foremost, I would like to express my heartily appreciation and sincere gratitude to my mentor Prof. Dr. Alfred Fahr, for offering me kindly a great help by his fruitful supervision, research guidance, and valuable advice which enabled this work to be completed. I am grateful for the experience acquired from him that will help me to continue successfully in my scientific life. Many thanks to him for being all the time like a strong father to his students and for giving them advices that can help them to become successful scientists in any place of the world.

I would like to express my deep and sincere gratitude to my supervisor Dr. Judith Kuntsche for her keen supervision, continuous advice and constructive criticism in dealing with many problems encountered and helpful suggestions throughout this work. I am grateful for the knowledge acquired from her that helped to broaden my horizons.

I would like to express my gratitude to the Egyptian government for the financial support during my work for four years.

I am grateful to my colleague Anh Thy Nguyen, who guided my first steps as a beginner in cell culture, permeation experiments and DSC. I am also grateful to my colleague Mohamed Badran for supplying his experience in the penetration experiments.

Many thanks to Mrs. Herre for her support in cell culture and Mrs. Brabetz for her help in tape stripping. I am also grateful to Dr. Jana Thamm for adjusting the German language in the summary of my thesis.

I would like to thank Dr. Gruhl for providing the human abdominal skin and I am also grateful to Dr. Sabine Bischoff for supplying the rat skin.

I would like to express my deep thanks to my friends, Adel Saad, Mohamed Dawoud as well as Mrs. Chavez for proofreading this work and for the help in editing this work by adjusting the language.

I am grateful to all my colleagues in our department and to every one who cooperated in the completion of this work.

Last but not least, I give my deepest thanks to my family. I want to thank my wife, for her encouragement and support during the time of my PhD study. I express my deep thanks especially to my parents for their encouragement and decent support from my childhood.

Contents

Part I: Introduction and aim of work **1**

Chapter 1: Introduction and Aim of Work **1**

1.1. Introduction 1

1.2. Aim of work 2

Chapter 2: Background **4**

2.1. Dermal and transdermal drug delivery 4

2.2. Skin function 5

2.3. Skin structure 6

2.3.1. Epidermis 6

2.3.1.1. The non- viable epidermis (stratum corneum) 6

2.3.1.2. The viable epidermis 7

2.3.2. The dermis 7

2.3.3. Subcutaneous layer or Hypodermis 8

2.3.4. Skin appendages 8

2.4. Routes of drug penetration 8

2.5. In-vitro skin models for penetration and permeation measurements 10

2.5.1. Human and animals 10

2.5.2. Full-thickness and epidermis 11

2.5.3. Chemical lipid mixture of stratum corneum 12

2.5.4. Organotypic keratinocyte cultures 12

2.5.4.1. ROC epidermal model 13

2.6. Vesicles as a skin delivery system 15

2.6.1. Classification of vesicles 16

2.6.1.1. Conventional vesicles 16

2.6.1.2. Elastic vesicles 16

Part II: Experimental **20**

Chapter 3: Material and methods **20**

3.1. Materials 20

3.2. Methods 23

3.2.1. Preparation of human and animal skin models 23

3.2.1.1. Preparation of human skin 23

3.2.1.2. Preparation of human epidermis 24

3.2.1.3. Preparation of rat skin 24

3.2.1.4. Preparation of pig ear skin 24

3.2.2. Preparation of REK organotypic models 25

3.2.2.1. Keratinocyte culture 25
3.2.2.2. Collagen substrate 25
3.2.2.3. REK organotypic culture (ROC) 25
3.2.2.4. Preparation of ROC full-thickness model with and without collagen 27
3.2.3. Stratum corneum separation 28
3.2.4. Characterization of skin models 28
3.2.4.1. Morphology (light microscopy) 28
3.2.4.2. Differential scanning calorimetry (DSC) 29
3.2.4.3. Transepidermal water loss (TEWL) 29
3.2.4.4. Permeation studies 30
3.2.5. Correlation between the mass and absorbance for tape stripping in-vitro 30
3.2.5.1. Tape stripping procedure 32
3.2.5.2. Determination of stratum corneum thickness 32
3.2.6. Penetration of a radiolabeled solution of corticosterone and mannitol 33
3.2.6.1. Franz diffusion cell 33
3.2.6.2. Skin stripping 34
3.2.6.3. Cutting of stripped skin 34
3.2.6.4. Determination the drug concentration 34
3.2.7. Preparation of vesicles formulations 34
3.2.7.1. Preparation of vesicles with elastic bilayers containing 1mM CF 34
3.2.7.2. Preparation of vesicles with rigid bilayers containing 1mM CF 35
3.2.7.3. Preparation of invasomes containing 1mM CF 35
3.2.8. Particle size and zeta potential of liposomal and invasomal dispersions 36
3.2.8.1. Photon correlation spectroscopy (PCS) 36
3.2.8.2. Zeta potential measurements 36
3.2.9. Stability 36
3.2.10. In-vitro qualitative penetration studies 36
3.2.10.1. Dosage regime and incubation time 36
3.2.10.2. Fluorescence microscopic studies 37
Part III: Results and discussion **38**
Chapter 4: Cell culture **38**
4.1. Morphology 38
4.2. Transepidermal water loss (TEWL) 41
4.3. Thermal behavior of stratum corneum lipids 41
4.4. Permeation studies 42
4.5. Discussion 49
4.5.1. Morphology 49

4.5.2. TEWL measurements 51
4.5.3. DSC measurements 52
4.5.4. Permeation studies 54
4.6. Conclusion 56
Chapter 5: Evaluation of tape stripping and penetration of model drugs 58
5.1. Correlation between mass and absorbance for human skin in-vivo 58
5.2. Correlation between mass and absorbance for human skin in-vitro 59
5.3. Correlation between mass and absorbance for pig ear skin in-vitro 59
5.4. Penetration of corticosterone into pig ear skin 60
5.5. Penetration of mannitol into human skin and pig ear skin 61
5.6. Discussion 64
5.7. Conclusion 70
Chapter 6: Qualitative penetration and stability studies of vesicles 71
6.1. Fluorescence microscopic studies 71
6.2. Stability studies 71
6.3. Discussion 75
6.4. Conclusion 78
Chapter 7: Final discussion 79
Chapter 8: summary 84
Zusammenfassung 87
References 90

PART I

Introduction and Aim of Work

1. Introduction and aim of work

1.1. Introduction

Currently dermal and transdermal drug delivery remains an attractive route for local and systemic drug delivery, therefore scientists are very interested to work in this field. This route of administration is particularly attractive due to the drawbacks of oral drug delivery and the advantages of topical drug delivery which, include convenience, elimination of hepatic first-pass effect and improved patient compliance (Friend, 1990).

To estimate dermal and transdermal absorption of molecules, the most convenient membrane is human skin. However, ethical problems and religious restrictions make the use of human skin difficult for most investigators (Netzaff et al., 2005). Thus, animal skin is commonly used. There are many animal models such as pig, rabbit, mouse, rat and guinea pig that have been suggested as appropriate substitutes for human skin and have been used to estimate percutaneous permeation of molecules (Bronaugh et al., 1982). It has been reported that there are many similarities in the morphology of the different skin layers between human skin and pig ear skin (Jacobi et al., 2007). Pig ear skin is particularly compatible for permeation studies and gives comparable results to human skin (Bronaugh et al., 1982).

However, due to ethical issues, which arise from the use of animal skin in testing of pharmaceutical and cosmetic products, new laws have been developed that prevent the use of animals (Netzaff et al., 2005).

To overcome these ethical problems, several types of reconstructed skin equivalents have been developed to use as alternative models for human and animal skin models and some of them are commercially available. There are several kinds of reconstructed human skin equivalent models based on human epidermal keratinocytes such as EpiSkin, SkinEthic and EpiDerm. These epidermal models have similarities to human skin in morphology, lipid composition and biochemical markers. The reconstructed human skin equivalent models were produced by seeding normal human keratinocytes on a dermal or other appropriate substrate and culturing them at the air liquid interface (Netzaff et al., 2005).

The use of human epidermal keratinocytes in the generation of artificial skin models has some drawbacks; it is time consuming because it is dependent on the use of primary or early passage of cells from different donors and the produced barrier is not as strong as that of human skin. The rat epidermal keratinocyte (REK) organotypic culture model was used instead of human epidermal keratinocyte to generate artificial skin models. REK cells have several advantages over human epidermal keratinocytes; the culture is established from the

cell line and independent of the primary or early passage of cells, thereby saving time. The produced barrier was comparable to that of human skin (Pasonen-Seppanen et al., 2001b).
It was noted that the epidermal membrane was more permeable compared to full-thickness human skin especially for lipophilic substance. So the addition of the dermis to the epidermal models may improve the barrier properties for lipophilic substance (Nakamura et al., 1990).
The evaluation of drug penetration into SC by tape stripping needs an exact evaluation of the amount of the SC on each tape strip in order to determine the depth of the SC. There are several methods used to determine the amount of SC on each tape strip such as the weighing method, colorimetric method and infrared densitometry method (IR-D). The IR-D method is superior to the other methods, which are time consuming and lead to error. It has been reported that the IR-D method, which measures the indirect SC protein content by using SquameScan 850 A, is accurate, very fast and non-destructive (Voegeli et al., 2007).
The main challenge in dermal and transdermal drug delivery as a route of administration is the presence of SC, where it provides a strong barrier for dermal and transdermal delivery of the applied drugs (Ponec et al., 2002). Consequently, the dermal and transdermal drug delivery is very low due to the effect of the SC. One possibility for increasing the penetration of drugs is the use of vesicular systems such as liposomes (Ting et al., 2004).
Liposome vesicles are spherical colloidal particles composed of one or more concentric spheres of lipid bilayers separated by water or aqueous buffer compartments (Bangham et al., 1965). Mezei and Gulasekharam (1980) first reported the potential use of liposomes in topical applications for the skin (Mezei and Gulasekharam, 1980). Although there has been progress in percutaneous absorption, conventional liposomes were not efficient at delivering transdermally across skin because they did not penetrate deeply into the skin but were restricted to the upper layer of the SC. Thereby, intensive research led to the introduction and development of novel elastic vesicles to easily and deeply penetrate the skin. Elastic vesicles include transfersomes, detergent-based elastic vesicles, ethosomes and invasomes (Elsayed et al., 2007).
It was reported that conventional liposomes have mainly dermal or rarely transdermal effects, but elastic vesicles were reported to penetrate the intact skin, thereby having dermal and transdermal effects (Cevc and Blume, 1992).

1.2. Aim of work

The SC limits dermal and transdermal drug delivery. However, the SC acts as the main barrier for most compounds. One of the methods to increase the transport rate of the drug across the skin is incorporation of drugs into liposomal formulations. In this study characterization and qualitative evaluation of the potential of topical liposomal formulations

were done, with different composition of liposomes and bilayer fluidity, using the full-thickness human abdominal skin model. Three different topical liposomal formulations were used for the delivery of hydrophilic carboxyfluorescein into the skin, which included liposomes with a flexible bilayer, liposomes with a rigid bilayer and invasomes. The Franz diffusion cell and fluorescence microscopy were used for the qualitative evaluation of *in-vitro* skin penetration for the different liposomal formulations through human skin. Fluorescence microscopy and penetration experiments were conducted in order to investigate the penetration ability of the vesicles through human skin. Liposomes were prepared and characterized in terms of size, Zeta potential and stability upon storage at 4 °C.

However, the available amount of human skin is limited and there is a variation between different donors. So the animal skin models were used as an alternative for human skin. Due to the many similarities between human skin and pig ear skin, the investigation of the penetration behavior of radiolabeled hydrophilic and lipophilic drugs through human and pig ear skin was performed in this study. During these penetration experiments, the tape stripping process was used to evaluate the amount of drugs in the SC. Thus the determination of the amount of SC removed by each tape strip was very important to determine the exact amount of drug in the SC. As mentioned in the previous section, IR-D is superior to the weighing method. In this study an attempt was made to find a correlation between the absorption of SquameScan and the mass as measured by a balance to calculate SC depth because SquameScan reduced the experimental time considerably. After obtaining the equation that expressed the correlation between the mass and absorbance, penetration experiments were performed and this equation applied for the calculation of the SC depth.

As mentioned in the previous section, there are many problems in using human and animal skin models as *in-vitro* models for research and development in the pharmaceutical and cosmetic industries. So in this study, the development and evaluation of organotypic skin models, ROC epidermis and ROC full-thickness, have been attempted as an alternative model for human skin. ROC epidermis was compared to human epidermis with regards to morphology using light microscopy and SC lipids were investigated using differential scanning calorimetry, TEWL measurements and the permeation studies of three different solutes (mannitol, corticosterone and tritiated water) were performed to evaluate the barrier properties. Then the ROC full-thickness model was compared morphologically to the full-thickness human skin model by light microscopy to investigate the layer differences, TEWL measurements and the permeation studies with tritiated water were performed to evaluate the barrier properties.

2. Background

2.1. Dermal and transdermal drug delivery

Over the last three decades, topical drug delivery systems have been an active area of research for the delivery of pharmaceuticals and cosmetics. Topical drug delivery may act on the dermal or travel through the transdermal layer. Dermal drug delivery means the topical application of a drug to the skin for the treatment of dermal disease. With advanced technology, high concentrations of the drug in the form of ointments, creams and powders that can be localized at the site of disease. This method decreases systemic drug uptake and consequently decreases the systemic side effects (Thomas and Finnin, 2004).

Transdermal drug delivery means the application of a drug to the skin, which then passes through the skin layers to the systemic circulation to treat systemic disease. This route of administration is usually designed to offer a slow, sustained release of a drug over long periods of time. Current transdermal delivery systems such as transdermal occlusive patches are capable of delivering drugs where the oral administration is limited by poor bioavailability (Thomas and Finnin, 2004). Transdermal delivery systems, which are often in the form of a drug-impregnated patch, are used for drugs including fentanyl, nitro-glycerine, nicotine, estradiol, testosterone, scopolamine and clonidine (Naik A et al., 2000; Thomas and Finnin, 2004).

Although the skin forms a strong barrier to the penetration of drugs and chemicals, it also serves favourably as a route of drug administration.

These routes of administration have certain advantages (Friend, 1990) :

1. Both dermal and transdermal methods are very easy and painless, which in turn increase patient compliance.
2. Avoidance of first pass intestinal and hepatic metabolism (due to degradation in the gastrointestinal tract or by the liver), which leads to a lower daily dose.
3. Avoidance of variable rates of absorption and metabolism, as occurs with oral delivery treatment.
4. Avoidance of the risks associated with parental treatment.
5. Avoidance of the irritation of gastrointestinal tract, which results from active and inactive pharmaceutical ingredients.
6. Drug input can be terminated simply by removing the formulation from the skin.

However, dermal and transdermal routes of administration have many disadvantages such as:

1. The limitations of transdermal drug delivery are related to the skin's barrier function. This is the main reason that only a small percent of drugs can penetrate through skin layers to obtain a therapeutic effect.
2. The interaction between the topical formulation excipients and the skin, which may result in irritation, toxic and damaging effects to the skin (Godwin et al., 1997).

2.2. Skin function

The skin is the largest organ of the human body; it comprises approximately 16% of the total body weight and its thickness varies between 0.5 mm in the eyelid to 3-6 mm on the palm of the hands or the soles of the feet (Van den Bergh and B.A.I., 1999). It acts as a strong barrier to control loss of water and electrolytes from the body to the external environment and it protects the body from the invasion of microorganisms, viruses, chemicals and radiation. Also the skin stabilizes blood pressure and body temperature, and has sensors that allow the feelings of cold, touch and pain. In addition it expresses emotions such as the sweating of anxiety, and the redness of embarrassment and anger as well as the synthesis of vitamin D (Wickert and Visscher, 2006).

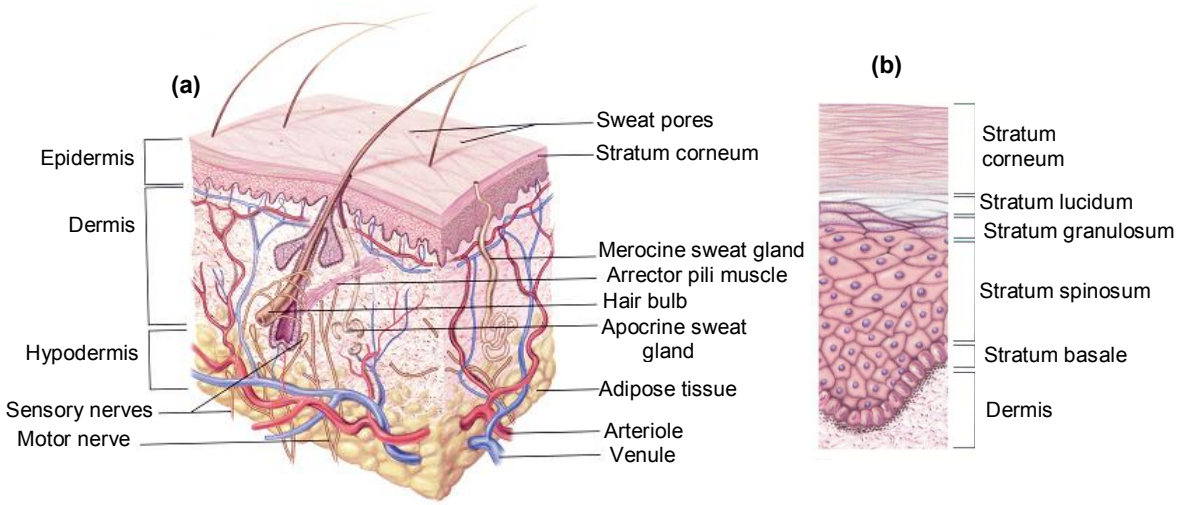

Figure 2.1: Structure of the human skin. (a) Layers of epidermis. (b) [taken from (Saladin and Porth, 1998)].

2.3. Skin structure

The skin is composed of three layers, the epidermis, the dermis and the hypodermis as illustrated in Figure 2.1 (a).

2.3.1. Epidermis

The uppermost layer of the epidermis, the stratum corneum (SC), is made up of stratified squamous epithelium. These cells are dead so the SC layer is considered the non-viable epidermis. The other three layers of the epidermis are called the viable epidermis as illustrated in Figure 2.1 (b).

2.3.1.1. The non-viable epidermis (Stratum corneum)

The stratum corneum is the outermost layer of the skin comprising 15-20 layers of corneocytes with the thickness of dry SC ranging from 10 to 15 μm (Christophers and Kligman, 1964). After hydration, the SC layers swell and its thickness can reach 40 μm (Scheuplein, 1967). The SC contains corneocytes, which are polyhedral-shaped non-nucleated cells. There is variation in the size of corneocytes, depending on the body site and age of the person (Schaefer and Redelmeier, 1996). The corneocytes are produced by the terminal differentiation of keratinocytes that are found in the viable epidermis. The cellular organelles and cytoplasm of corneocytes have disappeared during the process of cornefication. The keratin and thickened plasma membrane of cells in this stratum protect the skin against abrasion and penetration, where the glycolipid between these two structures acts as a waterproofing agent. Hence, the SC provides a durable support for the body, protects deeper cells from the hostile external environment and from water loss , and renders the body relatively insensitive to biological, chemical, and physical invasion. The structure of the SC is often depicted as bricks and mortar as illustrated in Figure 2.2, where the SC corneocytes and keratin microfibrils are considered the bricks and the layers of lipids that surround them as the mortar (Benson, 2005).

Keratins comprise approximately 60% of the dry weight of the SC and are considered as the major structural proteins of skin, nail, and hair. There are two types of keratins; type I, an acidic keratin, which has negative charges, and type II that has positive charges. These two types interact to form a structure called the coiled-coil and this structure is important in maintaining the integrity of the SC. Disturbance of the arrangement of the coiled-coil results in weakness of the keratinocytes that makes them rupture easily and finally leads to blistering (Wickert and Visscher, 2006).

The lipid mortar is crucial for the barrier function of the skin. The intracellular lipids are secreted from the lamellar bodies, which appear in the stratum granulsom layer. These lipids are released into the intracellular spaces where the SC forms. The intercellular lipids of the SC contain a mixture of ceramide, cholesterol, cholesterol esters and long chain fatty acid. Ceramides are sphingolipids linked to long chain fatty acids, which have a crucial role in the

barrier properties. The SC contains no phospholipid. The keratinocytes in the viable epidermis produce phospholipids that are disintegrated by phospholipase to produce fatty acids, which are very important for the formation of SC barrier and may lead to produce the acidic pH of the SC. Therefore the pH for the surface of SC around 4-5.5 and this acidic pH is known as the acid mantle of the skin (Wickert and Visscher, 2006).

2.3.1.2. The viable epidermis

The viable epidermis is located directly underneath the SC and is composed of 10-20 layers of keratinizing epithelial cells, which are responsible for the synthesis of the SC. The epidermis varies in thickness from 0.04 mm on the eyelids to 0.8-1.6 mm on the soles of the feet and the palms of the hand. Most epidermal cells are keratinocytes and responsible for the production of keratins and many other proteins, which are the structural proteins of the SC. The viable epidermis also contains other cells types such as melanocytes, langerhans cells and merkel cells. Melanocytes are responsible for skin pigmentation and protect the skin form ultraviolet radiation. Langerhans cells are dendritic immune cells, which arise from the bone marrow and migrate to the epidermis. They are important for antigen preservation and immune responses. Merkel cells are present at epidermal dermal junction and have a role as sensory receptors.
The viable part of the epidermis is composed of four layers, starting from the deepest layer the stratum basale, progressing to the stratum spinosom, stratum granulosum and stratum lucidum which lies just under the SC (Schaefer and Redelmeier, 1996).

2.3.2. The Dermis

The dermis is a fibrous layer, 3 to 5 mm thick that supports the epidermis and forms the bulk of the skin. It consists of a matrix of connective tissue that contains collagen and fibrous protein, which are embedded in a semigel matrix that contains water, ions and mucopolysaccharides. This matrix helps to hold the cells and allows oxygen and nutrients to diffuse to the epidermal cells. This layer contains an extensive blood vessel and nervous tissue network, hair follicles, sebaceous glands as well as sweat glands, which penetrate the dermis and epidermis to reach the surface of the skin. In addition, the dermis contains fibroblasts, which produce collagen, elastin and structural proteoglycans, together with immunocompetent mast cells and macrophages. Collagen fibers make up 70% of the dermis, giving it strength and toughness. Elastin maintains normal elasticity and flexibility while proteoglycans provide viscosity and hydration. The uppermost layer of the dermis is called

the papillary layer, which provides the nutritional support to the viable epidermis and has a role the temperature, pressure and pain regulation (Schaefer and Redelmeier, 1996).

2.3.3. Subcutaneous layer or Hypodermis

The subcutaneous layer or hypodermis is the innermost and thickest layer of the skin, which is located underneath the dermal layer. It is composed of a type of cells specialized in accumulating and storing fats, known as adipocytes. These cells are grouped together in lobules separated by connective tissue. This layer acts as energy storage, protection against injury and participates in thermoregulation since fat is a heat insulator. It acts as a depot for many compounds, which permeate the dermis and SC. Finally, the hypodermis contains an extensive network of circulatory vessels, so most permeated compounds can be considered to be distributed throughout the body (Schaefer and Redelmeier, 1996).

2.3.4. Skin appendages

Skin appendages include the nails, sweat glands, sebaceous glands, hair follicles and hair. Skin appendages penetrate the SC and the epidermis and provide various functions including thermal control and protective covering. Skin appendages form only about 0.1% of the total surface area of the skin (Schaefer and Redelmeier, 1996).

2.4. Routes of drug penetration

As mentioned above, any drug applied to the skin surface is delivered via dermal or transdermal delivery. In the case of dermal delivery, the drug penetrates the SC to reach its site of action within the skin. However, for transdermal delivery, the drug penetrates the SC is transmitted through the dermis and then taken up by systemic circulations. In both dermal and transdermal deliveries, the drug has to penetrate the SC, which is the main barrier for human skin.

For any skin applied molecules, there are two main routes of penetration through the SC, known as the transappendageal and transepidermal routes. In the transappendageal routes, known as shunt routes, the molecules pass through sweat glands and pilosebaceous units (hair follicles with their associated sebaceous glands). Skin appendages cannot be considered to be significant transdermal penetration routes because the appendages only contribute 0.1% of the total surface area of the skin. However, this does not take into account that the hair follicles extend deep into the dermis with a significant increase in the actual

surface area available for penetration, and so this method of penetration cannot be dismissed.

Many studies suggest that the transappendageal route of penetration may be especially convenient for hydrophilic and high molecular weight molecules (Benson, 2005).

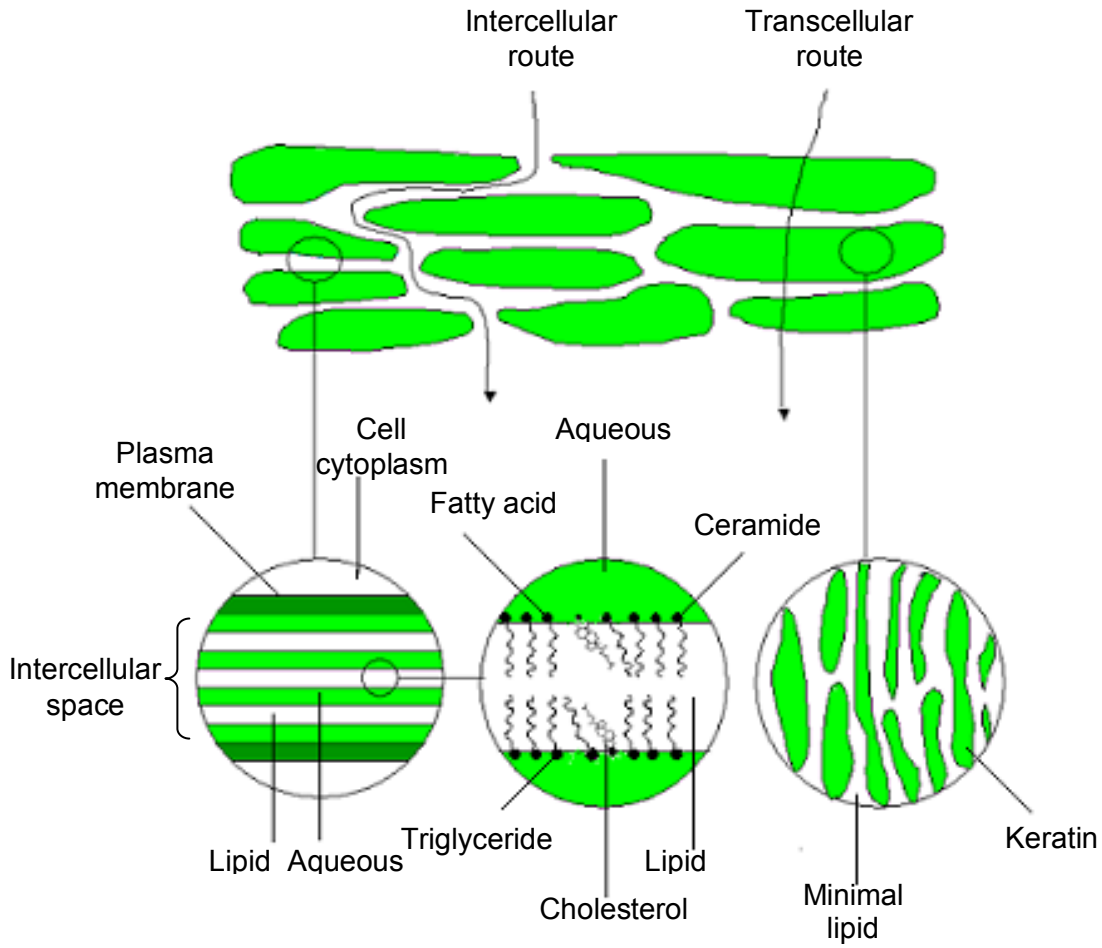

Figure 2.2: Simplified diagram illustrates the possible drug permeation pathways through intact SC, the transcellular or the tortuous intercellular pathways. Also illustrate the brick and mortar model of the SC with a simplified lamellar organization of intercellular domains showing the major stratum corneum lipids.

The transepidermal routes involve transport across the intact SC. There are two pathways through the intact SC as illustrated in Figure 2.2. First, the intercellular routes, where the applied molecules permeate through the intercellular lipid domains between the corneocytes. Second, the transcellular routes where the applied molecules cross through the keratinocytes and through the intercellular lipids. Most of the drug molecules prefer to permeate through the intercellular route (Benson, 2005).

2.5. In-vitro skin models for penetration and permeation measurements

2.5.1. Human and animals

Human skin is the best *in-vitro* model for research and development in the pharmaceutical and cosmetic industries. Possible sources for human skin are from cadavers, biopsies and cosmetic surgery. These have been used for the *in-vitro* assessment of percutaneous absorption (Friend, 1992). The need for human skin is increasing because research into transdermal drug delivery has expanded greatly in the last decades. However, the available amount of human skin is limited, there is a lack of viability and quality varies, so animal skin is used as an alternative model. Although animal models may have the same problem with biological variability they are more available and have small variations when compared to human skin due to the standardized conditions of animals.

A wide range of animal models have been suggested as suitable replacements for human skin, such as pig, mouse, rat, guinea pig and snake skin (Bronaugh et al., 1982). The histology of pig ear skin shows many similarities compared with human skin. The SC layers for both human and pig ear skin have orthokeratotic stratified squamous epithelium. The average thickness of the SC for pig ear skin is around 21 µm, while human skin ranges from 6 to 19 µm, and this thickness depends on the particular body site. The structure of the cell layers for viable epidermis in human and pig ear skin is the same and the thickness is similar; for pig ear skin around 72 µm, while for humans is 70 µm. The thickness of the dermal layer for pig ear skin is nearly 1.86 mm, while for human (on the back) is 1.8-1.9 mm. The follicular structure is also very similar. The hair is inserted deeply into the dermis in pig ear and human skin. The only difference between the pig ear and human skin is the diameter of the hair, where the diameter is larger in pig ear skin than in human skin. Therefore, the pig ear skin can be considered as the most suitable model for *in-vitro* assays of human skin (Jacobi et al., 2007). Also it was reported that, a big similarities between human skin and pig skin in terms of permeability and lipid composition (Bronaugh et al., 1982; Gray and Yardley, 1975).

The skin of rodents such as mice, rats and guinea pigs is the most commonly used in *in-vitro* and *in-vivo* percutaneous permeation studies. The advantages of these animals are their availability, small size, easy handling and relatively low cost. There are a number of hairless species such as nude mice and hairless rats in which the absence of hair coat mimics human skin better than hairy skin (Simon and Maibach, 1998). In these animals there is no need for hair removal by clipping or shaving prior to the experiment, consequently avoiding the risk of injury to the SC layer.

Rat skin showed the closest anatomical similarity to that of human skin, while the percutaneous absorption through it was one to three fold greater than in human skin

(Bronaugh et al., 1982). The skin permeability through human and animal models was arranged as follows; human < monkey < mini-pig < guinea-pig < rat < rabbit (Commission, 19 March 2004).

2.5.2. Full thickness skin and epidermis

The main difference between the full-thickness and an epidermal model is the presence of dermis. The human or animal epidermal models have been obtained by heat, chemical or enzymatic separation of epidermis from the underlying dermis (Commission, 19 March 2004), while in the human skin equivalent the epidermal models have been obtained by seeding of epidermal keratinocyte on the collagen gel or inert filter. Epidermal membranes are more fragile compared to full-thickness models (Van de Sandt J.J.M. et al., 2000). The full-thickness of human or animal skin models consists of three layers of SC, viable epidermis and dermis, whereas in the full-thickness skin equivalent models, the keratinocytes are proliferated on dermal substitutes, which include dead depidermized dermis (DED removed from native skin) or on the dermal equivalent consisting of fibroblast cells immersed in a collagen gel (Boelsma et al., 1999).

The DED retaining the basal lamina is a suitable substrate to induce epidermal cell differentiation in-vitro (Regnier M et al., 1981). In a culture that was made on DED and exposed to air, the feeding medium passed to the cell through the dermis and the epidermal morphogenesis was greatly improved. This suggests that any changes in cell differentiation may result from the dermal capacity of the dermal support (Regnier M et al., 1981).

However, the studies evaluating reconstructed human epidermal models have shown them to be more permeable than human skin particularly for lipophilic drugs. This has stimulated researchers to consider reconstructed full thickness models as more suitable models (Nakamura et al., 1990). The presence of dermal tissue may add some barrier to lipophilic drug permeation thus mitigating the higher permeability of the epidermal model especially for lipophilic drugs. However, reconstructed or cultured full thickness skin *in-vitro* lacks the vascular network present *in-vivo*. This vascular network should minimize the barrier role of the dermis, as it will clear any molecule crossing the dermoepidermal junction. Accordingly, the use of epidermal membranes *in-vitro* tends to provide a more representative model mimicking the *in-vivo* situation (Netzaff et al., 2005).

The presence of dermal constituents in some cell culture models contributes to wound healing, for example the treatment of severe burns, where these models act as a source of tissue and autologous skin grafts (Godwin et al., 1997).

Most of these models have been used to evaluate the cutaneous pharmacotoxicology of environmental agents including industrial products such as chemicals, pharmaceutical preparations, and cosmetics (Netzaff et al., 2005).

2.5.3. Chemical lipid mixture of Stratum corneum

The SC is the outer protective layer of mammalian skin and works as a main barrier to penetration of molecules through the skin and prevents water loss. The lipid composition of this layer plays an essential role in the determination of its flexibility, the partitioning and permeability of the drug into the skin. The SC lipids show a complex behavior that is dependent on the particular lipid composition in the SC matrix. The SC structure is depicted as the bricks and mortar model, where corneocytes (bricks) are surrounded by a lamellar lipid matrix (mortar). The SC lipid matrix mainly composed of ceramides, free fatty acids, cholesterol and cholesterol ester. Ceramides form the major components of the SC lipid matrix, where they represent approximately 50% of the total SC lipids. There are nine types of ceramides in human SC ranged from ceramide 1 to ceramide 9. Both cholesterol and free fatty acids form about 25% and 10% of SC lipid matrix respectively (Ponec et al., 2003; Wickert and Visscher, 2006).

Individual ceramides differ in their head group architecture and chain length distribution and in addition, ceramides 1 and 4 contain linoleic acid chemically bound to a long-chain ω-hydroxy acid. Ceramides affect the SC properties by decreasing the TEWL and skin scaliness and increasing the water content (Kessner et al., 2008).

Because SC intercellular lipids form bilayers, liposomes have been proposed as models for penetration of skin membranes. Simple phospholipid liposomes containing DPPC were originally used before, (Wertz et al., 1986) prepared liposomes from a lipid mixture approximating the lipid composition of the SC lipids (40% ceramides, 25% cholesterol, 25% palmitic acid and 10% cholesterol sulphate), termed SCL liposomes, were considered. These structures were used to investigate the mechanisms of enhanced skin drug delivery and used to investigate the mechanism of action of penetration enhancers (Kim et al., 1993). SCL liposomes have also been used as a model membrane to investigate the mechanism of action of phospholipid vesicles as skin drug delivery systems (Kirjavainen et al., 1996).

2.5.4. Organotypic keratinocyte cultures

The ethical problems due to the use of animals in experiments has led to new laws and regulations such as the 7th Amendment of the European Directive 76/768/EEC intended to limit the use of animals for testing purposes. Recently several commercial artificial skin

models have been developed such as human epidermis models EpiSkin, SkinEthic and EpiDerm. These models have similarities to human tissue in morphology, lipid composition and biochemical markers, so they are useful in toxicity studies. The models also have the advantage of being more consistent in permeability and responsiveness, compared to human skin. Unfortunately, the permeability barrier of these models is relatively weaker than excised human skin (Netzaff et al., 2005).

Human skin equivalents can be generated by seeding human keratinocytes on a dermal or other appropriate substrate and culturing them at the air liquid interface. Under these conditions a fully differentiated epidermis is formed (Netzaff et al., 2005).

However, improving the reconstructed barrier function towards drugs or chemicals is one of the main challenges in this field. So the most important character for the evaluation of an *in-vitro* skin culture model is the formation of a permeability barrier where any topical dermal or transdermal compound has to pass through the SC before it affects the viable cells (Ponec et al., 2002).

Different supports have been used for seeding of keratinocytes, e.g., inert filter, de-epidermized dermis (DED), dermal fibroblasts populated in a collagen matrix (Boelsma et al., 1999) and a combination of type IV collagen film and mixed collagens I and III (Tinois et al., 1991).

Although the main similarities between reconstructed human epidermis and native tissue have been achieved, some differences in SC function have remained and these illustrate the higher permeability of these models than that of native human skin (Ponec et al., 2001).

Reconstructed skin equivalent models have several advantages; their reproducible quality, the possibility of standardization (Pasonen-Seppanen et al., 2001a), and the potential for studying the irritation, toxicity and corrosivity of applied substances (Lotte et al., 2002). Although the cultured skin equivalent models are lacking hair follicles and sweat glands, this may not be significant since these appendages offer a minor route of penetration (Godwin et al., 1997).

2.5.4.1. ROC epidermal model

A tighter, easily maintained reproducible organotypic epidermal culture model has been developed, however the keratinocyte cell line was derived from newborn rat skin (rat epidermal keratinocytes; REK). These cells were grown for 3 weeks on a collagen gel as support and showed the ability to differentiate into epidermis and SC when grown at the air liquid interface as for the other models. This model exhibited normal SC structural and functional properties (Pasonen-Seppanen et al., 2001b). The permeability of this model to drugs was comparable to that of human epidermal cadaver membranes with an average of

only a two-fold higher permeability (Suhonen et al., 2003). This model showed only minor differences in its lipid composition and thermal phase behavior compared to human skin, explaining the minor differences in permeability (Pappinen et al., 2008). The functional permeability barrier was measured by transepidermal water loss (TEWL) and by permeability of corticosterone and mannitol (Pasonen-Seppanen et al., 2001a).

The REK organotypic culture (ROC) is a three-dimensional skin model, which exhibits a normal SC ultrastructure and functional properties (Pasonen-Seppanen et al., 2001a; Pasonen-Seppanen et al., 2001b). The ROC has several advantages involved in epidermal differentiation and permeability. First, the cultures are established from a cell line and independent on the primary or early passage of cells from different donors, where epidermal skin models are dependent on primary or early passage of human keratinocyte. This reconstruction of human keratinocytes is a time consuming process, which does not give an identical epidermal barrier to the human skin. Second, the REK cell line is different from other continuous cell lines, where it differentiates without support from connective tissue feeder cells (Pasonen-Seppanen et al., 2001b). Thirdly, ROC models respond to dermal penetration enhancers in the same way as human skin (Pappinen et al., 2007). Fourthly, the permeability barrier that is formed by REKs is comparable to the permeability barrier of human skin. This is a very important character of REKs. The ROC has a well developed permeability barrier, which closely resembles human skin (Suhonen et al., 2003). This is important with respect to solute permeation, permeation enhancement effects, and chemical irritation (Pappinen et al., 2007; Suhonen et al., 2003).

Organotypic cultures supplemented with vitamin C have shown better ultrastructure properties and this has been accompanied by an improvement in the barrier permeability of corticosterone and reduced TEWL (Pasonen-Seppanen et al., 2001b).

It has been reported that ROC models contain lamellar bodies that are completely extruded into the interface between stratum granulosum and SC (Pasonen-Seppanen et al., 2001a; Pasonen-Seppanen et al., 2001b). Most of the intercellular lipids form a typical repeating pattern of Landmann units (Landmann, 1986). ROC also contains the cornified envelopes and its components, such as keratin filaments, involucrin and filaggrin. So these lipid matrixes of the SC form the major barrier for ROC models, which is the main advantage of ROC models in pharmaceutical and chemical testing which is often decreased in other skin culture models.

2.6. Vesicles as a skin delivery system

The SC is the outermost layer of the skin and it acts as strong barrier in human skin. In order to improve transdermal drug delivery, several methods have been used to overcome the

barrier properties of the SC, such as chemical penetration enhancer, electroporation, iontophoresis, ultrasound, microneedles and vesicular systems, that is, liposomes (Ting et al., 2004).

Liposomes, first discovered by Bangham in 1960s (Bangham et al., 1965), are microscopic hollow colloidal particles, consisting of one or more lipid bilyers. These lipid bilayers have amphiphilic properties, that is, a polar hydrophilic head group and a non-polar hydrophobic tail. For this amphiphilic property, the lipid bilayers in the presence of aqueous phase form one (unilamellar vesicle) or more (multilamellar vesicles) concentric bilayers that are surrounded by an equal number of aqueous compartments (Vemuri and Rhodes, 1995). Liposomes can entrap both hydrophilic and lipophilic drugs as illustrated in Figure 2.3, where hydrophilic drugs can be entrapped in the internal aqueous of vesicles (in) and locate in the external aqueous compartment (out). The lipophilic drugs entrap into the liposome bilayer or partition between the bilayers and aqueous phase (if the drugs have solubility in both aqueous and non-aqueous phase) (Juanjuan Liu and Hu, 2007).

Liposomes are composed mainly of phospholipid, so the effects of phospholipids on flexibility of SC lipid bilayers and drug partitioning into them were estimated, using the SCL liposomes as a model for human SC (Kirjavainen et al., 1999). The study suggested that different phospholipids have different effects on drug partitioning into the SC lipid bilayers. Thus, incorporating egg-PC, soya-PC or DOPE into skin lipid liposomes increased the partitioning of drugs into these SC liposomes while distearyl-PC did not change this partitioning. It was suggested that fluid state phospholipids could disturb the rigid structure of the skin lipids, thus increasing drug partitioning into the lipid phase. However, gel state phospholipids made only minor or no effects. It was concluded that the phospholipid-improved skin permeation of drugs may be at least partially be due to increased drug partitioning. These results were in good agreement with those obtained after a partitioning study employing human SC *in-vitro* (El Maghraby et al., 1999), which further indicated the value of SCL liposomes as skin models.

The vesicles act as dermal or transdermal transporters and this depends on the different composition and physicochemical properties of the vesicles. However, some studies have suggested that the vesicles act as dermal transporters only while others have suggested that the vesicles act as transdermal transporters (Honeywell-Nguyen and Bouwstra, 2005).

2.6.1. Classification of vesicles

The classification of vesicles is based on the method of their preparation or the number of bilayers or their size. They are classified according to their method of preparation into; reverse phase evaporation vesicles (REV), French press vesicles (FPV) and ether injection

vesicles (EIV). The classification according to the size and number of bilayers is as follows: There are multilamellar vesicles (MLV) with a size > 100 nm with more than five lamella, large unilamellar vesicles (LUV), size > 60 and with only one lamellae, small unilamellar vesicles (SUL), size from 30 to 60 nm with only one lamellae and oligolamellar vesicles (OLV) size > 60 nm and containing from two to five lamellae (Verma, 2002). The classification of vesicles according to their lamellarity and size are more official than those according to the methods of preparation.
Vesicles were classified also according to the rigidity of the bilayer into:

2.6.1.1. Conventional vesicles

These can be defined as liposomes that are typically composed of only phospholipids and cholesterol. Most early work on liposomes as a drug-carrier system employed this type of liposomes. Conventional liposomes are a family of vesicular structures based on lipid bilayers surrounding aqueous compartments. They can vary widely in their physicochemical properties such as size, lipid composition, surface charge and number and fluidity of the phospholipid bilayers (Elsayed et al., 2007).
Mezei and Gulasekharam (Mezei and Gulasekharam, 1980) were the first to use liposomes as skin delivery systems. They incorporated triamcinolone acetonide in the vesicles of dipalmitoyl phosphatidylcholine (DPPC) and cholesterol. They reported that the concentration of triamcinolone acetonide in the epidermis and dermis was increased by four to five fold compared with a standard ointment. Incorporating these liposomes in a gel dosage form, similar findings were observed compared with a gel containing free drug and the liposome components at the same concentrations (Mezei and Gulasekharam, 1982).

2.6.1.2. Elastic vesicles

As mentioned above, elastic vesicles have a greater ability to deliver the drug into dermal layers or cross to general circulation than rigid or conventional vesicles especially under non-occlusive conditions. However, this is driven by an osmotic gradient through the skin that is caused by the difference in water concentration between the skin surface and the skin interior (Bouwstra and Honeywell-Nguyen, 2002).
Cevic and Blume introduced transfersomes as the first generation of elastic vesicles in 1992. Transfersomes consist of phospholipids such as phosphatidylcholine and an edge activator like sodium cholate. The elasticity of transfersomes depends on the ratio between the bilayer forming components, which work as a stabilizing molecule, and a micelle forming component, that is, a single chain surfactant (having a high radius of curvature), which acts as

a destabilizing molecule. However, an edge activator is often a single chain surfactant that destabilizes the lipid bilayer of the vesicles and increases their flexibility. The edge activator is used for preparation of transfersomes such as sodium cholate, sodium deoxycholate, span 80,span 60, span 65, tween 60, tween 20, tween 80, oleic acid and dipotassium glycyrrhizinate (Elsayed et al., 2007).

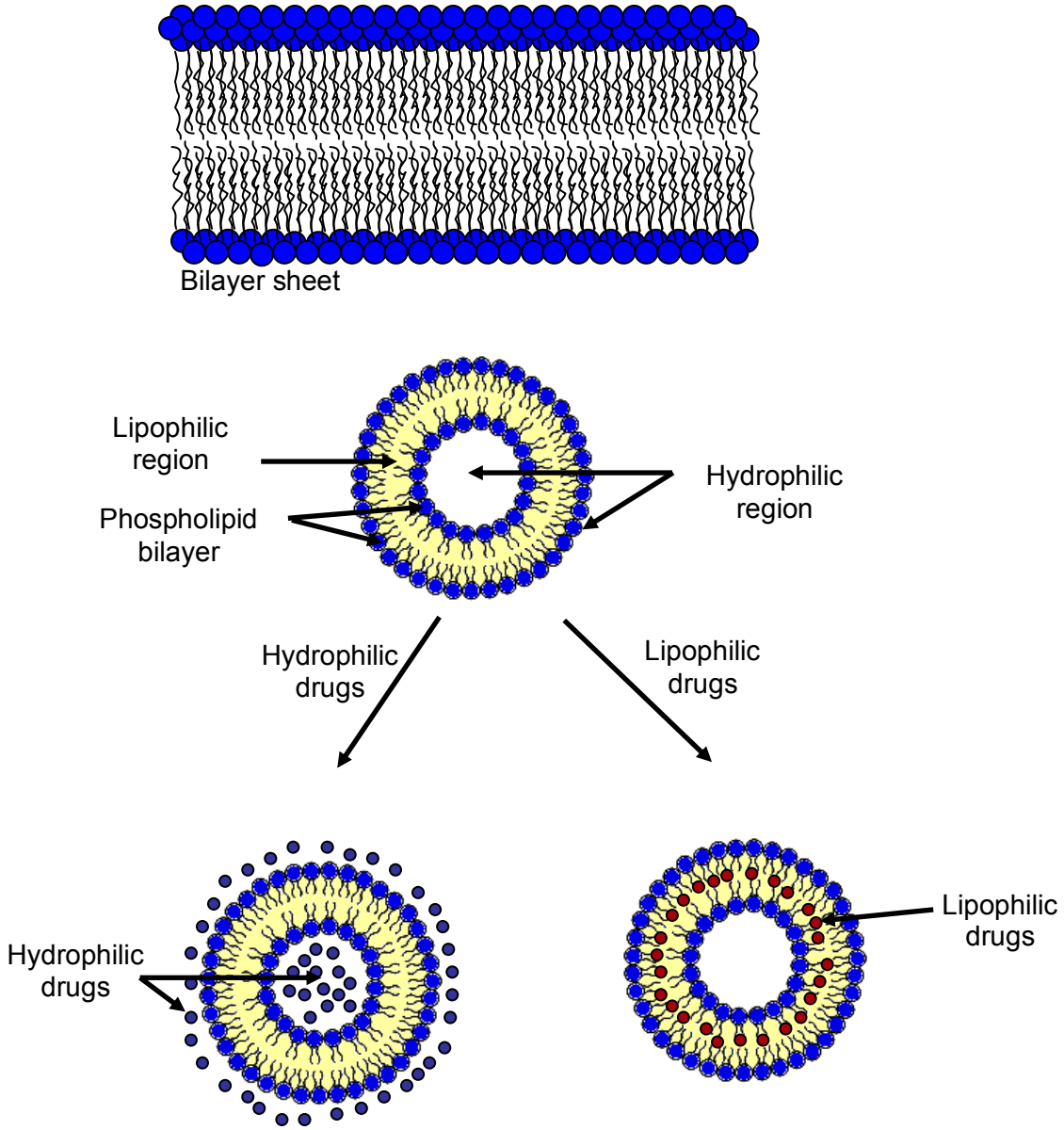

Figure 2.3: Illustrates the bilayer sheet and the general structure of vesicles and with hydrophilic and lipophilic drugs.

Van den Bergh (Van den Bergh and B.A.I., 1999) introduced the second generation of elastic vesicles based on a non-ionic surfactant or termed detergent-based elastic vesicles. It consists of a bilayer-forming surfactant L 595 (sucrose laurate ester), which acts as a stabilizing molecule, and a micelle-forming surfactant PEG-8-L (octaoxyethylene laurate

ester), which acts as a destabilizing molecule. These elastic vesicles are low cost, store easily and have slightly more elasticity compared to phospholipid elastic vesicles. These surfactant-based elastic vesicles were shown to be more effective than rigid vesicles in enhancing skin penetration of various chemical entities (Honeywell-Nguyen and Bouwstra, 2003).

Ethosomes are novel elastic vesicles containing phospholipids, a high concentration of ethanol (20-45%) and water. Touitou et al introduced the ethosomes (Touitou et al., 2000). The main features of this new vesicle are its soft structure, and flexible bilayers that carry the incorporated active agent into the skin lipid bilayers, enabling facilitated delivery. Ethanol acts as a permeation enhancer and has been added to prepare the elastic vesicles. Ethanol disturbs the organization of the SC lipid bilayer and enhances its lipid fluidity. It interacts with the polar head group region of the lipid molecules, which leads to a reduction of the melting point of the SC lipid, thereby increasing lipid fluidity, and cell membrane permeability. The release of a drug in the deep layers of the skin and its transdermal absorption could then be the result of fusion of ethosomes with skin lipids and drug release at various points along the penetration pathway. The high flexibility of bilayer membranes that result from the addition of ethanol permits the elastic vesicles to squeeze themselves through the pores, which are much smaller than their diameters. Ethosomes are much more efficient in delivering substances to the skin in terms of quantity and depth, than either conventional liposomes or hydroalcoholic solution (Touitou et al., 2000).

Verma and Fahr, introduced a novel generation of elastic vesicles termed invasomes, which consist mainly of a mixture of phospholipids in ethanol and mixture of terpenes (Verma and Fahr, 2004). Terpenes are very safe and effective penetration enhancers. The main sources of terpenes as essential or volatile oils are obtained from natural sources. The FDA classifies terpenes as generally safe. However, they cause low skin toxicity and low skin irritancy. Terpenes are hydrocarbons with the general formula $(C_5H_8)_n$. They increase the percutenous absorption of hydrophilic and lipophilic drugs (Aqil et al., 2007). Ethanol has been reported to act as a skin penetration enhancer for several drugs (Touitou et al., 2000). However Verma et.al (Verma and Fahr, 2004) reported that the combination of phospholipid, ethanol and a mixture of terpenes in the invasomes vesicles lead to a synergistic effect. His study reported a higher penetration for cyclosporine A into the skin from invasomes vesicles compared to an ethanolic solution. The enhancement of the skin penetration of various drugs is explained as a result of increased drug solubility in the SC, which has been treated with terpene. Furthermore, terpenes interact with intercellular lipids, perturbing the highly ordered intercellular lamellar packing of the SC lipids.

Ideal penetration enhancers should be non-toxic, non-irritating, non-allergenic and pharmacologically inactive compounds that work rapidly, with the activity and duration of their

effect being both predictable and reproducible. The skin's barrier properties should be restored rapidly and fully upon removal of the enhancer. The enhancers should work unidirectionally, that is, they should allow the passage of therapeutic agents into the body whilst preventing the loss of endogenous material. They should also be compatible with both excipients and drugs as well as be cosmetically acceptable (Williams and Barry, 2004).

PART II

Experimental

3. Material and methods

3.1. Materials

Materials for cell culture: Minimal Essential Medium (MEM with Earle's salts, without L-glutamine), Dulbecco's Modified Eagle's Medium (DMEM with glucose 4.5 g/l, and L-glutamine and without sodium pyruvate) as well as Hank's Balanced Salt Solution (HBSS without calcium, magnesium, and phenol red), Hank's balanced salt solution (HBSS) with antibiotics (penicillin 100 IU/ml, streptomycin 0.1 mg/ml), trypsin-EDTA solution (containing 500 U/ml porcine trypsin and 180 µg/ml EDTA in Dulbecco's Phosphate-Buffered Saline), penicillin-streptomycin solution (containing 10,000 IU penicillin and 10 mg/ml streptomycin) were purchased from PAA laboratories GmbH (Austria). Fetal bovine serum (FBS; 25 EU/ml endotoxin, 10 mg/dl hemoglobin, triple 100 nm filtered) was obtained from HyClone (Logan, Utah, USA). L-glutamine solution (200 mM) was obtained from Bio Whittaker Europe. Earle's Balanced Salt Solution (EBSS) without sodium bicarbonate and L-ascorbic acid (sodium salt) were supplied by Sigma-Aldrich.

Materials for light microscopy: Mayers Haemalaun solution and Euparal resin were purchased from Roth GmbH (Germany). Congo red powder was supplied from Fluka Sigma-Aldrich. Polysinecoated slides were obtained from Menzel GmbH & CoKG (Germany).

Materials for the separation of SC: Trypsin (TPCK treated, from bovine pancreas) and trypsin inhibitor (Type II: Soy bean) were obtained from Sigma-Aldrich.

Materials for permeation and penetration experiments: Phosphate-buffered saline (PBS) was composed of disodium hydrogenphosphate dihydrate ($Na_2HPO_4x2H_2O$) (Roth, Germany), potassium dihydrogenphosphate (KH_2PO_4) (Roth, Germany), sodium chloride (NaCl) (Merck, Germany), potassium chloride (KCl) (Merck, Germany) and Distilled water. Bovine serum albumin (BSA) was purchased from Sigma Aldrich. [1,2,6,7-3H]-corticosterone (37 MBq/ml) was supplied by GE Healthcare (Germany). Corticosterone has logP 1.94 and molecular weight (MW= 347g/mol), thereby it was used as a lipophilic model drug. D-[1-3H (N)] -mannitol (37 MBq/ml) was supplied by Perkin Elmer. It has logP -3.1 and molecular weight =182 g/mol). Mannitol was used as hydrophilic model drug. [3H]- triatiated water (37 MBq/ml) was supplied by GE Healthcare (Germany).

Carboxyfluorescein (CF) was purchased from Fluka (Buchs, Switzerland) and used a hydrophilic fluorescent marker. It has molecular formula ($C_{21}H_{12}O_7$), and molecular weight (MW= 376.32 g/mol). It was incorporated with different vesicles formulations to investigate the qualitative penetration through the different layers of human skin. Figure 3.1 illustrates the chemical structure of carboxyfluorescein, corticosterone and mannitol.

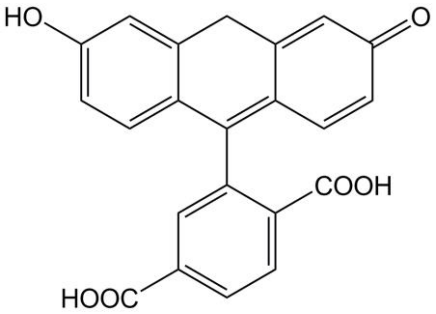

3′,6′-Dihydroxy-1-oxospiro[2-benzofuran- 3,9′-xanthen]-5-carbonic acid

Carboxyfluorescein

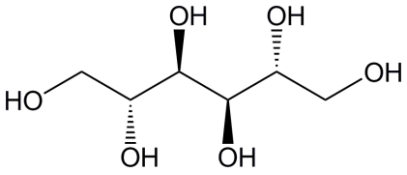

1,2,3,4,5,6-hexol

Mannitol

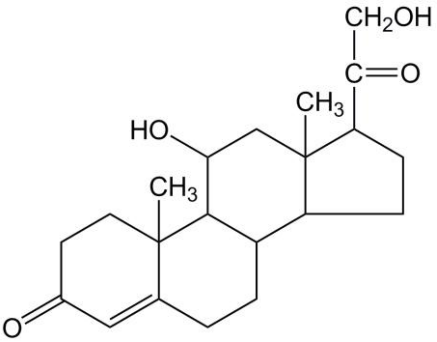

(11β)-11,21-dihydroxypregn-4-ene-3,20-dione

Corticosterone

Figure 3.1: Chemical structure of carboxyfluorescein, corticosterone and mannitol.

Materials for preparation of vesicles: Purified soybean phosphatidylcholine (SPC) dissolved in ethanol (NAT 8539, SPC: ethanol 75:25, w/w) was purchased from Phospholipid GmbH (Cologne, Germany). D-Limonene, citral and 1,8-cineole were purchased from Sigma–Aldrich. Tris buffer 10mM pH 7.4 was prepared from Trizma® Pre-set crystals pH 7.4 (Sigma-Aldrich). Soybean lecithin, hydrogenated lecithin (Lipoid S-100-3), Lipoid S-75 and hydrogenated phosphatidylglycerol from soybean (Lipoid S-PG-3), were purchased from Lipoid GmbH (Germany).

According to the manufacturers' certificates, Table 3.1 illustrates the main components of the lipids that were used for the preparation of the different vesicles.

Table 3.1: Composition of phospholipids (manufacturer's data)

Phospholipids (g/100 g)	NAT 8539	Lipoid S-75	Lipoid S-100-3	Lipoid S-PG-3
Phosphatidylcholine	73.0–79.0	68.0–73.0 (+LPC)	Min. 94.0	Max. 0.5
Phosphatidylglycerol	-----	-----	-----	Min. 98.0
Phosphatidylethanolamine	Max. 4.0	7.0–10.0	Max. 0.1	-----
N-Acyl-Phosphatidylethanolamine	-----	-----	Max. 1.0	-----
Lysophosphatidylcholine (LPC)	Max. 6.0	Max. 3.0	Max. 3.0	-----
Lysophosphatidylglycerol	-----	-----	-----	Max. 0.5
Phosphatidic acid	6.0	-----	-----	Max. 0.5
Dry residue	73.0–77.0	-----	-----	-----
Neutral oils, sterol	Max. 6.0	-----	-----	-----
Ethanol	23.0–27.0	-----	-----	-----
Non-polar Lipids (g/100 g)	-----	-----	Max. 3.0	Max. 0.5
Triglyceride	-----	Max. 3.0	Max. 2.0	Max. 0.5
Free fatty acids	-----	Max. 0.5	Max. 1.0	Max. 0.1
DL-α-Tocopherol	-----	0.1–0.2	Max. 0.1	Max. 0.1
Typical fatty acid composition (% of total fatty acid)				
Palmitic acid	-----	17.0–20.0	12.0–16.0	12.0–16.0
Stearic acid	-----	2.0–5.0	85.0–88.0	80.0–88.0
Oleic acid	-----	8.0–12.0	Max. 2.0	Max. 2.0
Linoleic acid	-----	58.0–65.0	Max.1.0	Max.1.0
Linolenic acid	-----	4.0–6.0	-----	-----

3.2. Methods

3.2.1. Preparation of human and animal skin models

3.2.1.1. Preparation of human skin

Human abdominal skin was obtained following plastic surgery. The subcutaneous fatty tissue was removed from the skin using a scalpel and surgical scissors as illustrated in Figure 3.2. Then, the skin was cleaned with PBS and allowed to dry for about 20 min at room temperature. The prepared skin was punched into 30 or 36 mm round samples. The punched skin samples were wrapped in aluminium foil and stored at -20°C. Under these conditions the skin was stable for up to 6 months (Harrison et al., 1984).

Prior to use, the skin was allowed to thaw at room temperature for about 15 min. The skin surface was then carefully wiped with cotton wool balls moistened with PBS. The cleaned punched skin samples were hydrated by placing on a filter paper saturated with PBS pH 7.4 in a petri dish and stored at 4°C for use on the second day.

Figure 3.2: Removing the fat tissue from human abdominal skin.

Figure 3.3: Illustrates the steps for shaving and separation of rat skin.

3.2.1.2. Preparation of human epidermis

Human epidermis was prepared by the heat separation method (Kligman and Christophel, 1963). The full-thickness skin sample was immersed in purified water at 60°C for 2 min. Then the epidermis was carefully separated from the dermis using a blunt scalpel. The separated epidermis was laid flat and dried overnight at room temperature. These samples were then put in plastic petri dishes, wrapped in aluminium foil and stored at -20°C. Prior to use, the frozen epidermis samples were allowed to thaw at room temperature for about 5 min, punched into rounds of 30 mm diameter and hydrated with PBS pH 7.4 overnight at 4°C.

3.2.1.3. Preparation of rat skin

Male or female Wistar rats weighed around 500 g and 2 years old were purchased from a breeding company (Harlan Winkelmann GMBH; Germany) and maintained on unlimited quantities of commercial stock ration and water. The process for shaving and separation of rat skin were done at the Institute for Animal Science and Animal Welfare (Friedrich Schiller University, Jena). As illustrated in Figure 3.3, the rat was killed using carbon dioxide followed by decapitation. The hair was removed from the dorsal and abdominal area using a shaver, and soap and water. The skin was dissected free from the underlying muscle and fat, and transferred to the laboratory in a cooling box. Freezing of skin was avoided during transport. In the laboratory, the skin was placed SC side down onto a clean surface. The residues of fat tissue on the dermal side were carefully removed. Then the SC face of the skin was cleaned with PBS pH 7.4 and the skin was used either fresh or stored at -20°C.

3.2.1.4. Preparation of pig ear skin

Domestic pigs came from farms to the slaughterhouse in Jena. The age of animals ranged from 6–12 months and their weight was around 100 Kg. The animal was shocked by electrical current to its head and the ears were separated from the head by knife. The animal was placed in a special container and scalded with hot water to clean the body. The ears were transported to the laboratory in a cooling box without pervious treatment. Freezing of the skin was avoided during transport. In the laboratory, the pig ear skin was washed carefully with tap water. The hair was removed from the external part of pig ear skin using a shaver. Then, the full-thickness skin of the external part of the pig's ear was separated from the underlying cartilage using a scalpel (Clowes et al., 1994). The best areas of the separated skin samples were selected and punched into round samples of 36 mm diameter. If fresh skin was required for the experiments, the punched samples were hydrated by

placing them on a filter paper moistened with PBS pH 7.4 in a petri dish and stored at 4°C for use on the second day. If the skin samples were not used fresh, they were wrapped in aluminium foil and stored at -20°C.

3.2.2. Preparation of REK organotypic models

3.2.2.1. Keratinocyte culture

The REK cell line was originally derived from a neonatal rat (Baden and Kubilus, 1983) and it was gift from the university of Kuopio (Finland). Stock cultures were put in the tissue culture flasks (Greiner Labortechnik GmbH Germany), Cell Star® (50 ml, 25 cm^2). The stock cultures were grown in MEM supplemented with 10% FBS, 4 mM L-glutamine, 100 IU penicillin and 100 µg/ml streptomycin at 37°C in a humidified mixture of 95% air and 5% CO_2. The REK were subcultured twice a week by incubating them for approximately 8 min at 37°C in trypsin-EDTA solution (Suhonen et al., 2003).

3.2.2.2. Collagen substrate

Collagen substrate was prepared as described before (Suhonen et al., 2003). The pure collagen was obtained from rat-tails. About 1 g of collagen strands were removed from 3–4 rat tails, washed with 70% ethanol and dried under UV light. The dried collagen was cut into small pieces and mixed with sterile aqueous acetic acid 0.1% (v/v) to give a final concentration of 3 mg/ml. The mixture was stirred for 48 h at 4°C and then centrifuged for 2 h at 2000 g. The clear supernatant was stored at 4°C. The collagen substrate was prepared by mixing the collagen solution with EBSS, 7.5% sodium bicarbonate and 1 M sodium hydroxide solution in a volume ratio of 8:1:0.3:0.2, respectively, on an ice bath. To cover the surface of the culture inserts Transwell® (polycarbonate membrane with 3 µm membrane pore size, 24 mm insert diameter, 4.67 cm^2 growth surface area) (Corning Inc. USA) or the de-epidermized dermis, 1 ml (REK epidermis) or 0.7 ml (REK full-thickness) of this mixture was pipetted into each insert and the plates were incubated overnight at 37°C in a humidified atmosphere to polymerize the collagen.

3.2.2.3. REK organotypic culture (ROC)

Firstly, the collagen coated inserts were washed with feeding medium DMEM (1 ml/insert). The feeding medium was aspirated carefully without touching the collagen surface. REK cells were trypsinized and diluted with DMEM supplemented with 10% FBS, 4 mM L-glutamine

(final concentration 8 mM) and 100 IU penicillin and 100 µg/ml streptomycin. 2 ml of cell suspension (400,000 cells/insert) (Kuntsche et al., 2008) was seeded onto the collagen coated inserts. The cultures were grown for three days with culture medium on top and below the cells. The culture medium was then removed from beneath as well as from the surface of cells and the level of culture medium beneath the insert was adjusted to the level of REK cells on the collagen gels (1.5 ml/insert). The culture medium was supplemented with 40 µg/ml L-ascorbic acid from the day after the culture was raised to the air-liquid interface. The medium was changed every two days for the first week and daily thereafter. The culture was incubated for three weeks at 37°C in a humidified mixture of 95% air and 5% CO_2.

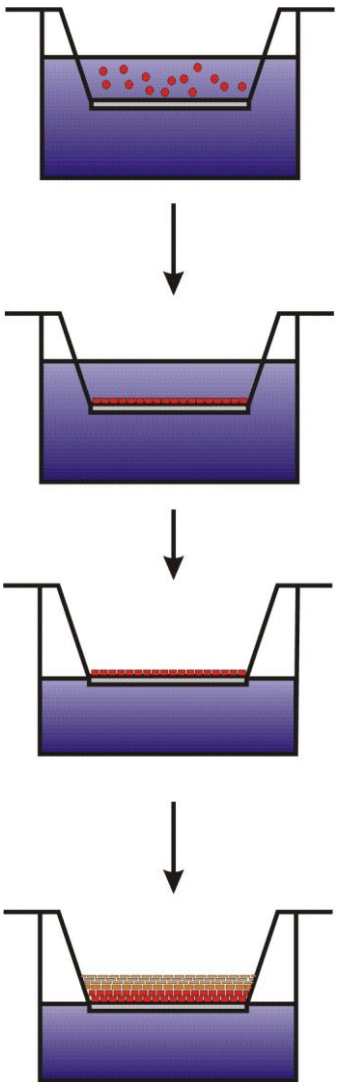

Figure 3.4: Illustrates the stages of REK organotypic culture model (ROC).

After three weeks of incubation the REK cells were differentiated into epidermis and stratum corneum as illustrated in Figure 3.4. The culture medium was removed and replaced by HBSS. The polycarbonate membrane with epidermis or with full-thickness sample were cut using a scalpel and placed on a filter paper soaked with PBS and used for the experiments (Suhonen et al., 2003).

3.2.2.4. Preparation of ROC full-thickness model with and without collagen

For preparation of the ROC full-thickness model, the de-epidermized dermis was prepared using the heat separation method, where the epidermis was separated from the underlying dermis as described above. The dermis was punched into rounds with a diameter of 25 mm. Each dermal sample was wrapped in disinfected aluminium foil to avoid damage by handling during cycles of freezing and thawing.

The dermal samples were rapidly frozen by immersing them in liquid nitrogen for 1 min and then allowed to thaw at room temperature for 7 min. The freezing and thawing cycles were repeated 9 times (Regnier et al., 1986).

After the last freezing/thawing cycle, the dermis was transferred under laminar air flow (LAF). The dermal samples were removed from the aluminium foil and placed into a sterile glass petri dish of a suitable size containing sterile-filtered 70% ethanol for 10 min. 5 ml of HBSS supplemented with penicillin (100 IU/ml) and streptomycin (0.1 mg/ml) were pipetted into each well of a sterile 6-well-plate (without inserts) (Greiner Labortechnik GmbH Germany). The dermal samples were transferred into the prepared well plates with the surface (epidermal side) upwards. The plates were incubated for approximately 12 h at 37°C.

The next day, the dermal support that was used for the preparation of the full-thickness model was prepared with and without collagen coating. The inserts of dermal support for the full-thickness model without collagen were prepared as follows: 2 ml HBSS supplemented with penicillin (100 IU/ml) and streptomycin (0.1 mg/ml) was added underneath each insert and the dermal samples were placed onto the filter of the inserts with the epidermal side upwards, avoiding wrinkles and air bubbles underneath the dermis. Then, the plates were incubated overnight at 37°C.

The inserts of dermal support for the full-thickness model with collagen were prepared as for the full-thickness model without collagen with a few differences. The underside of inserts did not contain HBSS and the surface of the dermis was rinsed with 1 ml HBSS supplemented with penicillin (100 IU/ml) and streptomycin (0.1 mg/ml). The buffer was aspirated carefully from the surface of the dermis and replaced with 0.7 ml collagen solution. Then, the plates were incubated overnight at 37°C.

Finally, for the REK full-thickness model with and without collagen, the organotypic models were seeded and cultured as described for ROC.

3.2.3. Stratum corneum separation

The human stratum corneum (SC) was separated from the epidermis by incubating the sample (SC uppermost) on a filter paper moistened with 0.1% (w/v) trypsin solution in PBS pH 7.4 in a petri dish at 4°C for 24 h and then at 37°C for 1 h. Then, using forceps, the SC was peeled off the underlying epidermis and immersed in a petri dish containing 0.1% (w/v) trypsin inhibitor in purified water for 30 s and washed twice in purified water. It was then placed on a wire mesh to dry at room temperature, and stored over silica gel in a dessicator containing nitrogen gas and protected from light until used.
The rat epidermal keratinocyte (REK) SC samples were prepared using the same method for separation of human SC, with the exception that the collagen and polycarbonate membrane filter were removed before incubation with 0.1% trypsin (Kuntsche et al., 2008).
The rat SC was separated from fresh or frozen full-thickness skin. Frozen full-thickness skin was allowed to thaw at room temperature. Then the full-thickness skin samples were punched into suitable sizes and placed dermal side down in contact with 0.1% trypsin solution in PBS and incubated at 37 °C for 12 h (Al-Saidan et al., 1998). If the SC did not peel off easily, the incubation time was increased and if necessary fresh trypsin solution was used. The procedure then continued as for the separation of human SC.
Prior to use the human, rat and ROC SC samples were hydrated over 27% w/w sodium bromide solution for 2 days to obtain a hydration level of about 20% (Bouwstra et al., 1995). The phase transition temperature of the SC is stable at a hydration level of 20% or more (Golden et al., 1987). For calculation of the hydration level, the SC samples were weighed before and after storage over sodium bromide solution.

3.2.4. Characterization of skin models

3.2.4.1. Morphology (Light microscopy)

Human epidermis, ROC epidermis, and ROC full-thickness skin samples were frozen at -26°C for 10 min in a cryomicrotome (Cryostat Reichert-Jung Frigocut 2800E) (Leica Instruments GmbH, Germany), while the human skin full-thickness was frozen in liquid nitrogen for 1 min. The vertical cross section (0.5 x 0.5 cm) for human epidermis and ROC epidermis was performed using a sharp scalpel, while the vertical cross section for the full-thickness model and human skin used a punch with a diameter of 8 mm. The vertical

cross sections of all samples were fixed on a pre-cooled microtome sample holder with a sufficient amount of embedding medium (Tissue-Tek®, Sakura (USA). Cross sections of human epidermis and ROC epidermis were cut with a thickness of 8 µm. The human skin full-thickness and ROC full-thickness model were cut with a thickness of 7 µm. The cross-sections were placed onto pre-cooled object slides and allowed to dry overnight at room temperature.

These sections were then fixed for 10 min with Baker´s Formol Potassium Fixation solution ($CaCl_2$, formol, $CaCO_3$) and then washed in purified water. Then, they were stained with Haemalaun solution (RothT865.1) for 5 min and rinsed in cold water to develop the blue color. Regressive staining was performed using Congo red solution (Fluka 60910, 20 mg/ml was obtained by dissolving 3 g of dye power in 150 ml warm distilled water) for 7 min, rapid washing with purified water and differentiated in 70% ethanol in order to remove the excess dye. The slides were rinsed then with 96% ethanol for 2 min, 100% ethanol for 3 min and propanol for 5 min twice. Finally, 3 drops of Euparal resin (Roth 7356.1) was added to the slices followed by covering the slides with the cover slips for storage. The slides were incubated at 60°C overnight to accelerate hardening.

The samples were examined under a light microscope (Leica DM RXP, Germany) with 100, 200, 400 and 1000- fold magnification in bright field mode.

3.2.4.2. Differential scanning calorimetry (DSC)

The hydrated SC samples (section 3.2.3) were folded and hermetically sealed in 50 µl large volume stainless-steel pans for analysis using a Pyris 1 differential scanning calorimeter (Perkin Elmer, GmbH, Germany) under nitrogen atmosphere. The hermetic seal prevented water vaporization from the tissue at 100°C. An empty pan was used as a reference. The calorimeter was calibrated using indium and purified water. The samples were heated from 10°C to 100°C. A heating rate of 10°C/min was selected. Then the samples were cooled to 0°C and reheated again to 100°C at the same rate of 10°C/min. Between the temperature scans, isothermal steps with durations of 30 s (100°C) or 60 s (0°C) were introduced respectively. The differential scanning calorimetry (DSC) curves were normalized to sample mass (hydrated SC) and the transition temperatures were referred to the peak maxima determined in the heating runs.

3.2.4.3. Transepidermal water loss (TEWL)

Transepidermal water loss (TEWL), as measured with an evaporimeter, was used as a rapid assessment of the integrity of the barrier properties of skin as part of *in-vitro skin* permeation

and penetration studies. The TEWL (g/m^2/h) was measured using a VapoMeter® (Delfin Technologies, Kuopio, Finland). The skin samples were placed on a filter paper moistened with PBS pH 7.4 in a petri dish. The samples were equilibrated for about 30 min at room temperature before measurements in triplicate were performed.

3.2.4.4. Permeation studies

After the TEWL measurements were done, permeability studies were carried out on the epidermal and full-thickness skin samples using Franz diffusion chambers (FDC) which purchased from PermeGear (USA) as illustrated in Figure 3.5. The skin samples were clamped between the donor and receptor sections with the SC facing upwards. The receptor compartment was filled with about 5 ml PBS at pH 7.4. Continuous magnetic stirring was maintained in the receptor compartment and the receptor fluid was thermostated at 32°C. An average effective area for diffusion of 0.64 cm^2 was used. Skin samples were mounted on FDC and allowed to equilibrate for at least 30 min before starting the experiment. 0.5 ml of PBS containing the radiolabeled model drug (5000 - 38000 dpm / 10 µl) was added to the donor chamber which was fully covered with parafilm and aluminium foil.

At predetermined time intervals (0, 1, 2, 4, 6, 8, 12, 22, 26, 30, 36 h), 0.7 ml of sample was taken from the receptor compartment and the same volume of fresh PBS pH 7.4 was replaced to maintain a constant volume.

The samples withdrawn were mixed with 3 ml of scintillation cocktail, Rotiszint® eco plus (Roth Germany) and analyzed by liquid scintillation counting (Tricarb 2100 TR, Perkin Elmer). The steady-state flux was calculated from the slope of the linear portion of the curve according to Fick's first law of diffusion. The permeability coefficient P (cm/s) of the model drugs was calculated at steady state under sink conditions according to equation (1):

$$P = \frac{1}{AC_D}\frac{dQ}{dt} \qquad (1)$$

Where A is the diffusion area of the diffusion cell (0.64 cm^2), C_D the concentration in the donor chamber (dpm/cm^3) and dQ/dt the slope of the linear region of the plot of the cumulative amount of drugs in the receptor chamber versus time (dpm/s). The lag time was obtained by extrapolation of the steady state slope to its intersection with the time axis (Kuntsche et al., 2008).

3.2.5. Correlation between the mass and absorbance for tape stripping in-vitro

The correlation between the mass by balance and the absorbance by infrared densitometry (SquameScan 850) for tape stripping of human abdominal skin and pig ear skin was done.

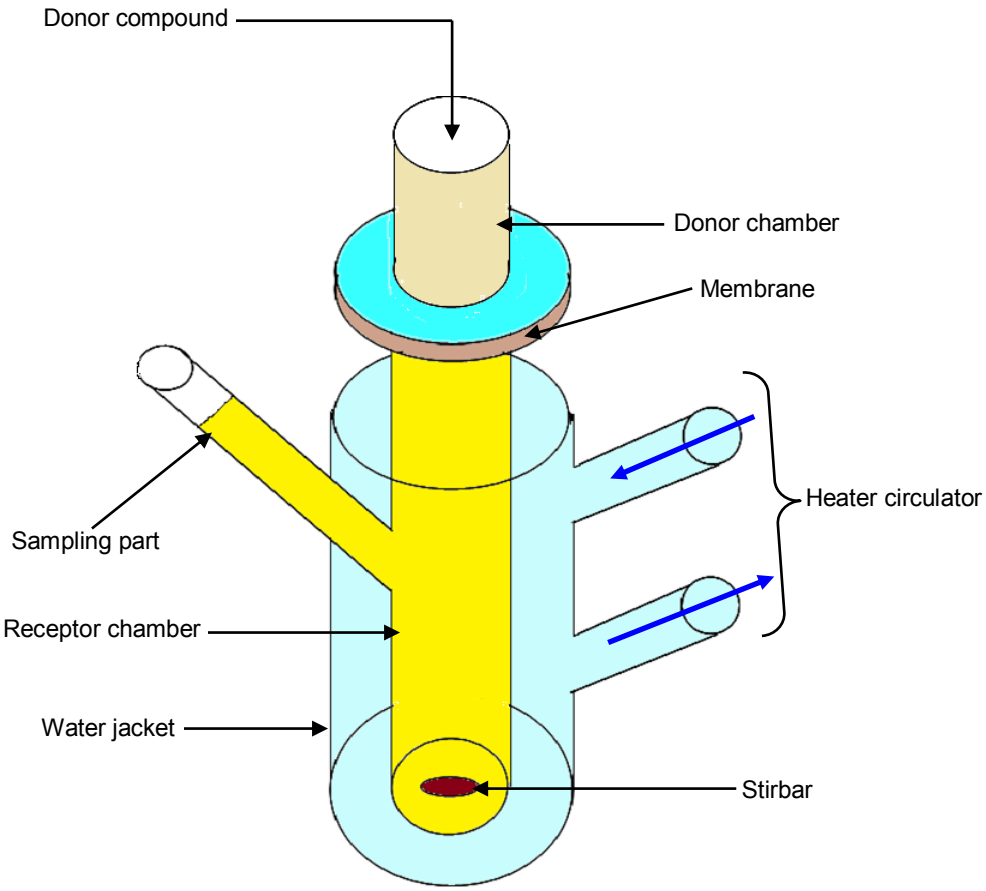

Figure 3.5: The component of Franz diffusion cell.

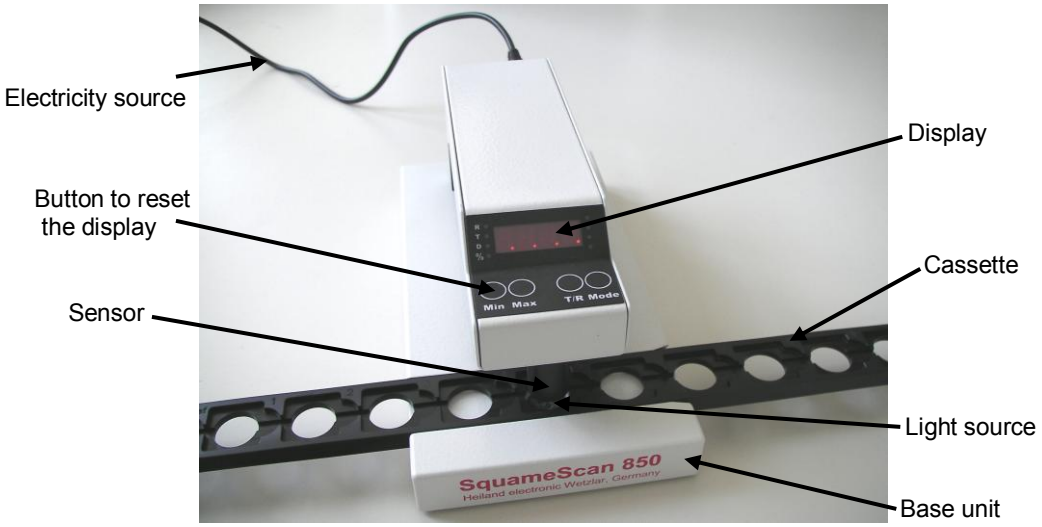

Figure 3.6: The components of the SquameScan.

Infrared densitometry (IR-D) is a new method for quantification of SC by using SquameScan 850A (Heiland electronic GmbH, Wetzlar, Germany). As illustrated in Figure 3.6 the IR-densitometer SquameScan 850A was designed to determine the optical absorption of tape strips and therefore to indirectly determine the SC amount on the tape (Voegeli et al., 2007). The instrument is equipped with a diode emitting light with a peak wavelength of 850 nm, which prevents thermal denaturation of biomolecules.
Immediately before the experiment, the SquameScan device was calibrated by setting the absorption of an empty sample holder to 0% absorption.
The balance and SquameScan determined the mass and absorbance for tape strips respectively before and after stripping. In case of SquameScan measurements, the tape strips were placed adhesive side up into a carrier that took up to 10 tapes with a measured diameter of 15 mm, thus covering more than half of the available disc area.

3.2.5.1. Tape stripping procedure

For tape stripping of human abdominal and pig ear skin, the skin samples were prepared and punched as mentioned above. The tape strips (Cristall Klar Tesa, Beiersdorf AG, Hamburg, Germany) were rolled out and fixed by length onto the template. The tapes were allowed to dry for 1 h before being weighed. In preparation for stripping 20 tapes were weighed by balance and measured by SquameScan for human skin, while 30 tapes were prepared for pig ear skin. One piece of human or pig ear skin was fixed in a metal block (filled with enough cork-plates to form a smooth surface) by 8 small pins and covered by a 15 mm diameter Teflon ring. Then the tape was placed in the middle of the skin, slightly pressed onto the skin and a 2 kg weight was lowered pressuring the skin for 10 s. The tape-strip was quickly removed from the skin surface and the procedure was repeated until the SC was completely removed. The absorbance for the tape strip was measured by SquameScan, and then weighed using a balance. This procedure was repeated with all the samples of human and pig ear skin.
All the data were transferred to a Microsoft Excel spreadsheet and a correlation was made between the weight and the absorbance.

3.2.5.2. Determination of SC thickness

The calculation of the thickness of the SC in case of mass was determined from the weight of the adhesive tapes before and after stripping and calculated according to the following equation (2) (Michel et al., 1992):

$$T = \frac{d}{ap} \quad (2)$$

Where *(T)* represents the thickness of the SC removed (µm), *(d)* is the difference in the strip weight before and after stripping (µg), *(a)* denotes the area of the strip (µm^2) and *p* is the density of the SC (1 X 10^3 µg/1 X 10^9 µm^3).

However, this equation was used to calculate thickness of SC in case of mass only, while in case of absorption by SquameScan the thickness of SC was calculated by the same equation but the difference in weight in this equitation was replaced by the difference in absorption.

3.2.6. Penetration of a radiolabeled solution of corticosterone and mannitol

3.2.6.1. Franz diffusion cell

An investigation into the penetration behavior of radiolabeled corticosterone and mannitol into human abdominal and pig ear skin was done. TEWL measurements of the skin samples were made, and the thickness of the skin samples was determined by micrometer. Then the skin sections were mounted on FDC with a diffusion area of 3.14 cm^2 and a receptor volume of about 14 ml and allowed to equilibrate for at least 30 min before starting the experiment. The epidermal side of the skin was exposed to ambient conditions while the dermal side was in contact with the receptor compartment. 0.5 ml of PBS containing the radiolabeled model drug (15000–40000 dpm/10 µl) was added to the donor chamber. Continuous magnetic stirring was maintained in the receptor compartment as illustrated in Figure 3.5 and the receptor fluid was thermostated at 32°C. Air bubbles were carefully removed from the contact region between the dermal side of the skin and the solution in the receptor compartment. The incubation period for these experiments was 6 h under occluded conditions. The receptor compartment contained PBS pH 7.4 in the case of mannitol and either PBS pH 7.4 containing 1% BSA or PBS pH 7.4 in the case of corticosterone. At predetermined time intervals (0, 1, 2, 3, 4, 5, 6 h), 0.7 ml of sample was taken from the receptor compartment and the same volume of fresh PBS pH 7.4 or PBS pH 7.4 containing 1% BSA was replaced to maintain a constant volume. After 6 h the experiments were stopped and the non-penetrated solutions were removed by wiping the skin 3–4 times with cotton wool pads moistened with PBS pH 7.4. Radioactivity of the used cotton wool pads was determined (skin retained). The donor compartment of the Franz chambers was wiped and analyzed together with the Eppendorf tip used for applying the formulation (Donor).

3.2.6.2. Skin stripping

For determining the drug concentration in the SC layer, the skin was stripped as in section (3.2.5.1) with few exceptions. Firstly, the SC thickness was calculated by using SquameScan device only. Secondly, the absorbance of empty tape stripes was measured by SquameScan before and after stripping and the adhesive side of the tape strips was mixed with glass beads. Thirdly, The tapes strips were collected in vials according the following scheme: vial 1 = strip 1, vial 2 = strips 2–3, vial 3 = strips 4–5, vial 4 = strips 6–8, vial 5 = strips 9–12, vial 6 = strips 13–16, vial 7 = strips 17–20. In the case pig ear skin the same procedure was completed with the addition of vial 8 = strips 21–25 and vial 9 = strips 26–30.

3.2.6.3. Cutting of stripped skin

After tape stripping, the stripped skin was frozen in liquid nitrogen and a 10 mm diameter skin disc was punched out of the stripped area. The skin disc was fixed with a sufficient amount of embedding medium (OCT Tissue-Tek) on a pre-cooled microtome sample holder, which was then transferred into the Cryomicrotome. The temperature in the Cryomicrotome box was -26°C, while the temperature of the object was -15°C.The skin sections were cut parallel to the surface into 25 µm thick layers. The skin sections were collected in vials according the following scheme: vial 1 = incomplete sections, vial 2 = 10 x 25µm, vial 3 = 10 x 25µm, vial 4 = 20 x 25µm, vial 5 = remaining skin. The thickness of incomplete sections and remaining skin was calculated from the total weight of the full thickness sections.

3.2.6.4. Determination the drug concentration

The liquid samples of receptor fluid were mixed with 3 ml of scintillation cocktail. The extraction of radiolabeled drugs from the adhesive tapes and skin sections was carried out after addition of 5 ml of scintillation cocktail. All samples were vortexed for at least 1 min and analyzed by liquid scintillation counting (Tricarb 2100 TR, Perkin Elmer). Blank samples were also prepared and the background was subtracted from the sample readings.

3.2.7. Preparation of vesicle formulations

3.2.7.1. Preparation of vesicles with elastic bilayers containing 1 mM CF

The elastic bilayer vesicles were composed of 10% w/w PC (Lipoid S75) and 1 mM CF in 10 mM Tris buffer pH 7.4. The vesicles were prepared by the conventional rotary evaporation

method (Bangham et al., 1965). Purified SPC (Lipoid S75) was dissolved in 2 ml chloroform in a round bottom flask. The organic solvent was evaporated under pressure (15 min at 400 mbar, 15 min at 300 mbar, 30 min at 100 mbar and 60 min at 50 mbar) at 50°C (Buchi RotaVapor). The lipid film was then flushed with nitrogen gas to remove possible traces of solvent and hydrated with an appropriate amount of Tris buffer pH 7.4 containing 1 mM CF to make a coarse lipid suspension. The obtained MLVs were extruded through polycarbonate membranes with different pore sizes (400, 100 and 50 nm, Armatis, Mannheim, Germany) using an Avestin Liposofast-Miniextruder (Ottawa, Canada). The prepared vesicles were extruded 21 times through each pore size at room temperature (Verma et al., 2003a).

3.2.7.2. Preparation of vesicles with rigid bilayers containing 1 mM CF

The rigid bilayer vesicles were composed of 9% w/w PC (Lipoid S100-3), 1% w/w PG (Lipoid SPG-3) and 1 mM CF in 10 mM Tris buffer. The vesicles were prepared as described in section 3.2.7.1 except that the evaporation was carried out at 60°C. The prepared vesicles were extruded 21 times through each pore size using a water bath (Julabo Labortechnik GMBH Germany) to maintain the temperature at 80°C.

3.2.7.3. Preparation of invasomes containing 1 mM CF

The invasomes vesicles were composed of 13.3% (w/v) SPC in ethanol (75:25 w/w), that is, NAT 8539, corresponding to 10% SPC, 1% w/v of a terpene mixture as the penetration enhancer (PE = citral: cineole: d-limonene 0.45:0.45:0.10 v/v) and 1 mM CF in 10 mM Tris buffer.

The invasomes were prepared at room temperature by dissolving the terpene mixture (PE) in the ethanolic solution of the phospholipid, vortexing the mixture for 5 min followed by sonication to produce a clear transparent solution. Care was taken of the obtained solution to prevent evaporation of the terpene mixture and ethanol. The aqueous phase, which includes 1ml Tris buffer contain 1mM CF was then added with the aid of a syringe under constant vortexing. The vortexing was continued for an additional 5 min. The last step was the extrusion of the obtained MLVs through polycarbonate membranes of different pore sizes (400 nm, 200 nm, 100 nm, 50 nm) using an Avestin hand-extruder. The invasomes were extruded through each polycarbonate membrane 21 times (Badran et al., 2009).

3.2.8. Particle size and zeta potential of liposomal and invasomal dispersions

3.2.8.1. Photon correlation spectroscopy (PCS)

The mean z-average and polydispersity of the different vesicles were determined by photon correlation spectroscopy (PCS) measurements using a Zetasizer Nano (Malvern Instruments, Malvern, UK). For size measurements, 10 µl from each vesicle suspension was mixed with 990 µl purified water (filtered through a 0.2 µl pore size). Each sample was measured four times over 5 min at 25ºC. The polydispersity index (PI) was determined as a measure of the homogeneity of the vesicle suspensions.

3.2.8.2. Zeta potential measurements

For measurements of zeta potential for the different vesicles, 10 µl liposomes or invasomes were diluted with 990 µl of Tris buffer 10 mM pH 7.4 (filtered through a 0.2 µl pore size). The solution was placed in a special cell for measurement of zeta potential and placed in the Zetasizer Nano. The measurements were done at 25°C. Each sample was measured four times and the mean value was calculated.

3.2.9. Stability

The stability of liposomal and invasomal formulations was determined for up to 8 months. For the stability evaluation, vesicles were stored at 4°C. At predetermined time intervals the stability of vesicles was determined by measuring their particle size, PI and Zeta potential using PCS.

3.2.10. In-vitro qualitative penetration studies

3.2.10.1. Dosage regime and incubation time

The dose applied was 10 µl/cm^2 of the skin surface without occlusion. Sufficient light protection was assured during the whole experiment (aluminium foil was used but avoiding occlusion). The skin samples were incubated with the different formulations for 6 h.

3.2.10.2. Fluorescence microscopic studies

The qualitative penetration into human skin of invasomes, liposomes with rigid bilayers and liposomes with elastic bilayers was investigated. The human skin was prepared as described

above. The qualitative penetration experiments were carried out as described in section 3.2.6.1 with some differences. A finite dose (10 µl formulation per cm²) of invasomes, liposomes with rigid or flexible lipid bilayer was added to the donor chamber and the receptor compartment was filled with PBS pH 7.4. The formulations were labeled with CF as a hydrophilic marker. Light protection was assured by covering the FDC loosely with aluminium foil. After incubation for 6 h, the surface of the skin was wiped with cotton wool moistened with PBS to remove any formulation left on the skin surface until the color on the cotton wool had disappeared. The skin samples were taken off the FDC and immediately frozen in liquid nitrogen. From each treated skin sample 2 small samples were punched out with diameter 8 mm. The punching skin samples were embedded in Tissue-Tek and 10 cross sections were cut in the cryomicrotome with a thickness 7 µm from each small skin sample. These cross sections were investigated by light (bright field) and fluorescence microscopy (CF: excitation 470 nm/emission 520 nm; 100-fold magnification, Leica DMRXP, Germany).

PART III

RESULTS AND DISCUSSION

4. Cell culture

4.1. Morphology

The results for the morphology of the different skin models used in this study are illustrated in Figures 4.1 and 4.2 and Table 4.I. The morphology of the ROC models was compared to that of human abdominal skin. The results of this work showed no distinct difference in thickness of the SC and the average thickness of epidermis between the ROC epidermis model and the ROC full-thickness models. The SC thickness of the ROC epidermis model and the ROC full-thickness models was 2-3 fold more than human skin. The average thickness of viable epidermis was nearly half of that in human skin. The thickness of the SC of ROC epidermis and the ROC full-thickness models was nearly the same: 42.50 ± 5.24 µm and 38.33 ± 4.08 µm respectively, while in human epidermis and human full-thickness skin it was 19.2 ± 3.8 µm and 15.33 ± 2.08 µm as illustrated in Figures 4.1 and 4.2 and Table 4.1. As shown in Figure 4.1, ROC epidermis and the ROC full-thickness model were devoid of skin appendages. As compared to ROC epidermis, the rete ridges were observed in case of ROC full-thickness model.

In the case of the ROC full-thickness models (cultivated with or without collagen) the epidermal layers were often separated from the dermis after sample preparation for light microscopy. This separation was observed especially after freezing the ROC full-thickness model without collagen at -80°C for two weeks (Figure 4.1 G-H).

Table 4.1: Thickness of the skin layers for different skin models

Skin type	n	Stratum Corneum (µm)	The average thickness of viable epidermis (µm)	Total thickness (µm)
Human epidermis	6	19.2 ± 3.8	26.7 ± 2.58	45.83 ± 3.76 [a]
ROC epidermis	6	42.50 ± 5.24	11.67 ± 2.58	54.17 ± 5.85 [a]
ROC full-thickness model	6	38.33 ± 4.08	16.67 ± 5.16	518.3 ± 95.17 [b]
Human skin	6	15.33 ± 2.08	30.07 ± 3.21	1150.5 ± 120.22 [b]

a SC + viable epidermis

b SC + viable epidermis + dermis

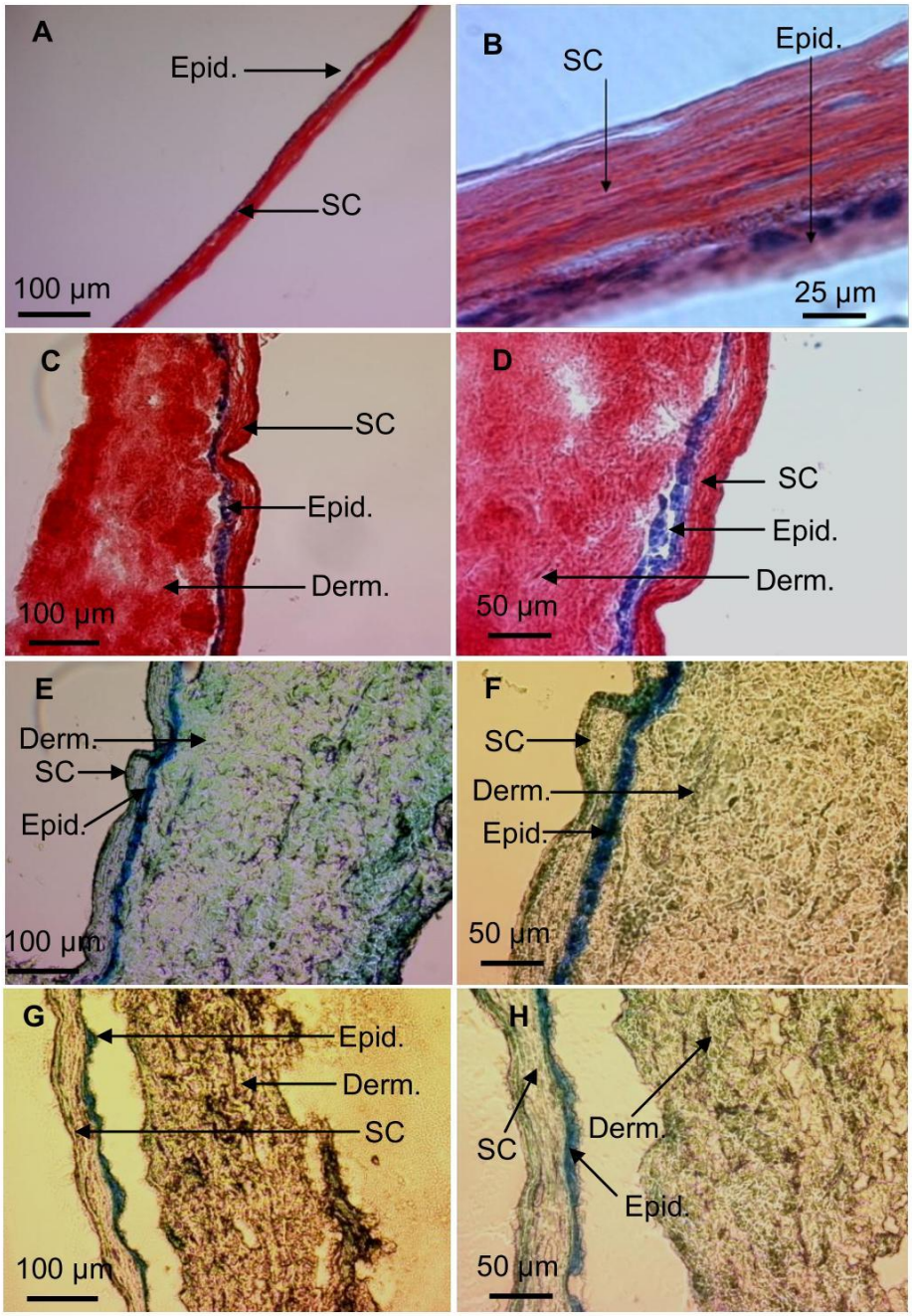

Figure 4.1: ROC epidermis **(A)** and **(B)**. ROC full-thickness model with collagen **(C)** and **(D)**. ROC full-thickness model without collagen **(E)** and **(F).** All of previous models were frozen in cryomicrotome for 10 min**.** ROC full-thickness model without collagen was frozen at -80°C for two weeks **(G)** and **(H),** the epidermis (blue colure) and the dermis (red color). Magnification X100, X200 and X1000.

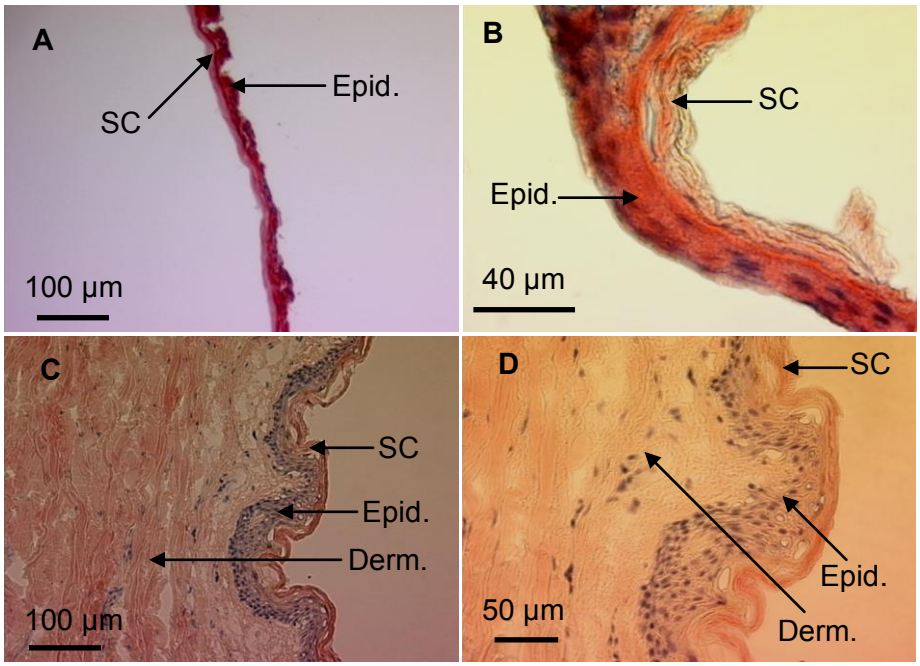

Figure 4.2: A light microscopic image of cross-sections of human epidermis was frozen in cryomicrotome for 10 min **(A)** and **(B).** Human abdominal skin full-thickness was frozen in liquid nitrogen for 2 min **(C)** and **(D),** the epidermis (blue colure) and the dermis (red color). Magnification X100, X200 and X400.

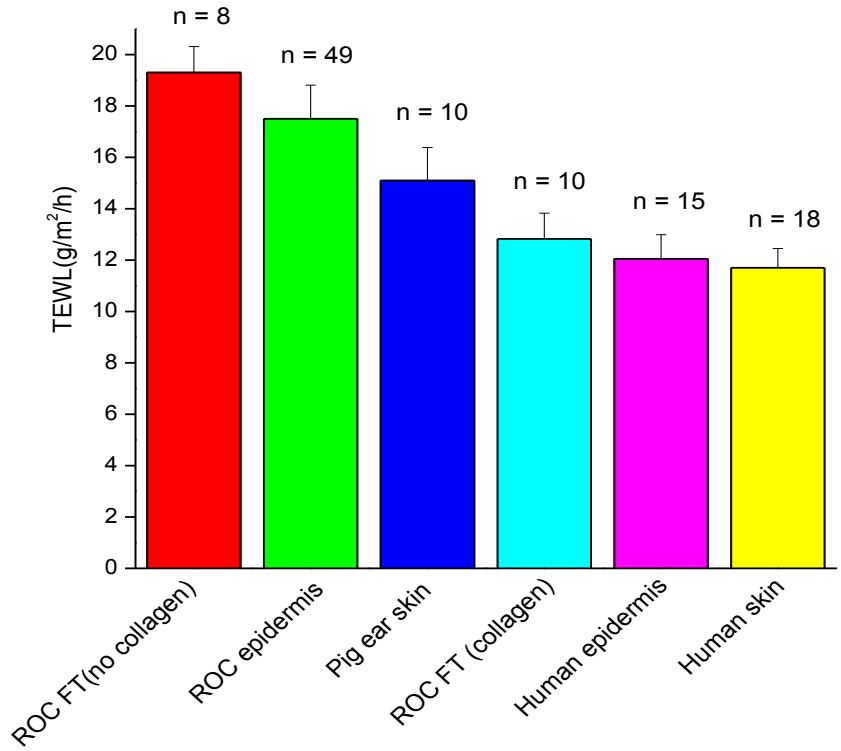

Figure 4.3: TEWL of human abdominal skin, pig ear skin, human epidermis, ROC epidermis, ROC full-thickness (FT) model with and without collagen. The data represent the mean values ± SD from (n = 6–49).

4.2. Transepidermal water loss (TEWL)

Organisation for Economic Co-operation and development (OECD) guidelines 428 request integrity testing for the skin samples before permeation experiments (OECD, 2004b). Also, guidance document 28 (OECD, 2004a) suggests the measurements of TEWL as one of some several methods that are used to evaluate the integrity barrier of the skin samples.whereas an increase in the TEWL values indicates a defect in the barrier properties of the SC (Pinnagoda et al., 1990).

As shown in Table 4.2 and Figure 4.3, the TEWL values were 19.13 ± 1.01 for the ROC full-thickness (FT) model without collagen, 17.50 ± 1.25 for ROC epidermis, 15.09 ± 1.29 for pig ear skin, 12.82 ± 1.01 for ROC full-thickness (FT) model with collagen, 12.05 ± 0.94 for human epidermis and 11.70 ± 0.75 g/m^2 /h for human abdominal skin.

Table 4.2: TEWL for different skin models

Skin type	TEWL (g/m^2/h)
ROC FT model (no collagen) (n = 8)	19.13 ± 1.01
ROC FT model (collagen) (n = 10)	12.82 ± 101
Human skin (n = 18)	11.70 ± 0.75
ROC epidermis (n = 49)	17.50 ± 1.25
Human epidermis (n=15)	12.05 ± 0.94
Pig ear skin (n = 10)	15.09 ± 1.29

4.3. Thermal behavior of stratum corneum lipids

The results of DSC measurements for human, rat and ROC SC are illustrated in Table 4.3 and Figure 4.4. For human SC, the results of first heating showed three phase transitions, T_1, T_2 and T_3, occurred at 36°C, 72°C and 83°C respectively. These phase transitions T_1, T_2 and T_3 were observed in all samples analysed. These results were reported by some workers (Al-Saidan et al., 1998; Bouwstra et al., 1989; Cornwell et al., 1996; Kuntsche et al., 2008). Upon reheating these samples a second time, the results did not detect the first transition T_1 and only one broad transition was shown at 70°C. This new broad transition was related to a combination between phase transitions T_2 and T_3 (Bouwstra et al., 1989). Three phase transition temperatures were observed as the results of the first heating for rat SC T_1, T_2 and T_3 at 35°C, 64°C and 79°C respectively. These results for T_1 and T_3 were in agreement with

the results reported by AL-Saidan et al.(Al-Saidan, 2004; Al-Saidan et al., 1998) But the T_2 result appeared lower than T_2 reported in literature data (Al-Saidan, 2004; Al-Saidan et al., 1998). In some measured samples T_x was detected at 53°C and this result agreed with that detected in literature data (Al-Saidan, 2004; Al-Saidan et al., 1998).

Table 4.3: Phase transition temperatures of SC samples from different skin models

SC type	n	First heating (°C)				Second heating(°C)	
		T_1	T_x	T_2	T_3	T_1	T_2
Human	3	36.3 ± 1.5	-----	72.7 ± 1.5	83.0 ± 1	-----	70.3 ± 0.5
Rat	3	35.0 ± 5.0	-----	64.3 ± 1.2	79.5 ± 2.1	34.0 ± 3.61	51.5 ± 3.5
ROC	5	39.2 ± 3.7	56.8 ± 0.8	64.8 ± 1.1	-----	-----	64.2 ± 1.3

Upon reheating, thermal transition T_1 appeared at nearly the same transition as in the first heating, and T_3 disappeared. These results also agreed with those of Al-Siadan et al.,(Al-Saidan, 2004). In contrast with the results of Al-Sidan et al.,(Al-Saidan, 2004) the T_2 transition shifted from 64°C to 52°C. A similar thermal behavior with three transitions, T_1, T_x and T_2 (39°C, 56°C, and 64°C respectively), was observed from the first heating of the ROC SC. On reheating the ROC SC only theT_2 phase transition temperature was reversible at the same temperature and this result agreed with the results reported in literature (Kuntsche et al., 2008). In some measured samples the transition T_1 was detected at a second heating of 46°C.

4.4. Permeation studies

Permeation studies were carried out on three radiolabeled model solutes with different physicochemical properties (mannitol, corticosterone and tritiated water), under occlusion and with an infinite dose applied. The permeation of mannitol was very slow as seen in Figure 4.5. After 5 hours only 0.01% had permeated the ROC epidermis and human epidermis. As illustrated in Table 4.4 and Figures 4.5 and 4.6, the permeability coefficient of mannitol through human epidermis was higher than for ROC epidermis, while the lag time was nearly the same. However, the lag time is the time required for the penetrant to establish a uniform concentration gradient within the membrane separating the donor from the receptor compartments. The early stage is the nonsteady state. At a later stage, the rate of diffusion is constant, the curve is essentially linear, and the system is at a steady state.

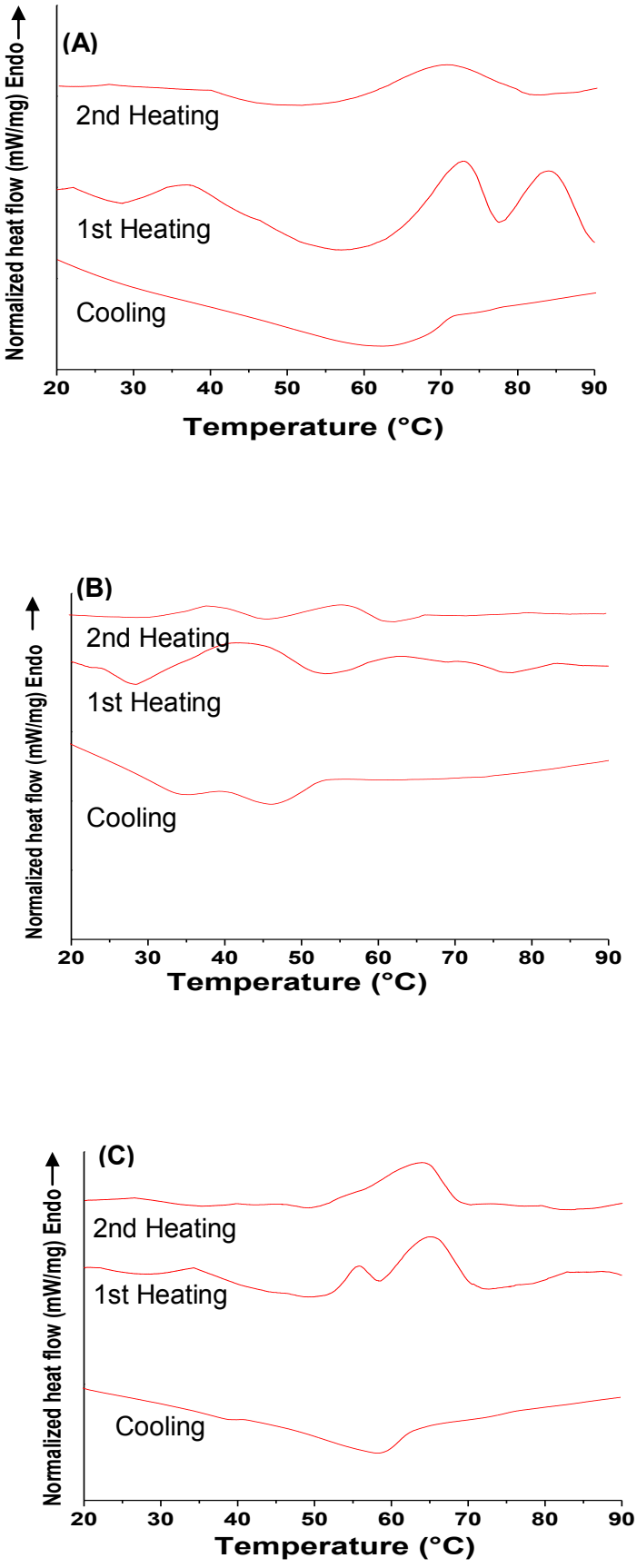

Figure 4.4: DSC heating and cooling curves (10°C/min) for human (A), rat (B) and ROC (C) stratum corneum samples.

When the steady state portion of the line is extrapolated to the time axis, the point of intersection is known as the lag time.

The percentage of mannitol that had permeated through human epidermis was nearly the same as the ROC epidermis during the first 8 hours, but after 8 hours the percentage of permeated mannitol was greater in human epidermis than in ROC epidermis. This difference in the permeation of mannitol increased with time as seen in Figure 4.5. This means that permeation after 35 h was higher than at 30 h, 25 h and 20 h.

In contrast to mannitol, the permeability coefficient of corticosterone through ROC epidermis model was 1.5 fold higher than for human epidermis and the lag time was different for the ROC epidermis model and human epidermis as illustrated in Table 4.4 and Figures 4.7 and 4.8. At the beginning of the permeation (4 h), the permeation of corticosterone through human epidermis and ROC epidermis was nearly the same. However, after that the percentage of permeated corticosterone was greater for ROC epidermis than for human epidermis. The difference in permeation of corticosterone between ROC epidermis and human epidermis increased with the time as seen in Figure 4.7.

As illustrated in Table 4.4 and Figures 4.9 and 4.10 there was no distinct difference in the permeability coefficient and lag time of tritiated water through the ROC epidermis model and human epidermis, while the permeability coefficient of tritiated water through the ROC full-thickness model (without collagen) was higher than for the full-thickness human abdominal skin and the ROC full-thickness model with collagen.

As expected, the percentage of permeated tritiated water through full-thickness human skin and ROC full-thickness with collagen models was less than for human epidermis and the ROC epidermis models as seen in Figure 4.9. These results illustrate the effect of the dermis. With respect to permeability coefficient and the lag time, the ROC full-thickness model with collagen was nearly the same as full-thickness human abdominal skin. These results illustrate the effect of collagen, which increases the permeability barrier.

By comparing the percentage of permeation for different penetrates used in this study, it was observed that the lowest permeation was obtained with mannitol through ROC epidermis and human epidermis. On the other hand, the highest permeation was observed with tritiated water through the ROC epidermis. The permeation of tritiated water through human epidermis was higher than corticosterone, while in the case of ROC epidermis the permeation of tritiated water was slightly higher than corticosterone, as seen in Table 4.4. The permeation of tritiated water through human epidermis and ROC epidermis were nearly the same. Also, the results of this work showed no distinct difference between the permeation of tritiated water through full-thickness human skin and ROC full-thickness model with collagen, as showed in Figure 4.9 and Table 4.4.

Table 4.4: Permeability coefficients of different models substance through different skin models

Skin type		Mannitol			Corticosterone			Tritiated water		
		n	P X 10^{-7} (cm/s)	T_L (h)	n	P X 10^{-7} (cm/s)	T_L (h)	n	P X 10^{-7} (cm/s)	T_L (h)
Human	Full-thickness	----	----	----	----	----	----	6	1.59 ± 0.18	2.05 ± 0.23
	Epidermis	6	0.18 ± 0.12	13.79 ± 0.30	12	1.04 ± 0.74	11.57 ± 0.43	6	2.43 ± 0.22	2.08 ± 0.15
ROC	Epidermis	13	0.025 ± 0.01	12.07 ± 0.24	16	2.24 ± 1.75	3.40 ± 0.54	20	2.84 ± 0.78	2.14 ± 0.23
	Full-thickness with collagen	----	----	----	----	----	----	7	1.46 ± 0.26	2.54 ± 0.77
	Full-thickness without collagen	----	----	----	----	----	----	8	25.6 ± 9.1	1.37 ± 0.22

n: Number of samples

P: Permeability coefficient

T_L: Lag time

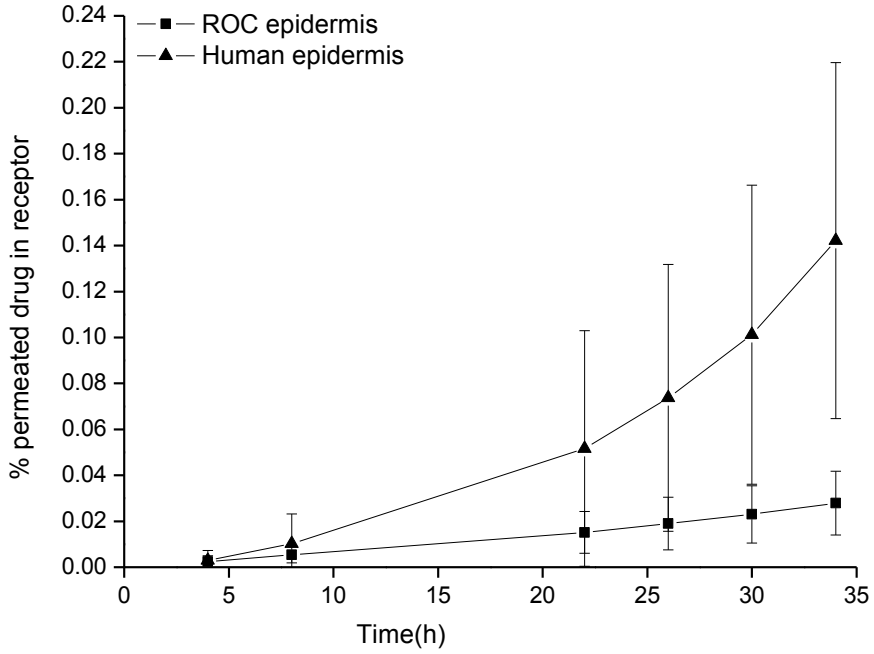

Figure 4.5: Permeation curves of mannitol through human epidermis and ROC epidermis. The data represent the mean values ± SD from (n = 6–13).

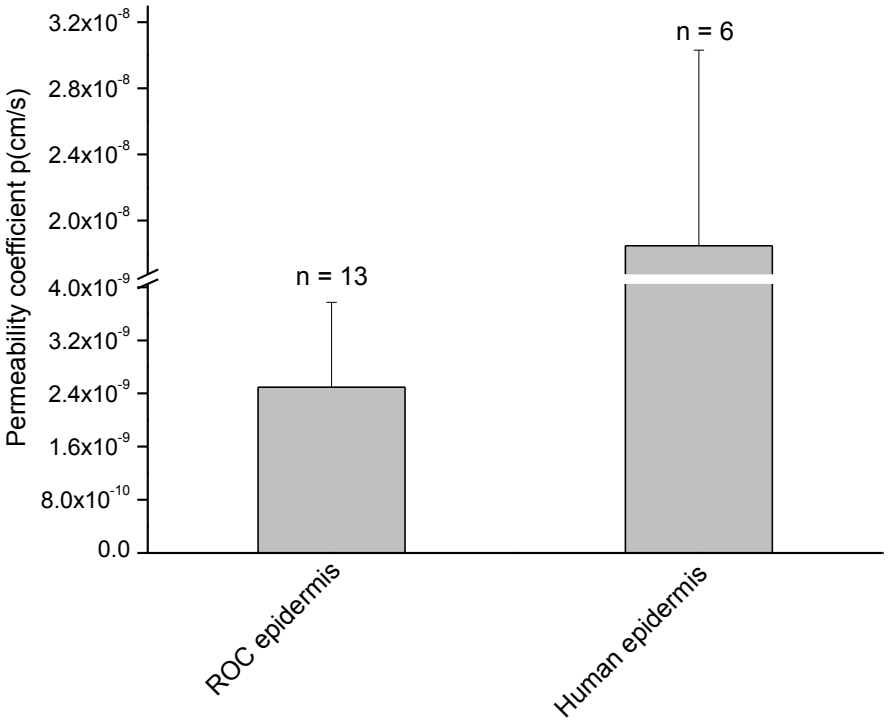

Figure 4.6: Permeability coefficients of mannitol through human epidermis and ROC epidermis. The data represent the mean values ± SD from (n = 6–13).

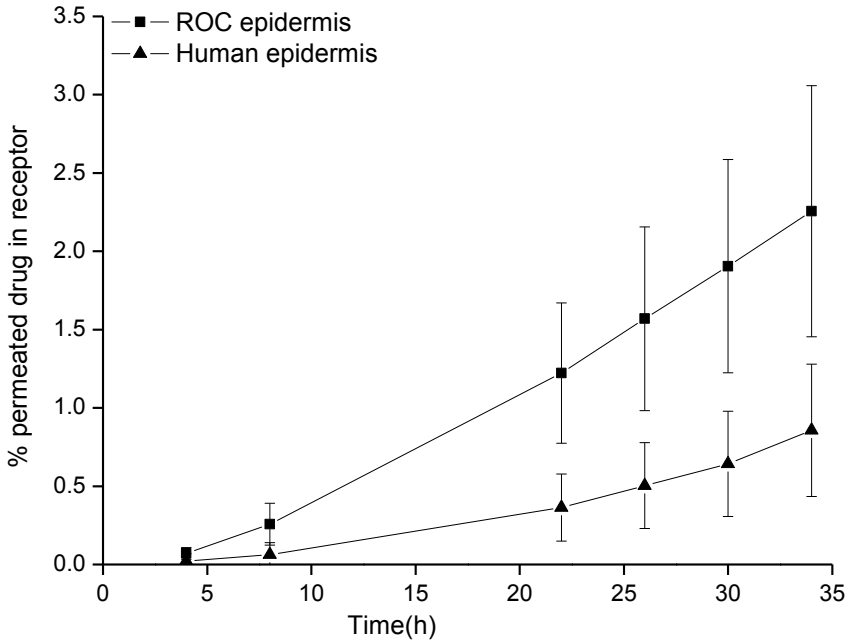

Figure 4.7: Permeation curves of corticosterone through human epidermis and ROC epidermis. The data represent the mean values ± SD from (n = 12–16).

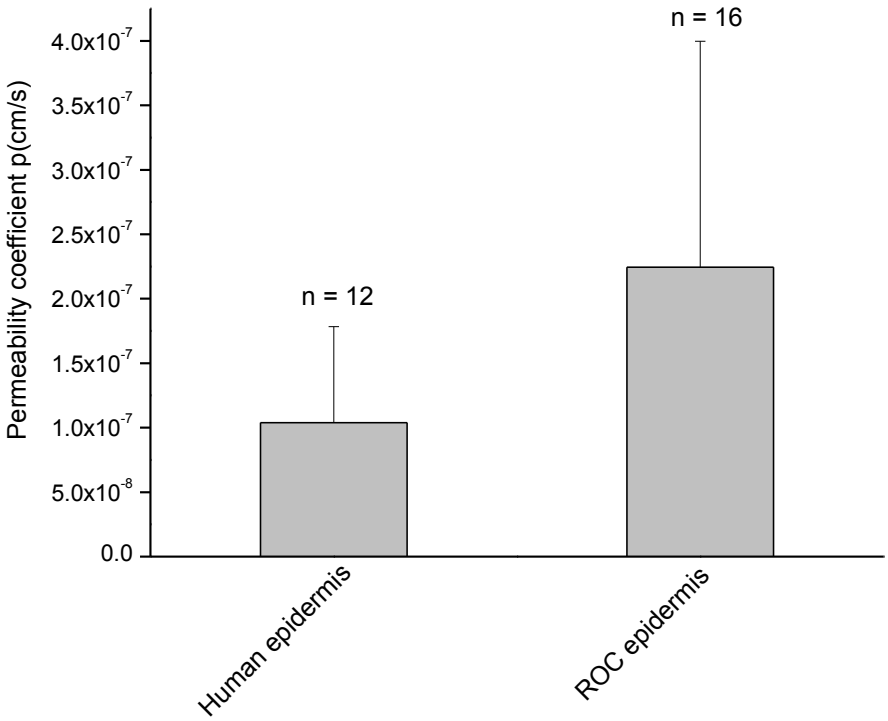

Figure 4.8: Permeability coefficient of corticosterone through human epidermis and ROC epidermis. The data represent the mean values ± SD from (n = 12–16).

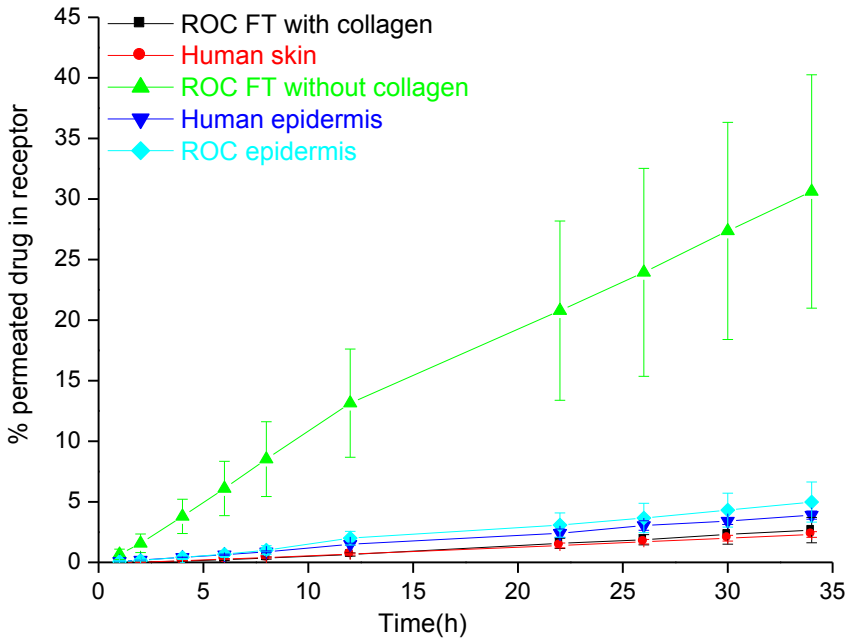

Figure 4.9: Permeation curves of tritiated water through human epidermis, ROC epidermis, full-thickness human skin and ROC full-thickness model with and without collagen. The data represent the mean values ± SD from (n = 6–22).

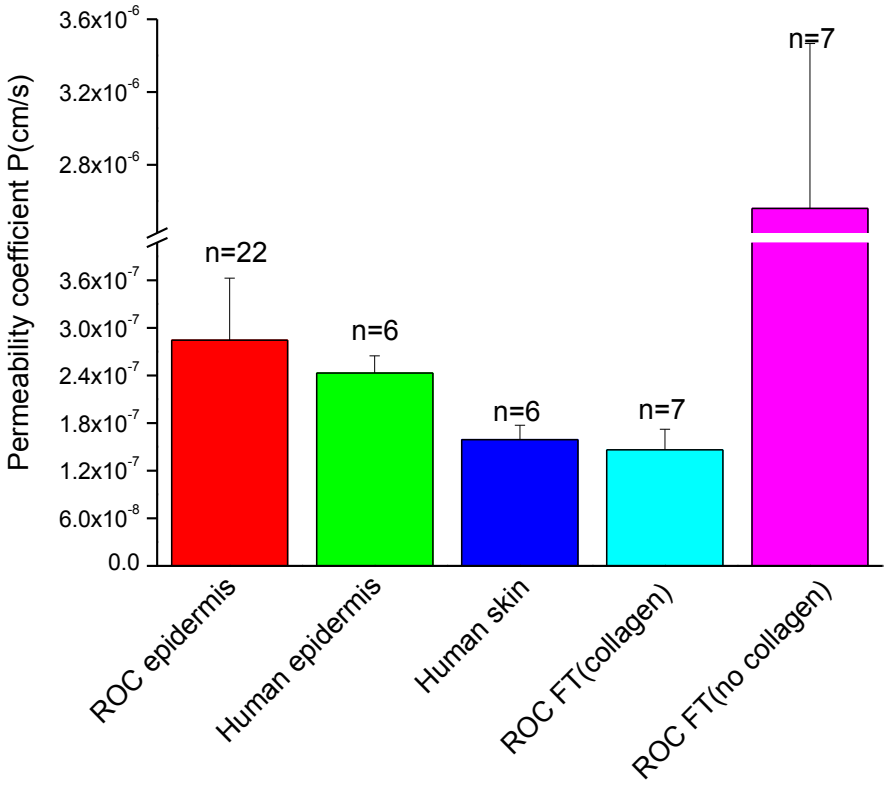

Figure 4.10: Permeability coefficient of tritiated water through human epidermis, ROC epidermis, full-thickness human skin and ROC full-thickness model with and without collagen. The data represent the mean values ± SD from (n = 6–22).

4.5. Discussion

4.5.1. Morphology

In the present study we explored the development and evaluation of ROC cultured skin models as alternatives for human skin. Thus, ROC models including the ROC epidermal model and the ROC full-thickness models (with and without collagen) were compared with human skin models. This work was interesting in that it improved the morphology of the ROC epidermal model by seeding REK cells onto dead human de-epidermized dermis (DED) to mimic full-thickness human skin. However the importance of the dermis for human skin was illustrated previously in section 2.3.2. Recently, there have been several types of dermal equivalents developed *in-vitro* to resemble dermis *in-vivo*. The dermal substrates which are used for the production of reconstructed epidermis may be acellular like DED or a cellular like fibroblast-populated collagen matrix (Ponec et al., 1997).

In order to replace human skin with these models for *in-vitro* study, they should be as close as possible to human skin in morphology, in thermal behavior of lipids in the SC and in permeability barrier.

In this thesis work, the REK cell line, originally isolated by Baden and Kubilus (1983) (Baden and Kubilus, 1983), was used for developing an organotypic keratinocyte culture. REK cells were grown at the air liquid interface for 3 weeks on type I collagen gel or on human DED to produce the ROC epidermis model or the ROC full-thickness model respectively. The DED was selected because it is sterilized acellular connective tissue and retains the intact basement membrane which is important for the adherence of the epidermis to the dermis and for the differentiation of keratinocytes (Smola et al., 1998).

Generally, the overall ultrastructural appearance of the cultured epidermis in the skin models was very similar to that of native tissue. All layers of epidermis were present such as the stratum basale, stratum spinosum, stratum granulosum and SC (Pasonen-Seppanen et al., 2001a). It was found that the ROC cultures supplemented with vitamin C showed better ultrastructural organization of SC lipids. Additionally, the presence of vitamin C in the feeding medium was improved epidermal morphology by contributing to keratinocyte differentiation. Also it improved the organization of intercellular lipid lamella and increased the amount of ceramides 4- to 7-fold by facilitating their hydroxylation reaction. Consequently, it enhanced epidermal barrier function (Ponec et al., 1997).

The results of this work for the morphology of ROC models (epidermis and full-thickness) for the thickness of SC were in agreement with the results of other skin models (Ponec et al., 2002; Ponec et al., 2000). However, the thickness of the SC was 2-3 fold greater than human SC in the ROC models (epidermis and full-thickness) because there was no desquamation

(Vicanova et al., 1996) of the ROC models. The average thickness of the viable epidermis was nearly one fold less than in human skin experiments. When the thickness of SC and epidermis of the ROC models with other reconstructed human skin models was compared, it was noted that the thickness of SC for the ROC models was in agreement with some reconstructed human skin models, while the thickness of the epidermis was always lower than in all reconstructed human skin models (Ponec et al., 2002).

Although there is no difference in the thickness of SC and viable epidermis between the ROC epidermis and the ROC full-thickness model, the ROC full-thickness model had rete ridges because REK cells were seeded on the DED, which had ridges (Lee et al., 2000).

The dermis in human skin was thicker than that of the ROC full-thickness model. This difference was due to removal of some dermal layers during preparation of DED. In addition, it was found that, like the other reconstructed human skin models, ROC epidermis and the ROC full-thickness model were free of skin appendages unlike human skin because ROC epidermis was grown on flat polycarbonate membrane (Rosdy and Clauss, 1990) and the ROC full-thickness model was grow on dead DED. The results of this work for ROC epidermis were in agreement with the results reported in the literature (Suhonen et al., 2003).

As shown in this thesis results for the ROC full-thickness model, after freezing at -80°C the epidermis was often separated from the dermis. Although this separation mostly appeared in the ROC full-thickness model without collagen, sometimes it occurred in the ROC full-thickness model with collagen. This separation may be due to the absence of a fully developed basement membrane (Ponec et al., 2000).

As compared to the ROC full-thickness model, the histology of reconstructed human epidermis on the DED after 28 days was well stratified with basal cells attached to the dermal-epidermal junction and a thick and compact multilayered SC (Regnier et al., 1993). Therefore, the organization of epidermis reconstructed in-vitro on DED at the air liquid interface shows an excellent morphological equivalence to in-vivo skin (El Ghalbzouri et al., 2002). Consequently, there is no separation of the epidermal layers from the underlying dermis as had happened in the ROC full-thickness model.

To avoid separation of the epidermis from the underlying dermis for the ROC full-thickness model and improve the thickness of its epidermis in future studies, the dermal support may be improved by cultivating human dermal fibroblasts or rat dermal fibroblasts to facilitate the adhesion and improve the differentiation of the REK cells.

It has been reported that the presence of fibroblasts in the dermal substrate was very important for establishment of suitable epidermal differentiation. Additionally, increasing the fibroblast numbers improved the tissue architecture of the viable epidermis while the absence of fibroblasts led to defects in the some layers of the viable epidermis. In the presence of fibroblasts, the stimulation of keratinocytes was dependent on the number of

fibroblasts incorporated into the DED and on the culture time. The combination of a fibroblast populated collagen matrix and DED in the dermal substrate led to improved epidermal differentiation of human keratinocytes and dermis substrate that closely resembled human dermis in-vivo (El Ghalbzouri et al., 2002).

4.5.2. TEWL measurements

TEWL is a measurement of the water vapor pressure gradient between the skin surface and the ambient air expressed in grams per square meter per hour. The TEWL values will vary with anatomical location and this is due to the variation in corneocyte size at different anatomical sites (Hadgraft and Lane, 2009). The barrier properties are reduced in cases of skin diseases or in chemically or physically damaged skin in which the TEWL value is increased relative to the degree of impairment (Welzel et al., 1996). The TEWL measurement is relatively insensitive for minor damage of the SC and this damage will lead to increased permeation of substances (Netzlaff et al., 2006). Although the SC works as a strong barrier for the skin, the rate of water evaporation from the underlying tissue and sweat glands to the outer environment is constant. There are some factors which affect the rate of water evaporation to the outside environment such as; low temperatures, decrease of air across the skin and high humidity. Also, under these conditions the rate of water evaporation is continuous through SC but this rate is decreased compared to normal conditions (Machadoa et al., 2010). As illustrated in the results of this work, the TEWL values were arranged in the following decreasing order: ROC full-thickness model without collagen, ROC epidermis model, pig ear skin, ROC full-thickness model with collagen, human epidermis and full-thickness human abdominal skin. The results of this study indicated that there was no distinct difference between the ROC full-thickness without collagen and the ROC epidermis models, but these TEWL results were higher compared to other models that were used in this study. These results indicate that the barrier properties for all these models were retained during sample preparation. From these results it could be observed that there was no distinct difference between human epidermis, full-thickness human skin and the ROC full-thickness model with collagen. A comparison between the TEWL measurements of the ROC full-thickness model with and without collagen indicates that collagen was necessary for increasing the barrier properties. The results of TEWL for the ROC epidermis model were in agreement with the results of Pasonen et al., (Pasonen-Seppanen et al., 2001a). Also the TEWL results for human epidermis agreed with those of J. Kuntsche et al., (Kuntsche et al., 2008), but were slightly higher for ROC epidermis. In this study the TEWL results for full-thickness human abdominal skin agreed with Marta's et al., (Machadoa et al., 2010), although his data was measured *in-vivo*. The TEWL results for pig ear skin were higher

compared to full-thickness human abdominal skin and also higher compared to other studies (Simonsen and Fullerton, 2007). The slightly higher TEWL values for pig ear skin compared to full-thickness human abdominal skin may be related to the larger diameter of hair follicles in pig ear skin and also the greater abundance of hairs (Jacobi et al., 2007).

4.5.3. DSC measurements

Thermal changes in the SC can provide information on structural alterations within the sample. This information may help us to understand the nature of the skin barrier. The thermal behavior of the hydrated SC was investigated by DSC. Although I did not study the morphology, TEWL and the permeability coefficient of rat skin, I measured the thermal behavior of the rat SC to make a comparison between rat cells that were used for preparation of the ROC models and the original rat skin. It has been reported that human and rat keratinocytes are different and have different permeation barriers. Although the ROC model is weaker than human skin, it is considerably less permeable (i.e. stronger barrier) than rat skin (van Ravenzwaay and Leibold, 2004).

According to the DSC measurements of the different skin models, I observed three endothermic transitions related to lipids in human and rat SC. The major phase transitions related to SC lipids are at T_1= 35–39°C, T_2 = 64–72°C and T_3 = 79–83°C for human and rat skin models. In the ROC epidermis model three phase transitions appeared, T_1, T_x and T_2, with T_x occurring at 56°C. Upon reheating, the phase transition T_1 was detected in the rat skin model. T_1 and T_x were irreversible for ROC and human skin. The transitions T_2 and T_3 coalesced into a single endotherm in all skin samples. The main reason for the absence of transition T_1 for human skin was its reduced peak size upon reheating (Cornwell et al., 1996). The absence of T_1 for the ROC model may reflect the differently distributed lipid domains during keratinocyte differentiation (Bouwstra et al., 1992) or the absence of sebaceous lipids that were found on the surface of the SC (Cornwell et al., 1996).

Fourier Transformations-IR- Spectroscopy (FTIR) measurements indicate that T_1 is related to the solid to fluid transition of subsidiary SC lipids (Gay et al., 1994). Wide angle x-ray diffraction (WAXD) measurements on human skin indicate that T_1 is related to the arrangement of lipid alkyl chains from orthorhombic lipid packing to hexagonal form (Bouwstra et al., 1992).

The phase transition, T_x, detected at 53–56°C, has been related to structural changes in covalently bound lipids present on the outside of the corneocytes envelope proteins. However, this transition remained after lipid extraction, indicating that this transition arises from a protein or protein bound component of the SC. According to FTIR, this phase

transition is related to the loss of the crystalline, orthorhombic lattice structure of covalently bound lipids (Cornwell et al., 1996).

The transition T_x in this study was detected in some samples but not in all. The main reason for this result was related to the hydration of samples as it has been reported that there is an inverse relationship between the hydration level and the size of the peak for T_x transition (Cornwell et al., 1996).

It has been reported that small angle x-ray diffraction (SAXD) measurements have shown that T_2 phase transition is related to disordering of a lamellar lipid phase (Bouwstra et al., 1991). Additionally, FTIR and WAXD measurements have supported that the T_2 phase transition is due to transformation of SC lipids from a gel to a liquid crystalline phase (Bouwstra et al., 1992; Cornwell et al., 1996). In this study, the T_2 phase transition occurred for the human skin model at 72°C, higher than for rat and ROC membrane (64°C), the latter of which contained similar amounts of cholesterol, ceramide and free fatty acid. Although the total amounts of ceramides in human skin and ROC were similar, previous results using TLC measurements have shown there is a clear difference in the proportions of ceramide subclasses between human skin and ROC. Ceramides 9, 3 and 7 were not found in ROC. ROC contained ceramide 2 more than human skin. Also, the content of free ceramide 1 was higher in ROC, while the content of ceramides covalently bound to proteins was lower in ROC than in human skin (Pappinen et al., 2008). In addition, mass-spectrometric analysis of the total lipid extract has indicated a lower level of bound ceramide 1 to linoleic acid in ω-hydroxyceramides for the ROC compared to that found in human skin (Pappinen et al., 2008). As a result of these previous studies, the higher T_2 and T_3 transition in human skin indicates that human lipid molecules are more highly ordered and more closely packed than those of the rat and ROC skin models. Consequently, this illustrates the human skin has a greater barrier compared to the rat and ROC skin models.

Previous FTIR and WAXD measurements have illustrated that the T_3 phase transition has been related to transformation from a gel to a liquid crystalline phase of the associated lipids covalently linked to the cornified envelope (Cornwell et al., 1996). Some studies have reported that the polar lipids alone have melted at temperatures similar to T_2 and polar lipids and cholesterol have melted at temperatures similar to phase transition T_3. These results illustrate that at both T_2 and T_3 phase transitions, the lipid lamella is converted from a gel to a liquid state and also indicate which lipids would melt in the T_2 and T_3 phase transition (Cornwell et al., 1996). From the results of this work for the rat skin and ROC skin models, it was shown that theT_3 phase transition was detected in the rat skin model at around 80°C, but not detected in the ROC model. This result may be related to both ceramides 3 and 7 which were deficient in the ROC but detected in rat keratinocytes (Wertz et al., 1984). Thus the ROC model is different from the original rat skin model in its composition of SC lipids.

4.5.4. Permeation studies

It was reported earlier that the permeation of reconstructed human epidermis models was higher compared to human skin, which probably reflects abnormalities in the SC lipid profile (Ponec, 1991; Vicanova et al., 1996) as well as in the intercellular organization of the lamellar body contents (Boyce and Williams, 1993; Fartasch and Ponec, 1994), which are the main determinants of the permeability barrier (Elias, 2004). Therefore, the addition of dermal substrate to these models led to improvement in their barrier properties and improvement in the differentiation of epidermal cells, which comprise only a few cell layers. In addition, the full-thickness models provide the possibility of evaluating drug penetration into different skin layers that resemble full-thickness human skin *in-vivo*, which enables the study of dermal-epidermal interaction (Netzaff et al., 2005).

The permeation experiments in this study were done under occlusive and hydration conditions. It was reported that occlusion and hydration increase the permeability of most molecules into the skin. The hydration of SC influences the permeation rate because the hydration allows water to open up the dense structure of the SC, thereby altering the barrier function of the SC. Additionally, the occlusion of the skin surface leads to the entrapment of water, thus leading to an increase in skin hydration, particularly within the SC. As a consequent, swelling of corneocytes takes place, so that the intercellular spaces become distended and the lacunae dilated. Thus, the distention of lacunae creates pores in the SC through which polar and non-polar substances can penetrate (Williams and Barry, 2004).

Human epidermis and full-thickness human skin were hydrated overnight prior to use in the permeation experiments to ensure that the water content of the tissue would be comparable to that of the ROC epidermis model and ROC full-thickness models (i.e., which is maintained in constant contact with the culture medium, and therefore, is considered to be fully hydrated).

The permeation results of tritiated water in this study through the ROC models (epidermis and full-thickness with collagen) resembled human epidermis and full-thickness human abdominal skin. In this permeation study, tritiated water was selected as the radiolabeled marker because water is a suitable indicator for the integrity of the epidermis and one of the main functions of skin is the provision of a barrier to excess water. Thus, the ability of reconstructed epidermis to retard water penetration is an essential test for its functionality (Regnier et al., 1993).

In this thesis discussion of the results of the permeation experiments, the comparison between permeation results and the results of TEWL was done. Because the TEWL measurement provides first information about the barrier properties of the skin, an increase in the TEWL value indicates a defect in the barrier properties of the SC (Pinnagoda et al., 1990).

In contrast to the results of TEWL measurements, the permeability coefficient of mannitol through human epidermis was higher than for the ROC epidermis model. These results may be due to that the presence of hair follicles in human epidermis (Lademann et al., 2008), while ROC epidermis lacks hair follicles that may provide an additional route of permeation (Rosdy and Clauss, 1990). The lag time of 13 h was nearly the same for ROC and human epidermis. This result indicates the beginning of the steady state for the permeation of mannitol through both membranes. These results indicated that the barrier properties of these models for the permeation of mannitol were strong before this time. The increasing permeation percentage at 35 h was related to the occlusion effect, which increased with time (Zhai and Maibach, 2002).

In agreement with the results of the TEWL measurements, the permeability coefficient of corticosterone through the ROC epidermis model was slightly higher than for human epidermis. These results were due to the penetration of corticosterone which occurred via intercellular lipids in the SC; however, human lipid molecules are more highly ordered and more closely packed than those of the ROC skin models (Pappinen et al., 2008).

The lag time, detected at 3 h and 12 h, was different for ROC and human epidermis. These results indicate that the beginning of the steady state for the permeation of corticosterone through ROC epidermis was started before that of human epidermis. This means the barrier properties of corticosterone through these models was strong before this time. By comparing the results of lag time between ROC and human epidermis, it was observed that the human epidermis barrier was greater than the ROC epidermis barrier and this may be related to the highly ordered domains of human SC lipid compared with ROC epidermis (Pappinen et al., 2008). This difference in the lag time of corticosterone between human epidermis and ROC epidermis was not observed with mannitol and this may be due to corticosterone being a lipophilic drug which penetrates the skin through these lipid molecules while mannitol is a hydrophilic drug which penetrates the skin through the skin appendages (Lademann et al., 2008). The increase of the permeation percentage by time was related to the occlusion effect.

In agreement with the results of TEWL measurements, the permeability coefficient of tritiated water through the ROC full-thickness model without collagen was more permeable than for the other models. It was noted that the permeability coefficients of tritiated water through the ROC full-thickness model without collagen were higher than for the ROC full-thickness model with collagen. This difference in permeability coefficient could be attributed to the presence of collagen, which increases the barrier properties of this model by providing normal REK cells adhesion and differentiation.

The results of this work for the permeability coefficient of tritiated water through the ROC epidermis model and human epidermis indicated no distinct difference between the two models. The results reported in this study for the permeability coefficients of tritiated water

through human epidermis were in agreement with the results reported in the literature (Lawrence, 1997). The results of permeability coefficients for tritiated water through the ROC full-thickness model with collagen were similar to the results for full-thickness human abdominal skin. In this study, the results of permeability coefficients of titrated water through full-thickness human abdominal skin were in agreement with the results reported in the literature (Lawrence, 1997). The previous results were due to the water permeating through both hydrophilic and lipophilic pathways (Tezel et al., 2002).

The lag time for permeation of tritiated water was nearly the same for all models. This result indicates that the beginning of the steady state for the permeation of tritiated water through these models was almost the same time, except for the ROC full-thickness model without collagen. This means that the barrier properties of these models for the permeation of tritiated water are the same with the exception of the ROC full-thickness model without collagen.

By comparing the permeation of tritiated water through the ROC and human epidermis models with the full-thickness model of ROC with collagen and human skin, it was found that permeation through the epidermis models was 0.5 fold higher than for the full-thickness models. These results may be related to the presence of dermis which acts as an additional barrier (Netzaff et al., 2005).

By comparing the permeation of tritiated water with mannitol and corticosterone through human epidermis and ROC epidermis, it was found that the permeation of tritiated water was greater than corticosterone and mannitol. These results may be due to the molecular weight of water which is lower than corticosterone and mannitol, and it has been reported that the water permeated through both hydrophilic and lipophilic pathways in the SC (Tezel et al., 2002).

From these results it could be observed that there was no difference between the ROC full-thickness model with collagen and full-thickness human abdominal skin.

4.5.5. Conclusions

This study investigated the development and evaluation of ROC cultured skin models as alternatives for human skin. In this study a comparison between the ROC models and the human skin model was done. By comparing the general morphology of the ROC epidermis model with the ROC full-thickness models there was no distinct difference between the thicknesses of SC and epidermis. But in the case of the ROC full-thickness models, the epidermis often separated from the dermis and this was clear especially after freezing at -80°C for two weeks. However, the ROC models were different in morphology to human skin; the SC was 2–3 fold thicker than for human skin and the epidermis was thinner. In addition,

the ROC models were devoid of skin appendages. This was illustrated by the higher permeability coefficient of mannitol through human epidermis than through the ROC epidermis model. Thermal behavior of the ROC differed from that in human skin and rat skin indicating some structural differences in the lamellar lipid arrangement and a lower amount of covalently bound ceramides. The testing of the permeability barrier of the ROC full-thickness models, with and without collagen, compared to full-thickness human abdominal skin found that the ROC full-thickness model with collagen was similar to full-thickness human skin in TEWL measurements and in the permeability coefficient of tritiated water, while the ROC full-thickness model without collagen showed a higher TEWL measurement and permeability coefficient of tritiated water than the full-thickness human abdominal skin. These results illustrate the effect of collagen on the permeability barrier.

From the results of TEWL measurements for ROC full-thickness model with collagen and permeation studies of tritiated water through ROC models (epidermis and full-thickness with collagen), it could be concluded that these ROC models were nearly the same as human epidermis and human full-thickness skin. Thus, the ROC epidermis and the ROC full-thickness models with collagen appear promising as *in-vitro* alternative models for human epidermis and human full-thickness skin.

5. Evaluation of tape stripping and penetration of model drugs

5.1. Correlation between mass and absorbance for human skin in-vivo

In-vivo experiments performed on the SC of the right and left arm of a human showed good correlation between cumulative mass (µg) measured by a balance and the cumulative absorbance determined using infrared densitometry (IR-D) by SquameScan (Figure 5.1). On application of the linear equation that was constructed from this correlation, the thickness of the SC in all three samples was found to be about 8 µm. Additionally, by applying it to the absorption results that were obtained from SquameScan, the results were nearly the same as those obtained using the balance method. The calculated thickness of SC in the case of mass only was obtained by using the equation in section 3.2.5.2**.** Similarly, the thickness of SC was calculated using the same equation in section 3.2.5.2 but the difference of absorption by SquameScan was used instead of the difference of mass. The thickness of the SC was in agreement with the literature (Jacobi et al., 2007).

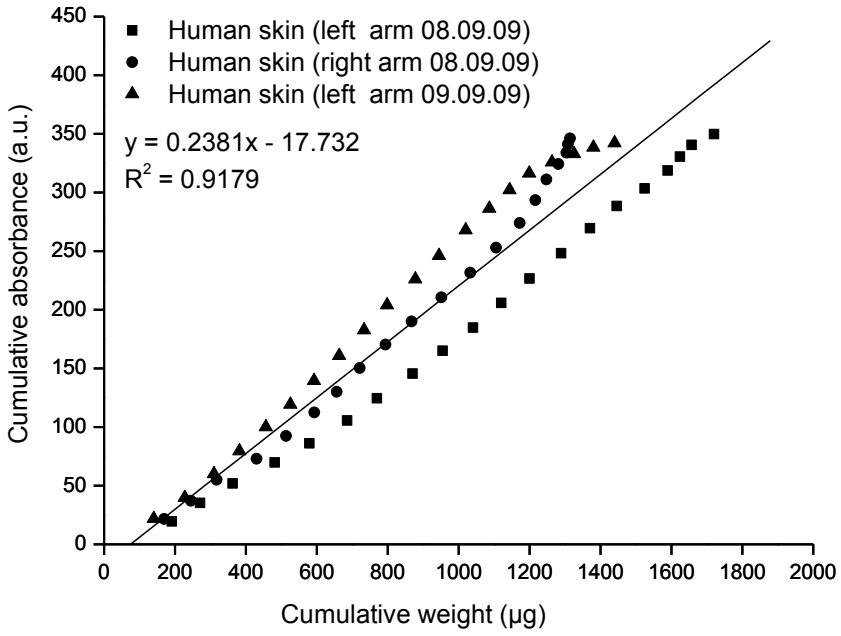

Figure 5.1: Correlation between cumulative weight and cumulative absorbance of tape stripping of human right and left forearm SC in-vivo where n = 3.

5.2. Correlation between mass and absorbance for human skin in-vitro

Figure 5.2 shows a good correlation between the cumulative weight (µg) and cumulative absorbance of tape stripping for human abdominal skin *in-vitro*. On application of the linear equation that constructed in Figure 5.2 to calculate the thickness of SC by absorption, the results were around 5 µm and nearly the same as to the thickness of SC calculated by mass only. By applying this equation to calculate the thickness of SC in the penetration experiments, however the absorption by SquameScan was used only; the results were in agreement with the results that were obtained by normal tape stripping prior to penetration experiments. In these experiments of tape stripping, skin samples from two different donors were used and all parameters of the tape stripping process were fixed.
The two linear equations obtained from the correlation between cumulative weight and cumulative absorbance in Figures 5.1 and 5.2 were nearly the same.

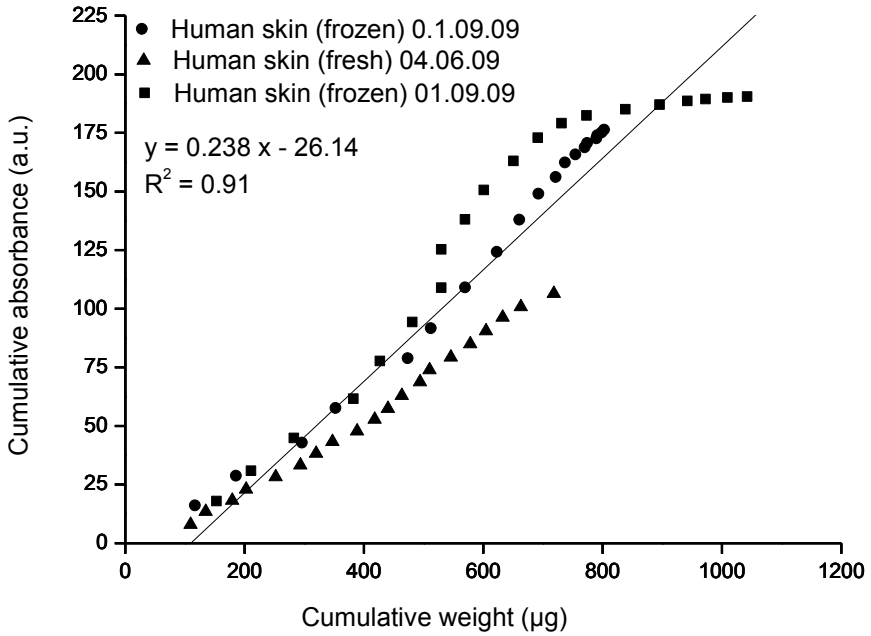

Figure 5.2: Correlation between cumulative weight and cumulative absorbance of tape stripping of human abdominal SC in-vitro where n = 3.

5.3. Correlation between mass and absorbance for pig ear skin in-vitro

Figure 5.3 shows the correlation between the cumulative weight (µg) and the cumulative absorbance for pig ear skin from which an equation and a correlation coefficient were obtained. In these experiments four samples of pig ear skin from three different donors were

used. The results from application of the linear equation to the results of SquameScan absorption were close to those obtained by mass measurements. Unfortunately, the thicknesses of the SC obtained by mass ranged between 5 and 6 µm and these results were not within the normal range (Jacobi et al., 2007). The results were nearly the same when the equation was used to calculate the thickness of the SC following tape stripping in the penetration experiments. However, there were some variations and these may be related to the use of different donors for each experiment.

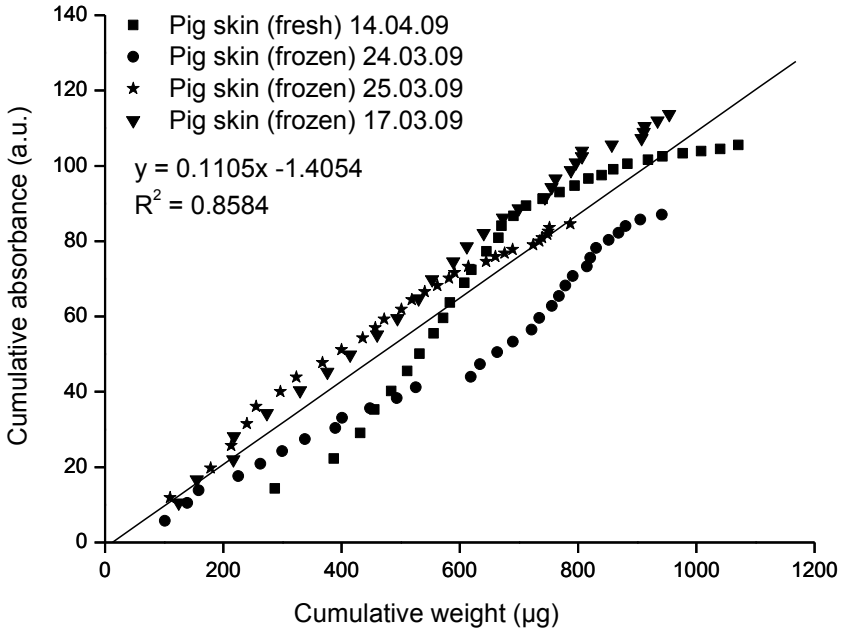

Figure 5.3: Correlation between cumulative weight and cumulative absorbance of tape stripping of pig ear SC where n = 4.

5.4. Penetration of corticosterone into pig ear skin

Figures 5.4 and 5.6 and Table 5.1 illustrate the cumulative permeation of corticosterone through fresh pig ear skin. In the first experiments, the receptor chamber contained PBS pH 7.4 and 1% BSA, whereas in the second experiments the receptor chamber contained PBS pH 7.4. These experiments were done under occlusive conditions with an infinite dose. In the second experiments the cumulative percentage of the applied dose in the receptor chamber for corticosterone was slightly higher than in the first experiments.

In Figures 5.5 and 5.6 and Table 5.1, the cumulative percentages of the applied dose in the SC layers, stripped skin and receptor part for second penetration experiments were higher than the first penetration experiments.

When comparing the cumulative percentage of the drug in the different skin layers and receptor chamber in both experiments, it was observed that the cumulative percentage of the drug in SC layers was higher than in the stripped skin (remainder of epidermis and dermis) and receptor chambers (Figure 5.6 and Table 5.1).

As illustrated in Table 5.1, there was a small difference in the percentage recovery approximately 86 % and 79 % for the first and second experiments, respectively. This difference in the percentage recovery could be attributed to the difference in the thickness of various skin samples.

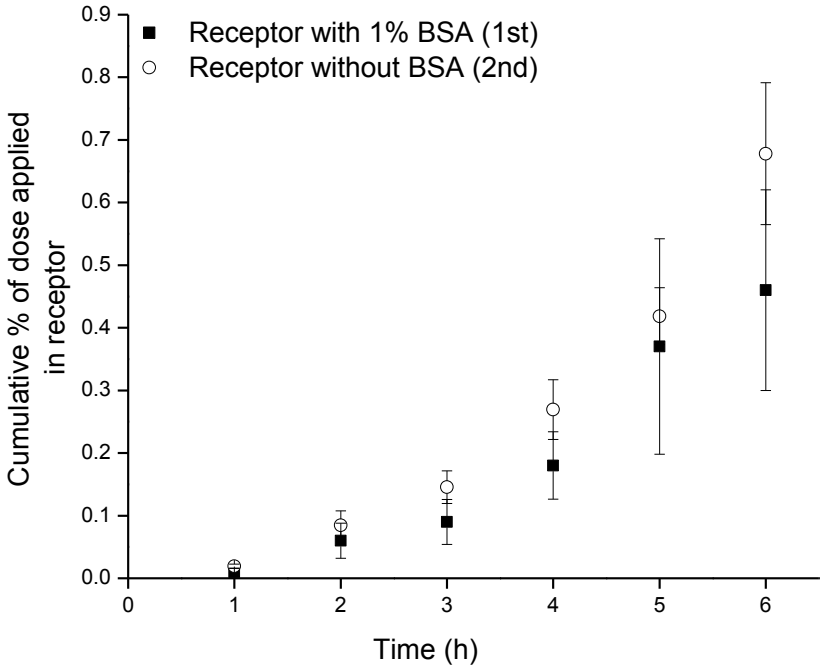

Figure 5.4: Cumulative amount of radiolabeled corticosterone in the receptor compartment for pig ear skin in-vitro. Incubation time 6 h at 32°C where n = 3 for each experiment.

5.5. Penetration of mannitol into human skin and pig ear skin

Figures 5.7, 5.8 and 5.10 and Table 5.2 illustrate the permeation of mannitol through fresh pig ear skin, fresh and frozen human abdominal skin. These experiments were performed using an infinite dose under occlusive conditions. The receptor chamber contained PBS, pH 7.4. It was observed that the cumulative percentage of the drug in the receptor chamber for the pig ear skin was higher than for both fresh and frozen human abdominal skin. Figure 5.8 and Table 5.2 also show that the cumulative permeation of mannitol through frozen human abdominal skin was slightly higher than for the fresh human abdominal skin.

Table 5.1: The amount of radiolabeled corticosterone (expressed as cumulative % of dose applied) in different layers of fresh pig ear skin

Radiolabeled corticosterone (%)							
Applied dose	Receptor medium	n	Stratum corneum	Deeper skin (epidermis + dermis)	Receptor chamber	Skin surface	Recovery
500 µl from solution (2 µl of corticosterone +2 ml of PBS	PBS	3	1.40 ± 0.37	1.24 ± 0.37	0.68 ± 0.11	82.21 ± 3.06	86.01 ± 2.54
	PBS + 1% BSA	3	1.11 ± 0.25	0.96 ± 0.11	0.46 ± 0.16	76.81 ± 5.01	79.33 ± 4.70

Table 5.2: The amount of radiolabeled mannitol (expressed as cumulative % of dose applied) in different layers of pig ear skin and human abdominal skin

Radiolabeled mannitol (%)							
Applied dose	Skin type	n	Stratum corneum	Deeper skin (epidermis + dermis)	Receptor chamber	Skin surface	Recovery
500µl of solution (2µl of mannitol in 2 ml of PBS)	Fresh pig ear skin	1	1.22	0.62	1.13	75.38	78.35
		1	1.10	1.68	1.50	64.14	68.42
	Frozen human skin	3	0.17 ± 0.04	0.08 ± 0.01	0.06 ± 0.04	77.47 ± 0.48	77.78 ± 0.42
	Fresh human skin	3	0.28 ± 0.19	0.03 ± 0.02	0.03 ± 0.01	67.35 ± 0.51	67.69 ± 0.68

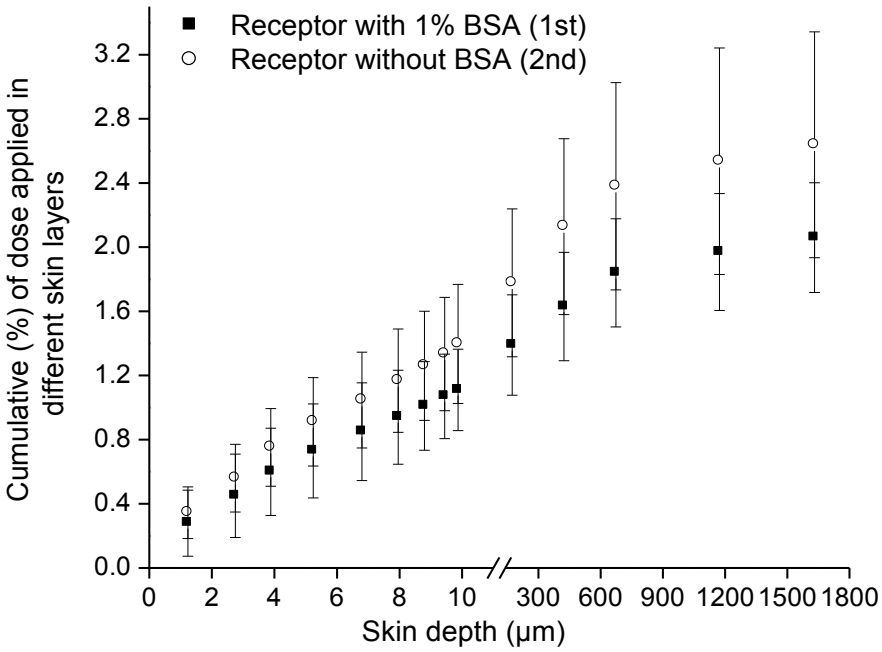

Figure 5.5: Skin depth profile of cumulative radiolabeled corticosterone detected in the SC and stripped skin for pig ear skin in-vitro after 6 h incubation at 32°C where n=3 for each experiment.

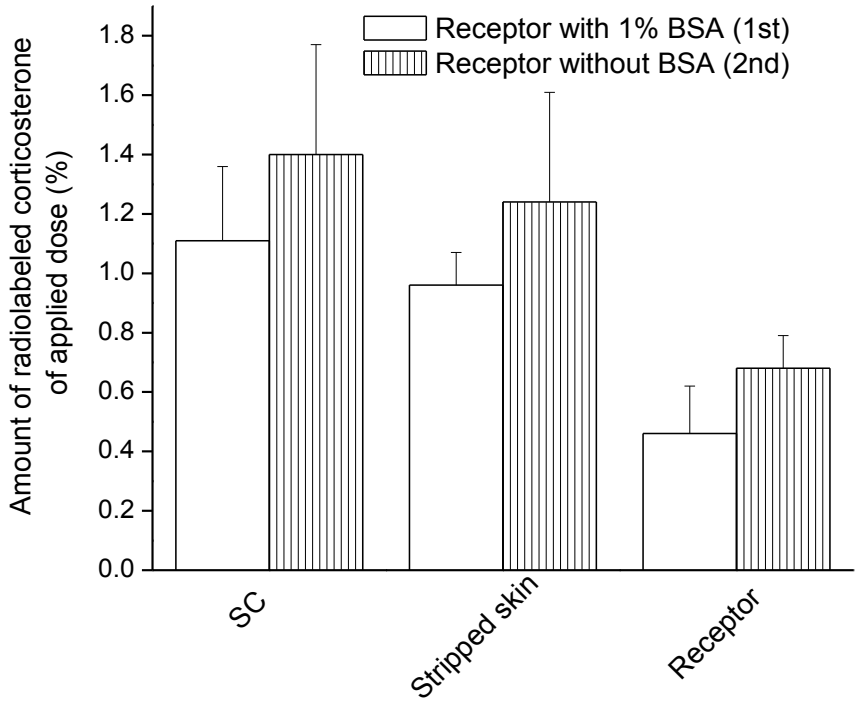

Figure 5.6: Amount of radiolabeled corticosterone detected in the SC, stripped skin and receptor for pig ear skin in-vitro after 6 h incubation at 32 °C. Where n = 3 for each experiments.

Figures 5.9 and 5.10 and Table 5.2 illustrate the cumulative percentage penetration of mannitol through different skin layers. There was no difference between the amount of mannitol found in the SC and stripped skin for pig ear skin, while it was slightly high in the receptor part as compared with SC and stripped skin. From these figures it was observed that the cumulative percentage of mannitol in pig ear SC and stripped skin was higher than for fresh and frozen human abdominal skin. In the case of both fresh and frozen human skin, it was observed that the percentage of mannitol found in the SC layers was higher compared with the amount found in the stripped skin and the receptor chamber. It was observed that, the amount of mannitol in the SC of frozen human skin was slightly lower than for fresh human skin. However, the amount of mannitol was slightly higher in frozen skin than in fresh skin when the stripped skin and the receptor chamber were compared with each other.

The two linear equations produced from the correlation between the mass and absorbance for human and pig ear skin were used to calculate the thickness of the SC.

Table 5.2 shows that the percentage recovery of mannitol was approximately 73% for pig ear skin, 77% for frozen human abdominal skin and 67% for fresh human abdominal skin.

The results for the penetration of mannitol through human abdominal skin were in agreement with those of Badran et al (Badran et al., 2009) for the presence of mannitol in the SC and stripped skin. However, their results showed no mannitol in the receptor chamber.

By comparing the penetration of corticosterone and mannitol through pig ear skin, it was found that the cumulative percentage of corticosterone in the SC and stripped skin was higher than the cumulative percentage of mannitol, while it was lower than that of mannitol in the receptor chambers (Tables 5.1 & 5.2).

5.6. Discussion

Penetration experiments are done to estimate the amount of a drug that can penetrate the SC, the remainder of epidermis and the dermis. The estimation of a drug in SC can be done by tape-stripping, where the process separates the SC layers into sections parallel to the skin surface. Analyses of the tapes at different depths of the SC are performed to estimate drug delivery inside the SC layers.

Tape stripping relies on the removal of the SC layers; however this is influenced by some factors which include, the adhesive quality (Bashir et al., 2001), pressure applied, duration of time of application and the removal of tape strips in the same direction from the skin surface (Loffler et al., 2004). In this study all these parameters were fixed, however, there was some variation in the skin samples due to different donors; human and pig.

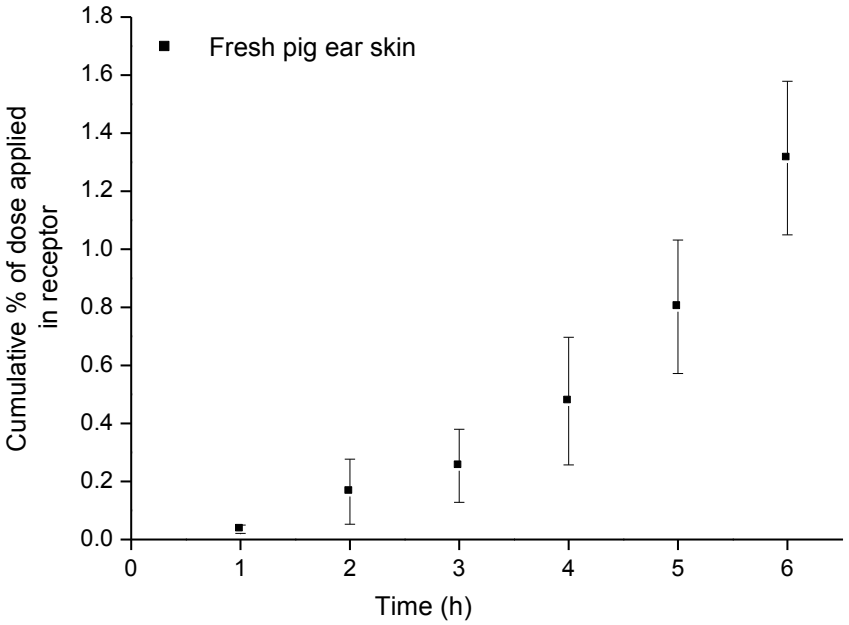

Figure 5.7: Cumulative amount of radiolabeled mannitol in the receptor compartment for pig ear skin in-vitro and incubation time 6 h at 32°C.

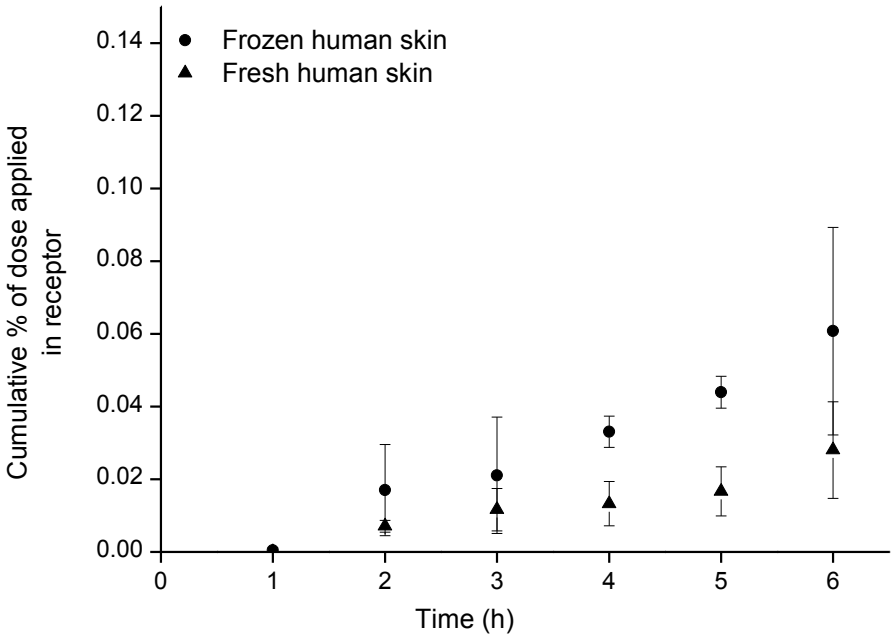

Figure 5.8: Cumulative amount of radiolabeled mannitol in the receptor compartment for fresh and frozen human abdominal skin in-vitro. Incubation time 6 h at 32°C where n = 3 for each experiment.

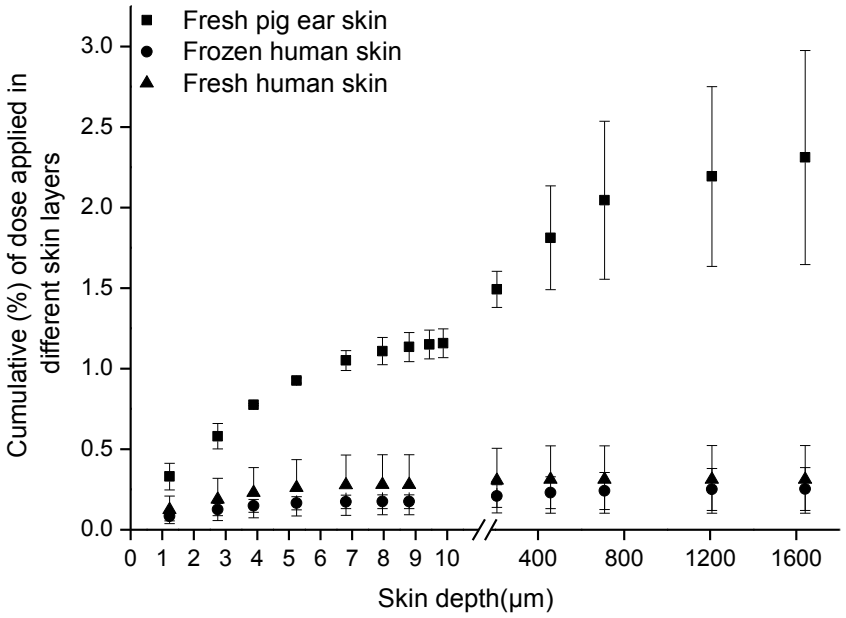

Figure 5.9: Skin depth profile of cumulative radiolabeled mannitol detected into the SC and stripped skin for pig ear skin and human abdominal skin in-vitro after 6 h incubation at 32°C where n = 3 for each experiment.

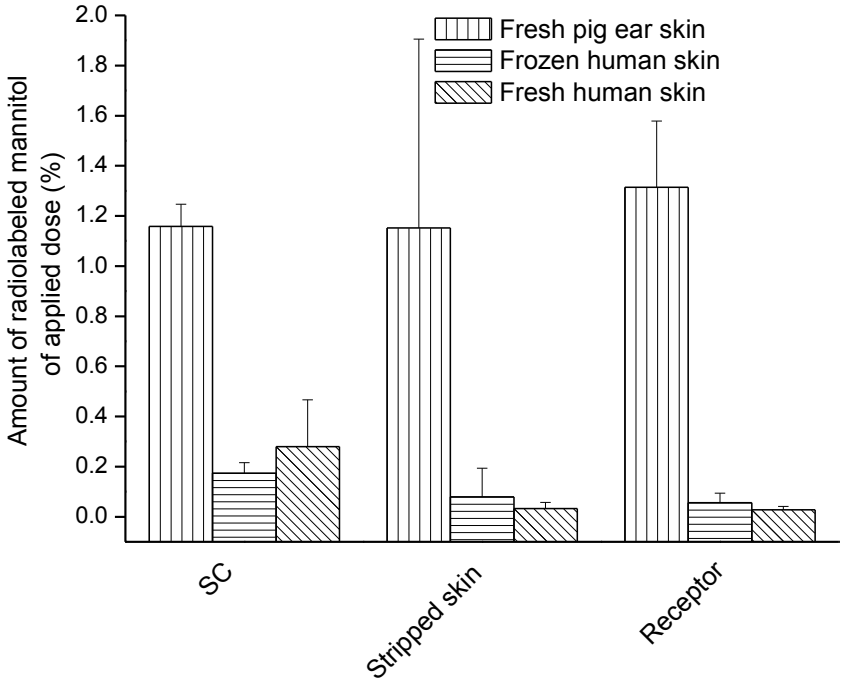

Figure 5.10: Amount of radiolabeled mannitol detected into the SC, stripped skin and receptor for pig ear skin and human abdominal skin in-vitro after 6 h incubation at 32°C. Where n = 3 for each experiment.

The evaluation of the SC thickness can be done by using experimental or mathematical methods. In the mathematical method, the SC thickness on each tape-strip is calculated by dividing the whole thickness of the SC by the number of tapes used in the stripping process (Wagner et al., 2000).

During the process of tape stripping in this study, different amounts of SC were removed by each tape strip and this difference was reported for each donor (Herkenne et al., 2008). The amount of the SC removed per strip decreased with increasing SC depth, due to an increase in cohesion between the corneocytes of the deeper SC layers (Chapman et al., 1991). The amount of SC removed by each tape stripping was determined by differential weighing (Marttin et al., 1996), protein quantification using the colorimetric method (Dreher et al., 1998) and optical methods using protein absorption at 278 nm or pseudo absorption at 430 nm (Marttin et al., 1996; Weigmann et al., 1999).

During tape stripping in the penetration experiments it was noted that the accuracy of the balance (gravimetric method) was not fixed at all times, which led to many errors. In addition to these problems this method was time consuming (Voegeli et al., 2007). The previous problems of the gravimetric method were due to formulation excipients, moisture, lipid content and interstitial fluid derived after removal of several tape strips, which may also increase the weight difference for the strips removed from deeper parts of the skin (Weigmann et al., 1999). Colorimetry is a destructive and time consuming method, and leads to error. The determination of protein content, other components of the same tape and cutting the same tape into parts is difficult and time consuming (Voegeli et al., 2007). The optical method leads to errors due to the other substances having absorption at 278 nm. Also, non specific pseudo absorption may occur at 430 nm due to sweat and lipids found within the SC and formulation excipients (Weigmann et al., 2003).

Therefore, a novel method is needed to quantify the amount of SC removed from each tape. IR-D is a non-destructive new method for quantification of SC by using SquameScan 850A. In IR-D, a beam of light of 850 nm is directed through a tape strip containing SC and the decrease in light intensity is measured. An empty tape is used for background correction. Thus the thickness of the SC and the amount of drug can be determined from the tape strips (Voegeli et al., 2007).

It was reported that the IR-D method was used to determine the thickness of SC *in-vitro* and there was no difference in using tape strips for both D-Squame and tesa Film kristall-klar for the quantification of SC. Additionally, IR-D allowed for determination of the endpoint for complete SC removal. Consequently, this method allowed adjustment for the total number of tape strips that were used for a single skin site during an experiment. Thereby, the SC-depth profiles could be determined more accurately. Furthermore, the exact number of tape strips

that were necessary for removal of the whole SC varied even between two skin samples from the same donor at the same site and time (Hahn et al., 2010).

SquameScan has several advantages such as its compact dimensions, easy handling and economy in that it reduces the measuring time to a few seconds per tape strip, consequently saving costs (Voegeli et al., 2007). Although this method was used to determine SC protein *in-vivo*, sometimes these experiments could not be done due to ethical problems (Netzaff et al., 2005).

From the results of this study, a good correlation coefficient between the cumulative weight and absorbance *in-vivo* and *in-vitro* for human skin and *in-vitro* for pig ear skin was obtained. Similar results of SC thickness were produced using the linear equations from these correlations as from the mass method. Thus, IR-D could have been used as an *in-vitro* method to determine the thickness of the SC.

Therefore, the linear equations obtained from the correlation between the mass by balance and the absorbance by SquameScan were used to calculate the thickness of SC for both human abdominal skin and pig ear skin during the penetration experiments.

The ability of topically applied substances to penetrate to sites within the layers of the skin and reach the systemic circulation to exert their pharmacological effects will depend on their physicochemical properties (Tezel et al., 2002). Thus in this study, the penetration behavior of corticosterone as a lipophilic model drug into pig ear skin and mannitol as a hydrophilic model drug into human abdominal skin and pig ear skin was investigated. The concentration of corticosterone and mannitol was estimated in all skin layers and in the receptor chamber.

The results of this work for the penetration of corticosterone through pig ear skin showed that the percentage of accumulated drug into SC was slightly higher than for stripped skin and the receptor part in the first and the second experiments. This was due to corticosterone being a lipophilic drug and there was a high partition coefficient between corticosterone and SC (Magnusson et al., 2006). Thus, the drug accumulated more in the SC. The increased accumulation of corticosterone in stripped skin more than in the receptor part was due to the fact that viable epidermis and dermis have an aqueous environment, which acts as a barrier to lipophilic substances (Netzaff et al., 2005). However the passage of solutes out of the SC is dependent on the partioning between SC and viable epidermis and dermis (Magnusson et al., 2006).

As a comparison between the first and second experiments, the cumulative percentage of corticosterone in the SC, stripped skin and receptor part was slightly higher in the second experiments than that in the first experiments. Although, BSA has the effect of binding the lipophilic solutes then generating a ‘sink condition’ that causes partitioning from the membrane into the receptor fluid (Cross et al., 2003), there was no effect generated by using BSA in the first experiments. The reason for these results is not clear but it may be related to

some interaction between BSA and the scintillation cocktail. However, the receptor chambers in the first experiments contained PBS and 1% BSA and during the penetration experiments the solution in the receptor part was diffused through the different skin layers.

The cumulative percentage of corticosterone in the SC and stripped skin was slightly higher than that of mannitol while the cumulative percentage of mannitol in the receptor part was higher than that of corticosterone. The highly cumulative amount of mannitol in the receptor part may be because mannitol is a hydrophilic drug and has an affinity to penetrate through skin appendages (Lademann et al., 2008), and pig ear skin has a high density and large diameter hair follicles (Jacobi et al., 2007). The high cumulative percentage of corticosterone in SC and stripped skin as compared with mannitol was because corticosterone is a lipophilic drug and has an affinity to dissolve in the SC lipids, and the partition coefficient between corticosterone and viable epidermis and dermis is very weak (Magnusson et al., 2006). Therefore, corticosterone accumulated more in the SC and stripped skin compared to mannitol.

Mannitol passively diffused through the SC and showed poor penetration into the skin due to the low partition between mannitol and the SC (Tezel et al., 2002). The penetration of mannitol into the pig ear skin was higher than for the human skin due to the higher density of hair follicles and larger diameter of the hair shafts in pig ear skin compared with human abdominal skin (Jacobi et al., 2007). The previous reason illustrates a higher percentage of mannitol in the SC, stripped skin and receptor chamber for pig ear skin compared with human skin. There was no distinct difference between the concentration of mannitol in the SC and stripped skin and it was slightly high in the receptor part of pig ear skin indicating that the drug had not accumulated in the SC. This may be due to the hair follicle, hair shaft and sebaceous glands extending deep into the dermis and passing through the epidermis and SC to skin surface (Harkey, 1993). On the contrary, mannitol was higher in the SC than in the stripped skin and receptor chamber for human abdominal skin.

There was a slight difference in the presence of mannitol in the SC, stripped skin, and receptor chamber between fresh and frozen human abdominal skin. The cumulative percentage of mannitol in SC for fresh human skin was slightly higher than for frozen human skin, while the cumulative percentage of mannitol in stripped skin and receptor chamber for fresh human skin was slightly lower than frozen human skin. The previous results were related to the effect of freezing. It was reported that the effect of freezing human skin leads to changes in the structure of the SC. These changes may be related to the formation of water crystals in the SC lipid or in the keratinized cells. Consequently, cells damage or disorder of the intercellular lipid matrix has occurred. This structural change is irreversible and leads to increased permeation of substances (Swarbrick et al., 1982).

The results of this work were in agreement with other results (Sintov and Botner, 2006) which reported that the freezing of skin leads to increase TEWL and penetration of hydrophilic substances. This study suggested that this effect was due to the freezing of skin which affects only the aqueous pathways in lipid bilayers. However, the freezing of skin leads to the formation of cracks that open the polar pathways in lipid bilayers or is related to the modification of the structural protein in the SC due to loss of adherence of corneocytes. Therefore, the barrier properties decrease especially for hydrophilic substances (Sintov and Botner, 2006).

These results were in agreement with those of Badran et al., (Badran et al., 2009) except for the receptor chamber. This may be due to experimental differences where the current study used an infinite dose (500 µl) of PBS containing radiolabeled mannitol under occlusive conditions, while Badran et al. used a finite dose (31.4 µl) of PBS containing radiolabeled mannitol under non-occlusive conditions.

The recovery percentage for all experiments in the current study was lower compared with other studies because a high infinite dose (500 µl) was used and this led to a high loss of drugs during the experiments.

5.7. Conclusion

In this study the thickness of the SC layer was determined by IR-D, a new method which is superior to gravimetric method. The correlation between the mass and absorbance for human abdominal skin *in-vivo* and *in-vitro* and for pig ear skin *in-vitro* gave a good correlation from which linear equations were produced that could be used for the calculation of the SC thickness *in-vitro*.

The penetration of the lipophilic drug, corticosterone, into pig ear skin was higher for the SC and stripped skin and lower for the receptor part compared with the penetration of the hydrophilic drug mannitol.

The penetration of mannitol into pig ear skin was higher compared to both fresh and frozen human abdominal skin. The penetration of mannitol in the SC was slightly higher in fresh human skin compared with frozen human skin, while the amount of mannitol in stripped skin and receptor chambers for frozen human skin was slightly higher than fresh human skin.

6. Qualitative penetration and stability studies of vesicles

6.1. Fluorescence microscopic studies

Fluorescence microscopy was used to visualize the qualitative penetration depth of fluorescent dye CF from different liposomal formulations after incubation for 6 h under non-occlusive conditions. Three different formulations containing CF were used in these penetration experiments: invasomes (92 nm), flexible liposomes containing S75 (74 nm), and rigid liposomes containing S100-3 (76 nm).

Figure 6.1 shows representative fluorescence microscope images of cross sections of skin samples incubated with invasomes (A), flexible liposomes (B) and rigid liposomes (C). The bright field images of the structure of the skin are shown in the left hand panel while the fluorescence images are shown in the right hand panel.

It can be seen from Figure 6.1 that the intensity of fluorescence in the SC layers was nearly the same in the case of invasomes and flexible liposomes while it increased with the rigid liposomes. The intensity of fluorescence in the viable epidermis and dermis was nearly the same in the case of invasomes and flexible liposome while it decreased in the rigid liposomes.

6.2. Stability studies

The long-term stability of the vesicles was investigated by storing the samples for up to 8 months at 4ºC as illustrated in Figure 6.2 and Table 6.1. Figure 6.2 and Table 6.1 shows the particle size of different liposomal formulations. From Figure 6.2 (A) it can be observed that the particle size of invasomes is larger than the flexible and rigid liposomes. The particle size of invasomes ranged between 88 and 94 nm with a very good polydispersity index (PI) of about 0.1 as seen in Figure 6.2 (B) and Table 6.1. There was almost no change in the particle size and PI during the 8 months of the experiment. Measuring the zeta potential proved the high stability of the invasomes. As seen from Figure 6.2 (C) and Table 6.1 the zeta potential of invasomes ranged from -45 to -60 mV, which indicates the high stability of these particles.

The flexible and rigid liposomes had particle sizes of less than 80 nm and these did not change during the stability period (8 months) as seen from Figure 6.2 (A). Figure 6.2 (B) shows the high homogeneity of the flexible and rigid liposomes where the PI was less than 0.15 for the rigid liposomes and 0.11 for the flexible liposomes. The zeta potential of the flexible liposomes ranged from -48 to -57 mV, which indicates the high stability of these particles as seen in Figure 6.2 (C). Also it can be seen in Figure 6.2 (C) that the zeta

potential of the rigid liposome was less than invasomes and flexible liposomes and ranged from -45 to -51 mV.

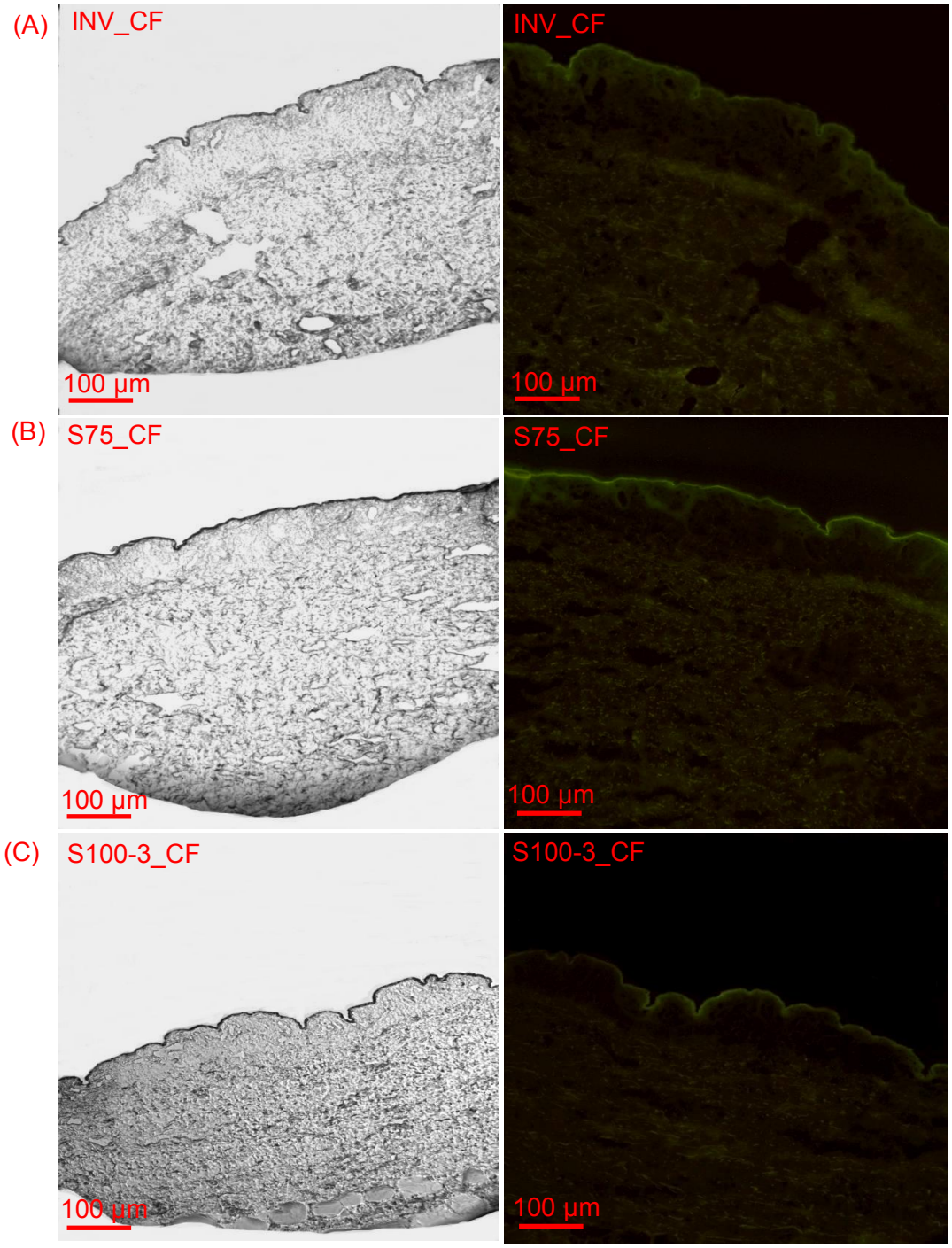

Figure 6.1: Fluorescence microscope images of a cross section of human abdominal skin incubated on a Franz diffusion cell with different liposomal formulations containing CF. The liposomal formulations were applied non-occlusively for 6 h. The left panel represents the bright field images and the right panel represents the fluorescence images of (A) invasomes, (B) liposomes S75 and (C) liposomes S100-3.

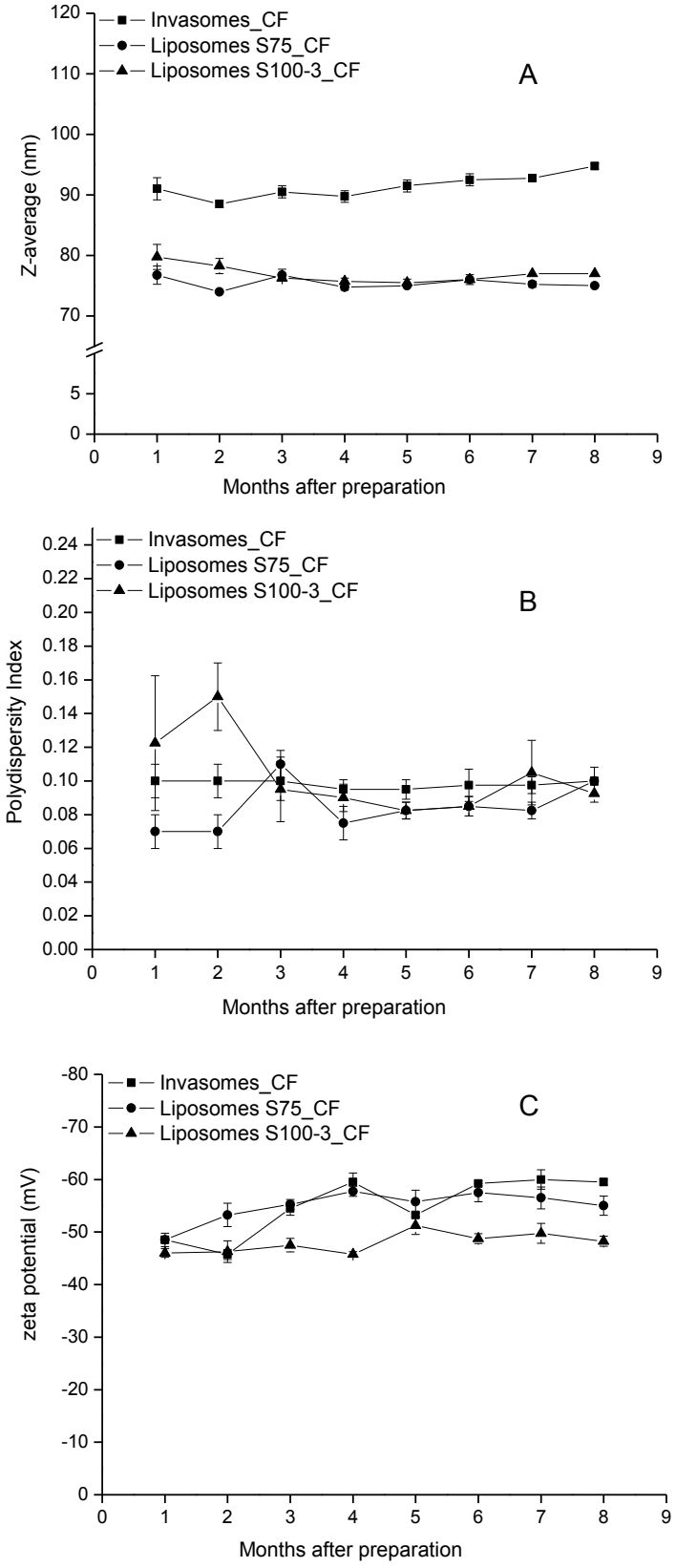

Figure 6.2: stability studies of invasomes, liposomes S75 and liposomes S100-3 containing CF for up to 8 months. (A) change of the particle size of vesicles (B) change of PI of vesicles (C) change of zeta potential of vesicles.

Table 6.1: Particle size, PI and Zeta-potential for invasomes, liposome S75 and liposome S100-3 containing CF stored for 8 months at 4ºC

Months	Invasomes			Liposome S75			Liposome S100-3		
	Size (nm)	PI	Zeta potential (mV)	Size (nm)	PI	Zeta potential (mV)	Size (nm)	PI	Zeta potential (mV)
1	91 ± 1.80	0.1 ± 0.01	-48 ± 1.29	76 ± 1.50	0.07 ± 0.01	-48 ± 0.60	79 ± 2.10	0.12 ± 0.04	-46 ± 0.80
2	88 ± 0.60	0.1 ± 0.01	-45 ± 0.96	74 ± 0.00	0.07 ± 0.01	-53 ± 2.20	78 ± 1.30	0.15 ± 0.02	-46 ± 2.10
3	90 ± 1.00	0.1 ± 0.01	-54 ± 1.29	76 ± 0.96	0.11 ± 0.01	-55 ± 0.90	76 ± 0.50	0.09 ± 0.02	-47 ± 1.30
4	89 ± 0.96	0.09 ± 0.01	-59 ± 1.73	74 ± 0.50	0.07 ± 0.01	-57 ± 0.90	75 ± 0.50	0.09 ± 0.01	-45 ± 0.50
5	91 ± 1.00	0.09 ± 0.01	-53 ± 0.50	75 ± 0.00	0.08 ± 0.01	-55 ± 2.20	75 ± 0.60	0.08 ± 0.01	-51 ± 1.70
6	92 ± 1.00	0.09 ± 0.01	-59 ± 0.50	76 ± 0.82	0.08 ± 0.01	-57 ± 1.70	76 ± 0.00	0.08 ± 0.01	-48 ± 0.96
7	92 ± 0.50	0.09 ± 0.01	-60 ± 1.82	75 ± 0.50	0.08 ± 0.01	-56 ± 2.10	77 ± 0.00	0.11 ± 0.01	-49 ± 1.90
8	94 ± 0.50	0.1 ± 0.01	-59 ± 0.58	75 ± 0.00	0.1 ± 0.00	-55 ± 1.80	77 ± 0.00	0.09 ± 0.01	-48 ± 0.90

6.3. Discussion

The SC is the outermost layer of the skin and acts as the main barrier for water and most solutes. There are several methods used to overcome the SC barrier, thereby increasing drug transport through the skin. Some of the most common methods are the use of vesicles and chemical penetration enhancers (Williams and Barry, 2004). Additionally, it has been reported that elastic vesicles have superior properties compared to rigid vesicles for enhancing drug transport through the skin (Elsayed et al., 2007). Also, the addition of ethanol and terpenes to the vesicles act as penetration enhancers. It has been reported that the combination of phospholipid, ethanol and a mixture of terpenes in invasomes leads to a synergistic effect in penetration through the skin (Dragicevic-Curic et al., 2008b). The presence of ethanol in vesicles fluidizes the intercellular SC lipids by decreasing their melting points, thereby disturbing the organization of the bilayer structure of the intracellular lipid matrix (Elsayed et al., 2007).

Terpenes can improve the permeation of lipophilic drugs (testosterone), hydrophilic drugs (propranolol) and amphiphilic drugs (6-mercaptopurine) (Aqil et al., 2007). Terpenes can improve skin permeation by interacting with SC lipids or keratin to increase the solubility of the drug into SC lipids. Additionally, terpenes increase skin permeability by increasing the partition coefficient of the drug into the skin and by increasing the thermodynamic activity of the drug in the vehicle (Yamane et al., 1995a), as well as interacting with intercellular lipids, perturbing their highly ordered intercellular lamellar packing (Dragicevic-Curic et al., 2008b).

The standard terpene mixture used in this thesis work was 1% citral, d-limonene and 1,8-cineole. However, limonene is a hydrocarbon lipophilic terpene, which enhances the permeation of lipophilic and amphiphilic substances (Aqil et al., 2007). It has been reported that limonene produced a freezing point-depression effect on SC lipids, thus perturbing the highly ordered lipid domain (Yamane et al., 1995b).

Cineole is cyclic ether monoterpene and is a most efficient penetration enhancer for hydrophilic substances. It has been reported that the application of 1,8-cineole on excised human skin changed the highly ordered lipid domain of the SC. This may be due to the interaction of cineole with the lipids and proteins forming hydrogen bonds thus, altering the organization of the SC (dos Anjos et al., 2007). Consequently, drug uptake was increased through the tissue after application of the penetration enhancer.

It has been reported that a 1% (w/w) concentration of terpene mixture enhanced the deposition of temoporfin in the SC more than 0.5% (Dragicevic-Curic et al., 2008b). However, a 1% combination of three different terpenes (cineol, citral and limonene) in invasomes preparations led to a higher penetration of temoporfin than in case of invasomes preparations containing 1% citral alone (Dragicevic-Curic et al., 2008a). The combination of three different

terpenes could have acted synergistically to enhance the penetration of temoporfin which would explain the higher efficacy of invasomes containing the 1% terpene mixture (Dragicevic-Curic et al., 2008b).

There are some factors such as physicochemical properties and chemical structure that influence the activity of terpenes as penetration enhancers as follows (Kang et al., 2007);

(1) Liquid terpenes tend to have better enhancing effects than solid terpenes and liquid terpenes may form more hydrogen bonds with intercellular lipids of the SC.

(2) Triterpenes and tetraterpenes usually have poor penetration compared with other terpenes.

(3) Terpenes with larger logP values are more successful enhancers than those with smaller log P because they mix more readily with the SC intercellular lipids.

(4) Terpenes with aldehyde and ester functional groups are found to be good enhancers.

(5) Smaller sized terpenes have a tendency to be more active than the larger terpenes as penetration enhancers. Additionally, smaller alcoholic terpenes with a higher degree of unsaturation appear to be good candidates for enhancing the permeation of hydrophilic drugs (Ghafourian et al., 2004).

The terpene mixture used in this study was a liquid monoterpene with a high logP value (limonene) and a small particle size.

A comparison of the qualitative penetration behavior of three different liposomal formulations containing CF as a hydrophilic marker into human skin was done under non-occlusive conditions. Previous literature (Verma et al., 2003a) designed liposomal formulations which could carry both entrapped as well as non-entrapped, hydrophilic CF into the skin. For this reason, non-entrapped CF in the three topically liposomal formulations used in this work was not separated, which means all these liposomal systems contained CF both inside and outside the liposomes.

These formulations included invasomes, and flexible and rigid liposomes. All formulations used were small in size, unilamellar and had a negative charge of less than -40 mV. The only difference between these vesicles was the rigidity and flexibility of the bilayer and the presence of penetration enhancers. Liposome S100-3 was used as the rigid vesicles and liposome S75 and invasomes were used as the flexible vesicles. The difference between liposome S75 and invasomes, is the presence of ethanol and a mixture of terpenes, which act as penetration enhancers and increase the flexibility of the invasomes.

It has been reported that the penetration of vesicles especially elastic vesicles is high under non-occlusive conditions. This is due to the non-occlusive conditions creating a transepidermal osmotic gradient that works as the driving force for the transport of elastic vesicles through the skin. This osmotic gradient is caused by the difference in the

concentration of water between different skin layers (Honeywell-Nguyen and Bouwstra, 2005).

From the results of penetration studies in this work, the intensity of fluorescence in images obtained from the SC, viable epidermis and dermis was nearly the same for invasomes and liposomes S75, while for rigid liposomes, the intensity of CF fluorescence was higher on the SC surface and lower in the viable epidermis and dermis compared to the other formulations. It has been reported that the flexibility of the vesicles facilitates their rapid penetration through the intercellular lipid pathways of the SC, allowing them to squeeze through the intact SC (Honeywell-Nguyen and Bouwstra, 2005). This illustrates that a decrease in intensity of CF fluorescence in the viable epidermis and dermis in the liposomes S100-3 is due to the accumulation of the vesicles on the surface of SC compared to liposomes S75 and invasomes, which penetrate the SC.

The results of this study are in agreement with other studies, which have suggested that elastic vesicles have performed better than rigid vesicles for interaction with human skin. After application of both elastic and rigid vesicles to human skin under non-occlusive conditions, it was found that the rigid vesicles formed collections of lipid bilayer on the skin surface. These collections led to reduced skin penetration. Also compared with elastic vesicles, there were no ultrastructural changes in the deeper layers of SC and no significant detection of the rigid vesicles in this layer. These results indicate that the rigid vesicles were restricted to the skin surface. However, when this study was done using elastic vesicles, ultrastructural changes were observed in the deeper layers of SC; with the creation of new channels in the SC lipids and the vesicles were detected in this layer (Honeywell-Nguyen et al., 2002).

The stability studies of the different liposomal formulations showed that all of the liposomal formulations had a particle size and PI below 93 nm and 0.11 respectively. These studies confirmed that these formulations had small particle size with very good homogeneity. The PI measures the homogeneity of the vesicle suspension. A small value of PI (< 0.1) indicates very homogenous vesicle particles, while a larger PI (> 0.3) indicates heterogeneity (Verma and Fahr, 2004).

From the results of this work, it was found that the particle size of invasomes was slightly larger than liposomes S75 and S100-3. These results were due to the presence of terpenes, which increased the particle size of the vesicles (Dragicevic-Curic et al., 2008b).

The results also indicated that these vesicles were very stable because the zeta potentials for all liposomal formulations were less -40 mV. It has been reported that the zeta potential influences electrostatic stability of the vesicles; where a zeta potential above 60 mV indicates excellent stability, 40 to 60 mV indicates very good stability, from 30 to 40 mV indicates good

stability, from 10 to 30 mV indicates very poor stability and below 10 mV indicates no stability (Juanjuan Liu and Hu, 2007).

Although the zeta potential measurements for all liposomal preparations were very good, the zeta potential for invasomes and liposomes S75 was slightly higher than for liposomes S100-3. This result was produced because according to manufacturer's specifications the invasomes contain phosphatidic acid which gave a negative charge for the vesicles. Also, in the case of liposomes S75, the manufacturer's specifications stated that the amount of fatty acid was higher in Lipoid S75 than in Lipoid S100-3.

6.4. Conclusion

There was no difference in the qualitative penetration of CF entrapped in invasomes and flexible liposomes in human skin. However, both showed increased penetration of CF compared with the rigid liposomes. All liposomal preparations showed very high stability for up to 8 months at 4ºC.

7. Final discussion

In recent years research into topical drug delivery has greatly expanded due to the advantages of dermal and transdermal drug delivery. Human skin is a suitable *in-vitro* model for research in the pharmaceutical and cosmetic industries. However, the available amount of human skin is not sufficient for experimental procedures and also there are variations between different skin donors. In addition, the ethical problems that have developed from the use of animals in toxicological experiments has led to new laws which prevent the use of human and animal skin models in some experiments (Netzaff et al., 2005). This thesis work was interested in improving the morphology and the barrier properties of the ROC epidermis model to resemble full-thickness human skin. This improvement was made by adding the dermis to the ROC epidermis model. So in the current study the development and evaluation of the ROC epidermis and the ROC full-thickness models (with and without collagen) were compared with the human skin model to ascertain whether these models could be used as alternatives for the human skin model. The ROC epidermis model was compared with human epidermis in terms of morphology, TEWL measurements, thermal behavior of SC lipids and permeation studies of radiolabeled mannitol, corticosterone and tritiated water. In addition, ROC full-thickness models were compared with full-thickness human skin in morphology and permeability barrier which included TEWL measurements and permeation of tritiated water. Thus, the important issue was the success of the ROC models in resembling the behavior of human skin with respect to morphology and permeability barrier.

According to the results of this study, there was a big difference between the morphology of the ROC models and human skin. The SC was thicker but the epidermis was thinner in the ROC model compared with human skin. However, the thickness of the SC was in agreement with other reconstructed skin equivalent (Ponec et al., 2002). The high thickness of the SC in this study was due to the impaired desquamation of the SC as had occurred in other reconstructed human skin studies (Vicanova et al., 1996).

The ROC models were devoid of skin appendages and the results were related to the dermal substrate, where REK cells were grown by seeding on polycarbonate membrane (Suhonen et al., 2003) or dead DED human dermis (Ponec et al., 2002) for ROC epidermis or ROC full-thickness model respectively. However, the epidermal layers of the ROC full-thickness model separated from the dermis during sample preparation for light microscopy. This separation could be due to the incomplete formation of the basement membrane (Ponec et al., 2000). In future, the dermal substrate could be improved by the addition of human or rat fibroblasts to prevent this separation and increase the thickness of the viable epidermis for the ROC model. It has been reported that the presence of fibroblasts has led to the

improvement of both of cell adhesion and differentiation of human epidermal keratinocytes (El Ghalbzouri et al., 2002).

The TEWL measurements for the ROC full-thickness model without collagen was slightly higher than for the ROC epidermis and both of these models were higher than those of pig ear skin, human full-thickness skin, human epidermis and the ROC full-thickness model with collagen. According to the previous results it was noted that the combination of collagen and DED led to improved barrier properties of the ROC models. From the comparison between the TEWL values for the ROC full-thickness model with and without collagen, it was observed that collagen increased the barrier properties. The TEWL values for full-thickness human skin, human epidermis and the ROC full-thickness model with collagen were nearly the same. The TEWL values for pig ear skin were slightly higher than for full-thickness human skin and this may be related to the high density of hair in pig ear skin (Jacobi et al., 2007).

The results of the thermal behavior for human and ROC SC showed that the thermal transition for human SC was different from ROC SC. The T_2 phase transition in ROC was detected at lower temperatures than the human SC and T_3 was absent in the ROC SC. Also, the thermal behavior of the ROC SC was different from the original rat SC. The previous results for the ROC model could be attributed to a very low amount of bound ceramides, the absence of two types of ceramide (3, 7) and incomplete replacement of linoleate for oleate in ω-hydroxyceramides (Pappinen et al., 2008). These differences may explain the difference in thermal behavior between ROC and human SC. The SC lipids in human skin are more highly ordered than those of ROC (Pappinen et al., 2008). These results illustrate why ROC models are slightly more permeable compared to human skin.

The permeation of mannitol, corticosterone and tritiated water through human epidermis and ROC epidermis was evaluated. The permeability coefficient of mannitol through human epidermis was higher than for ROC epidermis due to the hair follicles which were lacking in the ROC epidermis (Suhonen et al., 2003). The permeation of corticosterone through ROC epidermis was higher than through human epidermis because corticosterone is a lipophilic drug which permeates through the intercellular lipid pathway in the SC (Tezel et al., 2002) and the SC lipid bilayer in case of human skin is more ordered than in the ROC skin model (Pappinen et al., 2008). The permeability coefficient of tritiated water through ROC epidermis and human epidermis was nearly the same. To approach more closely the full-thickness human skin *in-vivo*, the ROC full-thickness model was developed. This model allowed better evaluation of drug penetration into different skin layers. The permeability coefficient of tritiated water through the ROC full-thickness model with collagen and full-thickness human skin was nearly the same and was higher for the ROC full-thickness model without collagen. These results illustrate the role of collagen in increasing the barrier properties and show that water permeated through both hydrophilic and lipophilic pathways in the SC (Tezel et al.,

2002). The lower permeation of tritiated water through the ROC full-thickness model with collagen and the full-thickness human skin compared to the ROC and human epidermis showed the importance of the dermis as an additional barrier (Netzaff et al., 2005). Finally from this study, it was observed that the permeation of tritiated water through human and ROC epidermis was higher than corticosterone and mannitol which could be related to the small particle size of water and its permeation through both hydrophilic and lipophilic pathways (Tezel et al., 2002).

As mentioned before, there are many problems in using human skin as an *in-vitro* model for research in the pharmaceutical industry. Therefore, animal skin models have been used as an alternative to human skin. This study, investigated the penetration behavior of model drugs into human and pig ear skin. Pig ear skin and human skin were used because of their similarities (Jacobi et al., 2007). The tape stripping process was used to evaluate the amount of drug in the SC layer (Dragicevic-Curic et al., 2008b). During penetration experiments the weighing method was used to determine the amount of SC removed by each tape stripping. To overcome the drawbacks of the weighing method, IR-D as a novel method was used to determine the amount of SC removed by each tape stripping by using SquameScan device (Voegeli et al., 2007). Thus, the weighing and IR-D methods were used to evaluate the amount of SC removed by each tape strip for human and pig ear skin. In order to use IR-D instead of the weighing method in this study, a correlation was done between cumulative weight by balance and cumulative absorbance by SquameScan for human skin *in-vivo* and *in-vitro* and for pig ear skin *in-vitro*. The results showed there was good correlation between cumulative weight and cumulative absorbance *in-vivo* and *in-vitro* for human skin and for pig ear skin *in-vitro*. The application of the linear equations that were produced from these correlations produced nearly the same SC thickness for human and pig ear skin in-vitro as that obtained in tape stripping only.

It was noted that BSA had no effect on the permeation of corticosterone, a lipophilic model drug, through pig ear skin. Also, the amount of corticosterone found in the SC was higher when compared with the stripped skin and the receptor chamber. These results are due to the hydrophobic behavior of the SC and the high partition between corticosterone and SC, which then works to dissolve corticosterone in the SC, so the drug accumulated more in the SC (Magnusson et al., 2006). Additionally, the amount of corticosterone was higher in the stripped skin when compared with receptor parts. These results were related to the hydrophilic behavior of the dermis, which acts as an additional barrier especially for lipophilic drugs (Netzaff et al., 2005). The penetration of corticosterone into SC and stripped skin for pig ear skin was higher than the penetration of mannitol. Furthermore, the amount of mannitol in the receptor part was higher than for corticosterone, because mannitol is a hydrophilic drug and there is no partition between mannitol and SC (Tezel et al., 2002),

thus there was no accumulation of mannitol in the SC. Additionally, it has been reported that mannitol permeates through skin appendages (Lademann et al., 2008) and the aqueous pathways in the SC of pig ear skin (Tezel et al., 2002), which has many hair follicles (Jacobi et al., 2007). So the drug penetrates through the SC, and there are no additional barriers preventing its permeation.

The penetration of mannitol into pig ear skin was higher than into human abdominal skin. These results are due to the hair density and the diameter of the hair shaft (Jacobi et al., 2007), which extends from the skin surface to deep within the dermis (Harkey, 1993). Hair shaft are much more prevalent in pig ear skin than in human skin. Thus, the accumulation of the mannitol in the SC layer of human skin compared to pig ear skin is due to the low number of hair follicles in human skin (Jacobi et al., 2007) and the fact that human SC lipids are highly ordered (Pappinen et al., 2008). The cumulative percentage of mannitol in the SC of fresh human skin was slightly high and in stripped skin and receptor part was slightly low compared with frozen human skin. These results were related to the effect of freezing on human skin which leads to water crystallize in the corneocytes and intercellular lipids, thus disrupting the barrier properties of SC and enhancing the permeation of drugs (Swarbrick et al., 1982).

The main challenge for the dermal and transdermal drug delivery system is the presence of the SC, which inhibits the passage of any applied molecules to the skin surface from penetrating into the deeper skin layers (dermal) or across skin layers into the general circulation (transdermal) (Benson, 2005). Vesicles were one of the methods that were used to overcome the barrier properties of this layer, thus enhancing drug transport across the skin (Elsayed et al., 2007). In this thesis, characterization and evaluation of the qualitative penetration of different vesicle formulations were done using the human skin model, fluorescence microscopy and FDC. The three different vesicle formulations used in this study were vesicles with rigid bilayers that contained Lipoid S100-3, vesicles with flexible bilayers that contained Lipoid S75 and invasomes that contained NAT 8539 (PC: ethanol = 75:25 w/w) and terpene mixture. The presence of negative or positive charged lipids in the bilayers will increase the interlamellar distance between the bilayers and thus increase the entrapped volume. In addition, the presence of charge on the vesicles reduces the tendency of vesicles to aggregate and fuse. The three liposomal formulations were prepared with different lipids which gave a negative charge to the vesicles (Vemuri and Rhodes, 1995). All these formulations contained CF as the hydrophilic marker. Before the penetration experiments, the prepared vesicles were characterized in terms of particle size, PI and zeta potential. After the penetration experiments, the stability of these vesicles was determined by storing them at 4°C for up to 8 months. The particle size, PI and zeta potential were measured at a predetermined time every month. It was noted from the results of the qualitative penetration

of different vesicle formulations into human skin, that there is no distinct difference between the intensity of CF in the SC, viable epidermis and dermis for invasomes and flexible liposomes. However, the intensity of CF was high on the SC surface and low in the viable epidermis and dermis for rigid vesicles. These results were due to liposomes S75 and invasomes that facilitated the penetration through intercellular lipid pathways by squeezing themselves through the intact SC (Honeywell-Nguyen and Bouwstra, 2005). Also, the presence of ethanol and terpene mixture in invasomes act as penetration enhancers, where both of them interact with intercellular lipids in the SC, consequently disturbing the organization of the intercellular lipid bilayer (Dragicevic-Curic et al., 2008b). Furthermore, the penetration was done under non-occlusive conditions and it has been reported that non-occlusive conditions facilitate the penetration of elastic liposomes due to the difference in the osmotic gradient between different skin layers (Honeywell-Nguyen and Bouwstra, 2005). The results for the characterization of different vesicle formulations in terms of particle size, PI and zeta potential illustrated that all formulations had small particle size with very good homogeneity and a negative zeta potential. Flexible liposomes and rigid liposomes had nearly the same particle size but invasomes were slightly larger, due to the terpene mixture, which is known to increase particle size (Dragicevic-Curic et al., 2008b). The three liposomal formulations were extruded with a 50 nm membrane filter to obtain small unilamellar vesicles, which have a high penetration compared with large multilamellar vesicles (Verma et al., 2003b). The results indicated that all of these formulations were very stable on storage at 4°C for up to 8 months due to the negative zeta potential of these formulations.

8. Summary

Recently, skin drug delivery has gained increasing attention as a route of administration because it can be used to overcome the drawbacks of oral drug delivery and other drug delivery systems. In-vitro skin models are used to investigate the efficacy of topical systems in order to choose a suitable dosage and formulation that could be used for humans. However, although human skin is the best *in-vitro* research model in skin drug delivery, its availability is limited and there is a large variation between different species and even between individuals. So, in this thesis work rat epidermal keratinocyte organotypic culture (ROC) was developed as an alternative model for human skin. This work included ROC epidermis and ROC full-thickness models with and without collagen. Hence, the ROC epidermis model was investigated for morphology by using light microscopy and its barrier properties by measuring differential scanning calorimetry (DSC), transepidermal water loss (TEWL) and permeation of three different solutes (mannitol, corticosterone and tritiated water) and compared with the human epidermal model. This thesis work also sought to improve the morphology and the barrier properties of the ROC epidermal model to resemble as closely as possible the full-thickness human skin model. Thus, the ROC full-thickness models was compared to full-thickness human skin in the morphology by using light microscopy and the barrier properties were evaluated by measuring TEWL and permeation of tritiated water.

The ROC models (epidermis and full–thickness) were different from human skin in the thickness of stratum corneum (SC) and viable epidermis. Moreover, these models were devoid of skin appendages. There is no distinct difference in the thickness of SC and viable epidermis between ROC epidermis and ROC full-thickness models. It was noted that, in the case of the full-thickness model with and without collagen, the epidermal layers separated from the underlying dermis particularly after freezing at -80°C.

The permeation of tritiated water through human epidermis and ROC epidermis was nearly the same. Also there is no distinct difference in the permeation of tritiated water through full-thickness human skin and the ROC full-thickness with collagen model. However, the permeation of mannitol and corticosterone through human epidermis was different compared to ROC epidermis.

The thermal lipid phase transitions of the ROC model were not the same as that of either the human or rat skin. It was found that the intercellular lipids for human skin were highly ordered compared with those of the ROC and rat skin.

The results of the TEWL measurements showed that the ROC full-thickness model without collagen was slightly higher than ROC epidermis. Furthermore, both of them were higher than other models. There is no distinct difference in TEWL between human skin (epidermis and full-thickness) and ROC full-thickness with collagen. TEWL values of pig ear skin were slightly higher than for human skin.

The results of the TEWL measurements and the permeation of tritiated water illustrated that collagen increased the barrier properties of the ROC full-thickness model and should therefore be used in future studies. These results allow us to conclude that the ROC epidermis and the ROC full-thickness with collagen models are promising alternative models for human skin in the pharmaceutical and cosmetic industries.

As a result of the close resemblances between human skin and pig ear skin, a comparison between the penetration behavior of different solutes into human skin and pig ear skin was evaluated using radiolabeled corticosterone for pig ear skin while, and radiolabeled mannitol for human and pig ear skin. The results showed that the penetration of corticosterone into SC and stripped skin for pig ear skin was higher than that of mannitol, while in receptor parts the amount of mannitol was higher than corticosterone. Also, the results indicated that 1% bovine serum albumin (BSA) did not enhance the permeation of corticosterone through pig ear skin probably due to the low concentration of corticosterone used in these experiments.The penetration of mannitol into pig ear skin was higher than that of human skin. There was a small difference in penetration of mannitol between fresh and frozen human skin. However, for fresh human skin the amount of mannitol was slightly higher in the SC and slightly lower in the stripped skin and receptor parts than for frozen human skin.

To estimate the amount of drug that penetrated into the SC it is necessary to determine exactly the depth of the SC. The tape stripping technique was applied to determine the depth of these layers and hence, the amount of the drug in the SC. The weighing method was used to determine the amount of SC on each tape strip but this method has been found to be inaccurate and this leads to errors. The Infrared densitometry (IR-D) method was used to determine the amount of SC on each tape strip and this method proved more accurate than the weighing method. So, the correlation between cumulative absorbance by SquameScan and cumulative weight by balance was done *in-vivo* and *in-vitro* for human skin and *in-vitro* for pig skin. The results indicated a good correlation between cumulative absorbance and cumulative weight for human skin *in-vivo* and *in-vitro* and also the same for pig ear skin *in-vitro*. The linear equations that were obtained from this correlation were used to calculate the SC thickness for the penetration experiments and the thickness was nearly the same as that obtained using the balance and SquameScan for tape stripping only.

The main challenge in skin drug delivery is the presence of SC which acts as the main barrier and vesicles may be used to overcome this barrier. A study of qualitative penetration of different vesicles formulation which included invasomes, flexible liposomes and rigid liposomes into human skin was performed. These vesicles formulations included flexible liposomes (Lipoid S75), rigid liposomes (Lipoid S100-3) and invasomes (Phosphatidylcholine, ethanol and terpene mixture) and all of these vesicles contained carboxyfluorescein (CF) as the hydrophilic marker. It could be observed that the intensity of CF in the SC, viable

epidermis and dermis for invasomes and flexible vesicles was approximately the same while in the case of rigid vesicles, the intensity of CF was higher on the SC surface and lower in the viable epidermis and dermis. According to the measurements of particle size distribution and zeta potential, all liposomal and invasomal formulations were small in size, highly homogenous and had zeta potentials less than -40 mV. These formulations were very stable in terms of particle size, polydispersity index (PI) and zeta potential on storage at 4°C for up to 8 months.

Zusammenfassung

In letzter Zeit gewann der Haut-Arzneistoff-Transfer zur Verabreichung von Medikamenten an Aufmerksamkeit, da er die Nachteile der oralen Anwendung von Arzneistoffen und anderen Darreichungsformen überwinden kann.
In-vitro Hautmodelle werden verwendet, um die Wirksamkeit topischer Systeme zu untersuchen, um geeignete Formulierungen zu entwickeln und Dosierungen einzustellen. Die Haut zeigt große Unterschiede zwischen den Arten. Die menschliche Haut ist deshalb das beste in-vitro Forschungsmodell für die Untersuchung des Haut-Arzneistoff-Transfers, aber sie steht nur in begrenztem Umfang zur Verfügung und weist auch individuelle Unterschiede auf.
In dieser Arbeit wurden organotypische Kulturen epidermaler Keratinozyten (ROC) der Ratte als ein alternatives Modell zur menschlichen Haut eingesetzt. Es wurden ROC-Epidermis und ROC-komplette-Schichten mit und ohne Kollagen als Untersuchungsmodelle eingesetzt. Die Morphologie des ROC-Epidermis-Modells wurde mittels Lichtmikroskopie charakterisiert und die Barriereeigenschaften durch DSC- und TEWL-Messungen sowie durch Permeation verschiedener Substanzen (Mannitol, Corticosteron, Tritium-Wasser) untersucht und mit dem humanen epidermalen Modell verglichen.
In der vorliegenden Arbeit wurde versucht, die Morphologie und die Barriereeigenschaften des epidermalen Modells zu verbessern, um eine große Ähnlichkeit zur menschlichen Haut zu erreichen. Außerdem wurden die morphologischen Eigenschaften der ROC-komplette-Schichten mit denen der menschlichen Haut lichtmikroskopisch verglichen und ihre Barriereeigenschaften mittels TEWL-Messung und der Permeation von Tritium-Wasser ausgewertet.
Die ROC-Modelle unterschieden sich von der menschlichen Haut in der Schichtdicke des SC und der lebenden Epidermis. Darüber hinaus haben diese Modelle keine Hautanhangsgebilde. Die Schichtdicken des SC und der lebenden Epidermis im ROC-Epidermis-Modell und im ROC-komplette-Schichten-Modell wiesen keine deutlichen Unterschiede auf. Es wurde festgestellt, dass sich beim ROC-komplette-Schichten-Modell mit und ohne Kollagen die Epidermis von der darunter liegenden Dermis nach dem Einfrieren bei -80°C trennte und dass die Permeation von Tritium-Wasser durch die menschliche Epidermis und ROC-Epidermis fast gleich war. Ebenso wurde gezeigt, dass es keine deutlichen Unterschiede in der Permeation von Tritium-Wasser durch die kompletten Schichten der menschlichen Haut und beim ROC-komplette-Schichten-Modell mit Kollagen gab. Allerdings war die Permeation von Mannitol und Corticosteron durch die menschliche Epidermis anders als durch die ROC-Epidermis.

Die temperaturabhängigen Phasenübergänge der Lipide der ROC-Modelle unterschieden sich von denen der menschlichen Haut und denen der Ratte. Es wurde festgestellt, dass die Interzellularlipide der menschlichen Haut im Gegensatz zu denen der ROC-Modelle und der Rattenhaut geordneter sind.

Die Werte der TEWL-Messung für das ROC-komplette-Schichten-Modell ohne Kollagen waren etwas höher als die der ROC-Epidermis und beide Modelle zeigten höhere Werte als die anderen Modelle. Es gab keinen deutlichen Unterschied zwischen den Ergebnissen der TEWL-Messung der menschlichen Haut (Epidermis und Vollhaut) und des ROC-komplette-Schichten-Modells mit Kollagen. Die TEWL-Werte der Schweineohrenhaut waren etwas höher als die der menschlichen Haut.

Die Ergebnisse der TEWL-Messungen und die Penetration von tritiiertem Wasser haben gezeigt, dass Kollagen die Barriereeigenschaften im ROC-komplette-Schichten-Modell erhöht, weshalb es in zukünftigen Studien eingesetzt werden könnte.

Aus diesen Ergebnissen kann man schließen, dass das ROC-Epidermis- und das ROC-komplette-Schichten-Modell mit Kollagen vielversprechende alternative Modelle für die menschliche Haut in der pharmazeutischen und kosmetischen Industrie darstellen.

Wegen der großen Ähnlichkeiten zwischen menschlicher Haut und Schweineohrenhaut wurde das Penetrationsverhalten verschiedener Lösungen in beide Hauttypen verglichen. Es wurden radioaktiv markiertes Corticosteron für die Schweineohrenhaut und radioaktiv markiertes Mannitol sowohl für die menschliche als auch für die Schweineohrenhaut verwendet.

Die Ergebnisse zeigten, dass die Penetration von Corticosteron in das SC und in die Schweineohrenepidermis und -dermis besser war als von Mannitol, während im Akzeptormedium eine höhere Mannitol-Konzentration nachgewiesen werden konnte. Ebenso wurde festgestellt, dass sich durch Hinzufügen von 1% BSA die Permeation von Corticosteron durch die Schweineohrenhaut nicht verbesserte. Grund dafür war wahrscheinlich die geringe Corticosteron-Konzentration. Die Penetration von Mannitol in die Schweineohrenhaut war höher als in menschliche Haut.

Geringe Unterschiede wurden bei der Penetration von Mannitol in frische und gefrorene menschliche Haut festgestellt. In der frischen Haut konnte im SC mehr Mannitol, in der Epidermis/Dermis und im Akzeptormedium dagegen weniger Mannitol nachgewiesen werden als in der gefrorenen Haut.

Die Tape-Stripping-Methode wurde angewendet, um Eindringtiefe und Menge des Wirkstoffs im SC zu bestimmen. Durch Auswägen wurde versucht, die Menge des SC auf jedem Klebestreifen zu bestimmen. Diese Methode hat sich als ungenau erwiesen und führte zu Fehlern. Deswegen wurde zusätzlich die Infrarot-Dichtemessung (SquameScan) eingesetzt, um die Menge des SC auf jedem Klebestreifen zu bestimmen. Diese Methode erwies sich

als genauer als die Wiege-Methode. Die Messwerte von kumulativer Absorption (SquameScan) und kumulativem Gewicht waren gut korreliert. Aus diesem Grund konnte eine lineare Abhängigkeit beider Größen angegeben werden. Die linearen Gleichungen, die sich aus dieser Korrelation ergaben, wurden verwendet, um die Schichtdicke des SC in den Penetrationsversuchen zu berechnen. Die Ergebnisse zeigten eine gute Korrelation zwischen kumulativer Absorption und kumulativem Gewicht für humane Haut, sowohl in-vivo als auch in-vitro und ebenso in-vitro für Schweineohrenhaut.

Die Ergebnisse zeigten fast die gleichen Werte für die Schichtdicke des SC sowohl nach der Wiege-Methode als auch nach dem SquameScan.

Das SC stellt das größte Hindernis bei der Übertragung von Arzneistoffen in die Haut dar. Vesikel sind ein gutes Trägersystem, um diese Barriere zu überwinden. Die Penetration verschiedener vesikulärer Formulierungen in die menschliche Haut wurde qualitativ untersucht. Es wurden Formulierungen mit flexiblen Liposomen (Lipoid S75), rigiden Liposomen (Lipoid S100-3) und Invasomen (Phosphatidylcholin, Ethanol und Terpengemisch) getestet. Alle Vesikel enthielten Carboxyfluorescein als hydrophilen Marker. Es konnte beobachtet werden, dass die CF-Intensität im SC, in der lebenden Epidermis und Dermis für Invasomen und flexible Liposomen etwa gleich war. Für rigide Liposomen dagegen war die CF-Intensität auf der Oberfläche des SC höher und in der lebenden Epidermis und Dermis niedriger. Durch Messungen der Partikelgrößenverteilung und des Zeta-Potentials wurde gezeigt, dass alle liposomalen Formulierungen (< 80 nm) und Invasomen (ca. 90 nm) klein und sehr homogen waren und ein Zeta-Potential von weniger als -40 mV besaßen. Die Formulierungen waren im Hinblick auf die Partikelgröße, PI und Zeta-Potential bei einer Lagerung bei 4°C bis zu 8 Monaten sehr stabil.

References

Al-Saidan, S.M. (2004). Transdermal self-permeation enhancement of ibuprofen. J Control Release *100*, 199-209.

Al-Saidan, S.M., Barry, B.W., and Williams, A.C. (1998). Differential scanning calorimetry of human and animal stratum corneum membranes. Int J Pharm *168*, 17-22.

Aqil, M., Ahad, A., Sultana, V., and Ali, A. (2007). Status of terpenes as skin penetration enhancers. Drug Discov Today *12*, 1061-1067.

Baden, H.P., and Kubilus, J. (1983). The Growth and Differentiation of Cultured Newborn Rat Keratinocytes. J Invest Dermatol *80*, 124-130.

Badran, M.M., Kuntsche, J., and Fahr, A. (2009). Skin penetration enhancement by a microneedle device (Dermaroller (R)) in vitro: Dependency on needle size and applied formulation. Eur J Pharm Sci *36*, 511-523.

Bangham, A.D., Standish, M.M., and Watkins, J.C. (1965). Diffusion of Univalent Ions across Lamellae of Swollen Phospholipids. J Mol Biol *13*, 238-&.

Bashir, S.J., Chew, A.L., Anigbogu, A., Dreher, F., and Maibach, H.I. (2001). Physical and physiological effects of stratum corneum tape stripping. Skin Res Technol *7*, 40-48.

Benson, H.A. (2005). Transdermal drug delivery: penetration enhancement techniques. Curr Drug Deliv *2*, 23-33.

Boelsma, E., Verhoeven, M.C.H., and Ponec, M. (1999). Reconstruction of a human skin equivalent using a spontaneously transformed keratinocyte cell line (HaCaT). J Invest Dermatol *112*, 489-498.

Bouwstra, J.A., Gooris, G.S., Bras, W., and Downing, D.T. (1995). Lipid Organization in Pig Stratum-Corneum. J Lipid Res *36*, 685-695.

Bouwstra, J.A., Gooris, G.S., Salomonsdevries, M.A., Vanderspek, J.A., and Bras, W. (1992). Structure of Human Stratum-Corneum as a Function of Temperature and Hydration - a Wide-Angle X-Ray-Diffraction Study. Int J Pharm *84*, 205-216.

References

Bouwstra, J.A., Gooris, G.S., Vanderspek, J.A., and Bras, W. (1991). Structural Investigations of Human Stratum-Corneum by Small-Angle X-Ray-Scattering. J Invest Dermatol *97*, 1005-1012.

Bouwstra, J.A., and Honeywell-Nguyen, P.L. (2002). Skin structure and mode of action of vesicles. Adv Drug Deliver Rev *54*, S41-S55.

Bouwstra, J.A., Peschier, L.J.C., Brussee, J., and Bodde, H.E. (1989). Effect of N-Alkyl-Azocycloheptan-2-Ones Including Azone on the Thermal-Behavior of Human Stratum-Corneum. Int J Pharm *52*, 47-54.

Boyce, S.T., and Williams, M.L. (1993). Lipid Supplemented Medium Induces Lamellar Bodies and Precursors of Barrier Lipids in Cultured Analogs of Human Skin. J Invest Dermatol *101*, 180-184.

Bronaugh, R.L., Stewart, R.F., and Congdon, E.R. (1982). Methods for in vitro percutaneous absorption studies. II. Animal models for human skin. Toxicol Appl Pharmacol *62*, 481-488.

Cevc, G., and Blume, G. (1992). Lipid Vesicles Penetrate into Intact Skin Owing to the Transdermal Osmotic Gradients and Hydration Force. Biochim Biophys Acta *1104*, 226-232.

Chapman, S.J., Walsh, A., Jackson, S.M., and Friedmann, P.S. (1991). Lipids, Proteins and Corneocyte Adhesion. Arch Dermatol Res *283*, 167-173.

Christophers, E., and Kligman, A.M. (1964). Visualization of the Cell Layers of the Stratum Corneum. J Invest Dermatol *42*, 407-409.

Clowes, H.M., Scott, R.C., and Heylings, J.R. (1994). Skin Absorption - Flow-through or Static Diffusion Cells. Toxicol in Vitro *8*, 827-830.

Commission, E. (19 March 2004). Guidance Document on Dermal Absorption. Health and Consumer Protection Directorate-General Doc *Sanco/222/2000 rev 6*.

Cornwell, P.A., Barry, B.W., Bouwstra, J.A., and Gooris, G.S. (1996). Modes of action of terpene penetration enhancers in human skin differential scanning calorimetry, small-angle X-ray diffraction and enhancer uptake studies. Int J Pharm *127*, 9-26.

References

Cross, S.E., Anissimov, Y.G., Magnusson, B.M., and Roberts, M.S. (2003). Bovine-serum-albumin-containing receptor phase better predicts transdermal absorption parameters for lipophilic compounds. J Invest Dermatol *120*, 589-591.

dos Anjos, J.L., de Sousa Neto, D., and Alonso, A. (2007). Effects of ethanol/l-menthol on the dynamics and partitioning of spin-labeled lipids in the stratum corneum. Eur J Pharm Biopharm *67*, 406-412.

Dragicevic-Curic, N., Grafe, S., Albrecht, V., and Fahr, A. (2008a). Topical application of temoporfin-loaded invasomes for photodynamic therapy of subcutaneously implanted tumours in mice: a pilot study. J Photochem Photobiol B *91*, 41-50.

Dragicevic-Curic, N., Scheglmann, D., Albrecht, V., and Fahr, A. (2008b). Temoporfin-loaded invasomes: Development, characterization and in vitro skin penetration studies. J Control Release *127*, 59-69.

Dreher, F., Arens, A., Hostynek, J.J., Mudumba, S., Ademola, J., and Maibach, H.I. (1998). Colorimetric method for quantifying human Stratum corneum removed by adhesive-tape-stripping. Acta Derm-Venereol *78*, 186-189.

El Ghalbzouri, A., Lamme, E., and Ponec, M. (2002). Crucial role of fibroblasts in regulating epidermal morphogenesis. Cell Tissue Res *310*, 189-199.

El Maghraby, G.M.M., Williams, A.C., and Barry, B.W. (1999). Skin delivery of oestradiol from deformable and traditional liposomes: Mechanistic studies. J Pharm Pharmacol *51*, 1123-1134.

Elias, P.M. (2004). The epidermal permeability barrier: From the early days at Harvard to emerging concepts. J Invest Dermatol *122*, Xxxvi-Xxxix.

Elsayed, M.M.A., Abdallah, O.Y., Naggar, V.F., and Khalafallah, N.M. (2007). Lipid vesicles for skin delivery of drugs: Reviewing three decades of research. Int J Pharm *332*, 1-16.

Fartasch, M., and Ponec, M. (1994). Improved Barrier Structure Formation in Air-Exposed Human Keratinocyte Culture Systems. J Invest Dermatol *102*, 366-374.

Friend, D.R. (1990). Transdermal Delivery of Contraceptives. Crit Rev Ther Drug *7*, 149-186.

References

Friend, D.R. (1992). Invitro Skin Permeation Techniques. J Control Release *18*, 235-248.

Gay, C.L., Guy, R.H., Golden, G.M., Mak, V.H.W., and Francoeur, M.L. (1994). Characterization of Low-Temperature (Ie, Less-Than-65-Degrees-C) Lipid Transitions in Human Stratum-Corneum. J Invest Dermatol *103*, 233-239.

Ghafourian, T., Zandasrar, P., Hamishekar, H., and Nokhodchi, A. (2004). The effect of penetration enhancers on drug delivery through skin: a QSAR study. J Control Release *99*, 113-125.

Godwin, D.A., Michniak, B.B., and Creek, K.E. (1997). Evaluation of transdermal penetration enhancers using a novel skin alternative. J Pharm Sci *86*, 1001-1005.

Golden, G.M., Guzek, D.B., Kennedy, A.H., Mckie, J.E., and Potts, R.O. (1987). Stratum-Corneum Lipid Phase-Transitions and Water Barrier Properties. Biochemistry-Us *26*, 2382-2388.

Gray, G.M., and Yardley, H.J. (1975). Lipid Compositions of Cells Isolated from Pig, Human, and Rat Epidermis. J Lipid Res *16*, 434-440.

Hadgraft, J., and Lane, M.E. (2009). Transepidermal water loss and skin site: A hypothesis. Int J Pharm *373*, 1-3.

Hahn, T., Hansen, S., Neumann, D., Kostka, K.H., Lehr, C.M., Muys, L., and Schaefer, U.F. (2010). Infrared Densitometry: A Fast and Non-Destructive Method for Exact Stratum Corneum Depth Calculation for in vitro Tape-Stripping. Skin Pharmacol Phys *23*, 183-192.

Harkey, M.R. (1993). Anatomy and Physiology of Hair. Forensic Sci Int *63*, 9-18.

Harrison, S.M., Barry, B.W., and Dugard, P.H. (1984). Effects of Freezing on Human-Skin Permeability. J Pharm Pharmacol *36*, 261-262.

Herkenne, C., Alberti, I., Naik, A., Kalia, Y.N., Mathy, F.X., Preat, V., and Guy, R.H. (2008). In vivo methods for the assessment of topical drug bioavailability. Pharm Res *25*, 87-103.

Honeywell-Nguyen, P.L., and Bouwstra, J.A. (2003). The in vitro transport of pergolide from surfactant-based elastic vesicles through human skin: a suggested mechanism of action. J Control Release *86*, 145-156.

Honeywell-Nguyen, P.L., and Bouwstra, J.A. (2005). Vesicles as a tool for transdermal and dermal delivery. Drug delivery formulation and nanotechnology *2*, 67-74.

Honeywell-Nguyen, P.L., de Graaff, A.M., Groenink, H.W.W., and Bouwstra, J.A. (2002). The in vivo and in vitro interactions of elastic and rigid Vesicles with human skin. Biochimica Et Biophysica Acta-General Subjects *1573*, 130-140.

Jacobi, U., Kaiser, M., Toll, R., Mangelsdorf, S., Audring, H., Otberg, N., Sterry, W., and Lademann, J. (2007). Porcine ear skin: an in vitro model for human skin. Skin Res Technol *13*, 19-24.

Juanjuan Liu, and Hu, G. (2007). Advances in studies of phospholipids as carriers in skin topical application. Journal of Nanjing Medical University *21*, 349-353.

Kang, L., Yap, C.W., Lim, P.F., Chen, Y.Z., Ho, P.C., Chan, Y.W., Wong, G.P., and Chan, S.Y. (2007). Formulation development of transdermal dosage forms: quantitative structure-activity relationship model for predicting activities of terpenes that enhance drug penetration through human skin. J Control Release *120*, 211-219.

Kessner, D., Ruettinger, A., Kiselev, M.A., Wartewig, S., and Neubert, R.H.H. (2008). Properties of ceramides and their impact on the stratum corneum structure: A review - Part 2: Stratum corneum lipid model systems. Skin Pharmacol Phys *21*, 58-74.

Kim, C.K., Hong, M.S., Kim, Y.B., and Han, S.K. (1993). Effect of Penetration Enhancers (Pyrrolidone Derivatives) on Multilamellar Liposomes of Stratum-Corneum Lipid - a Study by Uv Spectroscopy and Differential Scanning Calorimetry. Int J Pharm *95*, 43-50.

Kirjavainen, M., Monkkonen, J., Saukkosaari, M., Valjakka-Koskela, R., Kiesvaara, J., and Urtti, A. (1999). Phospholipids affect stratum corneum lipid bilayer fluidity and drug partitioning into the bilayers. J Control Release *58*, 207-214.

Kirjavainen, M., Urtti, A., Jaaskelainen, I., Suhonen, T.M., Paronen, P., Valjakka-Koskela, R., Kiesvaara, J., and Monkkonen, J. (1996). Interaction of liposomes with human skin in vitro--the influence of lipid composition and structure. Biochim Biophys Acta *1304*, 179-189.

Kligman, A.M., and Christophel, E. (1963). Preparation of Isolated Sheets of Human Stratum Corneum. Arch Dermatol *88*, 702-705.

Kuntsche, J., Bunjes, H., Fahr, A., Pappinen, A., Ronkko, S., Suhonen, M.U., and Urtti, A. (2008). Interaction of lipid nanoparticles with human epidermis and an organotypic cell culture model. Int J Pharm *354*, 180-195.

Lademann, J., Knorr, F., Richter, H., Blume-Peytavi, U., Vogt, A., Antoniou, C., Sterry, W., and Patzelt, A. (2008). Hair follicles - An efficient storage and penetration pathway for topically applied substances. Skin Pharmacol Phys *21*, 150-155.

Landmann, L. (1986). Epidermal Permeability Barrier - Transformation of Lamellar Granule-Disks into Intercellular Sheets by a Membrane-Fusion Process, a Freeze-Fracture Study. J Invest Dermatol *87*, 202-209.

Lawrence, J.N. (1997). Electrical resistance and tritiated water permeability as indicators of barrier integrity of in vitro human skin. Toxicol in Vitro *11*, 241-249.

Lee, D.Y., Ahn, H.T., and Cho, K.H. (2000). A new skin equivalent model: dermal substrate that combines de-epidermized dermis with fibroblast-populated collagen matrix. J Dermatol Sci *23*, 132-137.

Loffler, H., Dreher, F., and Maibach, H.I. (2004). Stratum corneum adhesive tape stripping: influence of anatomical site, application pressure, duration and removal. Brit J Dermatol *151*, 746-752.

Lotte, C., Patouillet, C., Zanini, M., Messager, A., and Roguet, R. (2002). Permeation and skin absorption: Reproducibility of various industrial reconstructed human skin models. Skin Pharmacol Appl *15*, 18-30.

Machadoa, M., Salgadoa, T.M., Hadgrafta, J., and Lane, M.E. (2010). The relationship between transepidermal water loss and skin permeability Int J Pharm *384*, 73-77.

Magnusson, B.M., Cross, S.E., Winckle, G., and Roberts, M.S. (2006). Percutaneous absorption of steroids: Determination of in vitro permeability and tissue reservoir characteristics in human skin layers. Skin Pharmacol Phys *19*, 336-342.

Marttin, E., NeelissenSubnel, M.T.A., DeHaan, F.H.N., and Bodde, H.E. (1996). A critical comparison of methods to quantify stratum corneum removed by tape stripping. Skin Pharmacol *9*, 69-77.

Mezei, M., and Gulasekharam, V. (1980). Liposomes - a Selective Drug Delivery System for the Topical Route of Administration .1. Lotion Dosage Form. Life Sci *26*, 1473-1477.

Mezei, M., and Gulasekharam, V. (1982). Liposomes - a Selective Drug Delivery System for the Topical Route of Administration - Gel Dosage Form. J Pharm Pharmacol *34*, 473-474.

Michel, C., Purmann, T., Mentrup, E., Seiller, E., and Kreuter, J. (1992). Effect of Liposomes on Percutaneous Penetration of Lipophilic Materials. Int J Pharm *84*, 93-105.

Naik A, Kalia YN, and RH, G. (2000). Transdermal drug delivery: overcoming the skin's barrier function. Pharm Sci Technolo Today *3*, 318-326.

Nakamura, M., Rikimaru, T., Yano, T., Moore, K.G., Pula, P.J., Schofield, B.H., and Dannenberg, A.M. (1990). Full-Thickness Human Skin Explants for Testing the Toxicity of Topically Applied Chemicals. J Invest Dermatol *95*, 325-332.

Netzaff, F., Lehr, C.M., Wertz, P.W., and Schaefer, U.F. (2005). The human epidermis models EpiSkin (R), SkinEthic (R) and EpiDerm (R): An evaluation of morphology and their suitability for testing phototoxicity, irritancy, corrosivity, and substance transport. Eur J Pharm Biopharm *60*, 167-178.

Netzlaff, F., Kostka, K.H., Lehr, C.M., and Schaefer, U.F. (2006). TEWL measurements as a routine method for evaluating the integrity of epidermis sheets in static Franz type diffusion cells in vitro. Limitations shown by transport data testing. Eur J Pharm Biopharm *63*, 44-50.

OECD (2004a). Guidance document for the conduct of skin absorption studies. OECD series on testing and assessment *2*.

OECD (2004b). Skin absorption : in vitro method. Test Guideline *428*.

Pappinen, S., Hermansson, M., Kuntsche, J., Somerharju, P., Wertz, P., Urtti, A., and Suhonen, M. (2008). Comparison of rat epidermal keratinocyte organotypic culture (ROC) with intact human skin: Lipid composition and thermal phase behavior of the stratum corneum. Bba-Biomembranes *1778*, 824-834.

Pappinen, S., Tikkinen, S., Pasonen-Seppanen, S., Murtomaki, L., Suhonen, M., and Urtti, A. (2007). Rat epidermal keratinocyte organotypic culture (ROC) compared to human cadaver skin: The effect of skin permeation enhancers. Eur J Pharm Sci *30*, 240-250.

Pasonen-Seppanen, S., Suhonen, T.M., Kirjavainen, M., Miettinen, M., Urtti, A., Tammi, M., and Tammi, R. (2001a). Formation of permeability barrier in epidermal organotypic culture for studies on drug transport. J Invest Dermatol *117*, 1322-1324.

Pasonen-Seppanen, S., Suhonen, T.M., Kirjavainen, M., Suihko, E., Urtti, A., Miettinen, M., Hyttinen, M., Tammi, M., and Tammi, R. (2001b). Vitamin C enhances differentiation of a continuous keratinocyte cell line (REK) into epidermis with normal stratum corneum ultrastructure and functional permeability barrier. Histochem Cell Biol *116*, 287-297.

Pinnagoda, J., Tupker, R.A., Agner, T., and Serup, J. (1990). Guidelines for Transepidermal Water-Loss (Tewl) Measurement - a Report from the Standardization-Group-of-the European-Society-of-Contact-Dermatitis. Contact Dermatitis *22*, 164-178.

Ponec, M. (1991). Lipid-Metabolism in Cultured Keratinocytes. Advances in Lipid Research *24*, 83-118.

Ponec, M., Boelsma, E., Gibbs, S., and Mommaas, M. (2002). Characterization of reconstructed skin models. Skin Pharmacol Appl *15*, 4-17.

Ponec, M., Boelsma, E., Weerheim, A., Mulder, A., Bouwstra, J., and Mommaas, M. (2000). Lipid and ultrastructural characterization of reconstructed skin models. Int J Pharm *203*, 211-225.

Ponec, M., Gibbs, S., Pilgram, G., Boelsma, E., Koerten, H., Bouwstra, J., and Mommaas, M. (2001). Barrier function in reconstructed epidermis and its resemblance to native human skin. Skin Pharmacol Appl *14*, 63-71.

Ponec, M., Weerheim, A., Kempenaar, J., Mulder, A., Gooris, G.S., Bouwstra, J., and Mommaas, A.M. (1997). The formation of competent barrier lipids in reconstructed human epidermis requires the presence of vitamin C. J Invest Dermatol *109*, 348-355.

Ponec, M., Weerheim, A., Lankhorst, P., and Wertz, P. (2003). New acylceramide in native and reconstructed epidermis. J Invest Dermatol *120*, 581-588.

Regnier M, Prunieras M, and D., W. (1981). Growth and differentiation of adult human epidermal cells on dermal substrate. Frontiers of Matrix Biology *9*, 4 -35.

Regnier, M., Caron, D., Reichert, U., and Schaefer, H. (1993). Barrier function of human skin and human reconstructed epidermis. J Pharm Sci *82*, 404-407.

Regnier, M., Schweizer, J., Michel, S., Bailly, C., and Prunieras, M. (1986). Expression of High-Molecular-Weight (67k) Keratin in Human Keratinocytes Cultured on Dead De-Epidermized Dermis. Exp Cell Res *165*, 63-72.

Rosdy, M., and Clauss, L.C. (1990). Terminal Epidermal Differentiation of Human Keratinocytes Grown in Chemically Defined Medium on Inert Filter Substrates at the Air-Liquid Interface. J Invest Dermatol *95*, 409-414.

Saladin, K.S., and Porth, C.M. (1998). Anatomy and physiology: The unity of form and function. WCB/McGraw-Hill.

Schaefer, H., and Redelmeier, T.E. (1996). Skin Barrier, Principles of Percutaneous Absorption. Karger, Basel

Scheuplein, R.J. (1967). Mechanism of percutaneous absorption. II. Transient diffusion and the relative importance of various routes of skin penetration. J Invest Dermatol *48*, 79-88.

Simon, G.A., and Maibach, H.I. (1998). Relevance of hairless mouse as an experimental model of percutaneous penetration in man. Skin Pharmacol Appl *11*, 80-86.

Simonsen, L., and Fullerton, A. (2007). Development of an in vitro skin permeation model simulating atopic dermatitis skin for the evaluation of dermatological products. Skin Pharmacol Phys *20*, 230-236.

Sintov, A.C., and Botner, S. (2006). Transdermal drug delivery using microemulsion and aqueous systems: Influence of skin storage conditions on the in vitro permeability of diclofenac from aqueous vehicle systems. Int J Pharm *311*, 55-62.

Smola, H., Stark, H.J., Thiekotter, G., Mirancea, N., Krieg, T., and Fusenig, N.E. (1998). Dynamics of basement membrane formation by keratinocyte-fibroblast interactions in organotypic skin culture. Exp Cell Res *239*, 399-410.

Suhonen, T.M., Pasonen-Seppanen, S., Kirjavainen, M., Tammi, M., Tammi, R., and Urtti, A. (2003). Epidermal cell culture model derived from rat keratinocytes with permeability characteristics comparable to human cadaver skin. Eur J Pharm Sci *20*, 107-113.

Swarbrick, J., Lee, G., and Brom, J. (1982). Drug Permeation through Human-Skin .1. Effect of Storage-Conditions of Skin. J Invest Dermatol *78*, 63-66.

Tezel, A., Sens, A., and Mitragotri, S. (2002). Incorporation of lipophilic pathways into the porous pathway model for describing skin permeabilization during low-frequency sonophoresis. J Control Release *83*, 183-188.

Thomas, B.J., and Finnin, B.C. (2004). The transdermal revolution. Drug Discov Today *9*, 697-703.

Ting, W.W., Vest, C.D., and Sontheimer, R.D. (2004). Review of traditional and novel modalities that enhance the permeability of local therapeutics across the stratum corneum. Int J Dermatol *43*, 538-547.

Tinois, E., Tiollier, J., Gaucherand, M., Dumas, H., Tardy, M., and Thivolet, J. (1991). In vitro and post-transplantation differentiation of human keratinocytes grown on the human type IV collagen film of a bilayered dermal substitute. Exp Cell Res *193*, 310-319.

Touitou, E., Dayan, N., Bergelson, L., Godin, B., and Eliaz, M. (2000). Ethosomes - novel vesicular carriers for enhanced delivery: characterization and skin penetration properties. J Control Release *65*, 403-418.

Van de Sandt J.J.M., Meuling W.J.A., Elliott G.R., C.N.H.P., and Hakkert B.C. (2000). Comparative in vitro - in vivo percutaneous absorption of the pesticide propoxur. Toxicological Sciences *58*, 15-22.

Van den Bergh, and B.A.I. (1999). Elastic liquid state vesicles as a tool for topical drug delivery. University of Leiden *Leiden*, 156-162.

van Ravenzwaay, B., and Leibold, E. (2004). The significance of in vitro rat skin absorption studies to human risk assessment. Toxicol in Vitro *18*, 219-225.

Vemuri, S., and Rhodes, C.T. (1995). Preparation and characterization of liposomes as therapeutic delivery systems: a review. Pharm Acta Helv *70*, 95-111.

Verma, D.D. (2002). Invasomes-novel topical carriers for enhanced topical delivery: characterization and skin penetration properties. Marburg/Lahn *Ph.D. Thesis*.

Verma, D.D., and Fahr, A. (2004). Synergistic penetration enhancement effect of ethanol and phospholipids on the topical delivery of cyclosporin A. J Control Release *97*, 55-66.

Verma, D.D., Verma, S., Blume, G., and Fahr, A. (2003a). Liposomes increase skin penetration of entrapped and non-entrapped hydrophilic substances into human skin: a skin penetration and confocal laser scanning microscopy study. Eur J Pharm Biopharm *55*, 271-277.

Verma, D.D., Verma, S., Blume, G., and Fahr, A. (2003b). Particle size of liposomes influences dermal delivery of substances into skin. Int J Pharm *258*, 141-151.

Vicanova, J., Mommaas, A.M., Mulder, A.A., Koerten, H.K., and Ponec, M. (1996). Impaired desquamation in the in vitro reconstructed human epidermis. Cell Tissue Res *286*, 115-122.

Voegeli, R., Heiland, J., Doppler, S., Rawlings, A.V., and Schreier, T. (2007). Efficient and simple quantification of stratum corneum proteins on tape strippings by infrared densitometry. Skin Res Technol *13*, 242-251.

Wagner, H., Kostka, K.H., Lehr, C.M., and Schaefer, U.F. (2000). Drug distribution in human skin using two different in vitro test systems: comparison with in vivo data. Pharmaceutical Resarch *17*, 1475-1481.

Weigmann, H.J., Lademann, J., Meffert, H., Schaefer, H., and Sterry, W. (1999). Determination of the horny layer profile by tape stripping in combination with optical spectroscopy in the visible range as a prerequisite to quantify percutaneous absorption. Skin Pharmacol Appl *12*, 34-45.

Weigmann, H.J., Lindemann, U., Antoniou, C., Tsikrikas, G.N., Stratigos, A.I., Katsambas, A., Sterry, W., and Lademann, J. (2003). UV/VIS absorbance allows rapid, accurate, and reproducible mass determination of corneocytes removed by tape stripping. Skin Pharmacol Appl *16*, 217-227.

Welzel, J., Wilhelm, K.P., and Wolff, H.H. (1996). Skin permeability barrier and occlusion: No delay of repair in irritated human skin. Contact Dermatitis *35*, 163-168.

Wertz, P.W., Abraham, W., Landmann, L., and Downing, D.T. (1986). Preparation of Liposomes from Stratum-Corneum Lipids. J Invest Dermatol *87*, 582-584.

References

Wertz, P.W., Downing, D.T., Freinkel, R.K., and Traczyk, T.N. (1984). Sphingolipids of the Stratum-Corneum and Lamellar Granules of Fetal-Rat Epidermis. J Invest Dermatol *83*, 193-195.

Wickert, R.R., and Visscher, M.O. (2006). Structure and function of the epidermal barrier. Am J Infect Control *34*, S98-S110.

Williams, A.C., and Barry, B.W. (2004). Penetration enhancers. Adv Drug Deliver Rev *56*, 603-618.

Yamane, M.A., Williams, A.C., and Barry, B.W. (1995a). Effects of Terpenes and Oleic-Acid as Skin Penetration Enhancers Towards 5-Fluorouracil as Assessed with Time - Permeation, Partitioning and Differential Scanning Calorimetry. Int J Pharm *116*, 237-251.

Yamane, M.A., Williams, A.C., and Barry, B.W. (1995b). Terpene penetration enhancers in propylene glycol/water co-solvent systems: effectiveness and mechanism of action. J Pharm Pharmacol *47*, 978-989.

Zhai, H., and Maibach, H.I. (2002). Occlusion vs. skin barrier function. Skin Res Technol *8*, 1-6.

Selbstständigkeitserklärung:

Hiermit erkläre ich, die eingereichte Arbeit selbstständig verfasst und keine anderen Hilfsmittel und Quellen als die angegebenen benutzt zu haben.
Diese Arbeit ist weder identisch noch teilidentisch mit einer Arbeit, welche an der Friedrich-Schiller-Universität Jena oder einer anderen Hochschule zur Erlangung eines akademischen Grades oder als Prüfungsleistung vorgelegt worden ist.
Die Promotionsordnung der Biologisch-Pharmazeutischen Fakultat der Friedrich-Schiller-Universität Jena ist mir bekannt.

Khaled Ahmed

Curriculum Vitae Khaled Ahmed

Personal data

First name	Khaled
Middle name	Shalaby
Family name	Ahmed
Nationality	Egyptian
Gender	Male
Military status	Completed
Marital status	Married
Date of birth	3 January, 1972
Place of birth	El-Dakahlia, Egypt
E-mail:	Khaled_shalabym@yahoo.com or Khaled.shalaby@uni-jena.de
Telephone	004917653361757

Present position

PhD student: at the department of Pharmaceutical Technology of the Friedrich Schiller University of Jena, Germany.
Topic: Characterization and evaluation of the barrier properties of different skin models as an alternative model for human skin.

Education

Master Degree of Pharmaceutics and Industrial Pharmacy, March, 2004, Faculty of Pharmacy, Al-Azhar University Cairo, Egypt.
Title of M.Sc. Thesis: Pharmaceutical Studies on the Availability of H_2 Blocker from Different Suppository Bases.
Bachelor in the Pharmaceutical Sciences with general grade of very good May 1995, Faculty of Pharmacy, Al-Azhar University, Cairo, Egypt.

Occupational backgrounds

2007 -2008: I helped my German colleagues in teaching practical courses for student in the sterilization part.
March, 2004: Assistant lecturer of Pharmaceutics and Industrial Pharmacy, Faculty of Pharmacy, Al-Azhar University, Cairo, Egypt. During this occupation shared in teaching of

practical courses of Physical Pharmacy, Industrial Pharmacy, Preformulation study, Bioavailability and Quality control.
1998 - December, 2003: Demonstrator of Pharmaceutics and Industrial Pharmacy, Faculty of pharmacy, Al-Azhar University, Cairo, Egypt.

Academic background

Post graduate courses

General courses: Organic Chemistry, Instrumental Analysis of Compounds, Physical Chemistry, Computer, Mathematics, Analytical Chemistry and English.
Special courses: Physical Pharmacy, Industrial Pharmacy, Preformulation study, Bioavailability and quality control.
Advanced courses: European Intensive Program- Galenos Course from 16th September 2007 – 2nd October 2007, skin barrier function "Cutaneous Absorption and Environmental Factors" Claude Bernard University, Lyon, France.

Laboratory skills

- I have experienced studying the suppository.
- During my master thesis I measured the bioavailability of Ranitidine suppository on human volunteers and then used the HPLC in the analytical chemistry department, Faculty of pharmacy, Al-Azhar University, Cairo, Egypt.
- I have experience in the cell culture field especially in rat epidermal keratinocyte.
- I performed drug transdermal penetration and permeation studies.
- I have experience in the preparation and separation of different skin layers of human, pig and rat skin.
- Preparation of different liposomal formulations like invasomes, flexible liposomes and rigid liposomes.
- Phase transition behavior of stratum corneum lipids for human, rat epidermal keratinocyte and rat by using Differential Scanning Calorimetry (DSC).
- I worked with photon correlation spectroscopy to measure particle size and zeta potential for different liposomal formulations.
- I worked on the liquid scintillation counting device to measure the radioactivity of different substances.

Language skills

Arabic: native
English: very good
German: Grundstufe

Computer Skills

Get ICDL degree

Publications

Conference Contributions

1- A.A. Kasem, A.M.S. Ahmed and **K.S. Ahmed.** Preformulation, Quality Control Testes, In-Vitro Release and Kinetic Studies of Ranitidine HCl Suppositories. Poster, Al-Azhar 4th-International Conference for Pharmaceutical & Biological Science, February, 13 - 15, 2006 Department of Pharmaceutics, Faculty of Pharmacy, AL-Azhar University Nasr City, Cairo. Egypt.

2- A.M.S. Ahmed, A.A. Kasem and **K.S. Ahmed.** Accelerated Stability and Shelf-Storage Stability Testing of Ranitidine HCl Suppositories. Poster, Al-Azhar 4th-International Conference for Pharmaceutical & Biological Science, February, 13 - 15, 2006, Department of Pharmaceutics, Faculty of Pharmacy, AL-Azhar University Nasr City, Cairo. Egypt.

3- **K.S. Ahmed**, A.A. Kasem, A.M.S. Ahmed and N. El-Abasawy. Bioavailability and Pharmacokinetic Parameters of Ranitidine HCl Suppositories using HPLC technique. poster, Al-Azhar 4th-International Conference for Pharmaceutical & Biological Science, February, 13 - 15, 2006, Department of Pharmaceutics, Faculty of Pharmacy, AL-Azhar University Nasr City, Cairo. Egypt.

4- J. Kuntsche, **K.S. Ahmed**, A.T. Nguyen, A. Fahr. Development of an organotypic skin model based on rat epidermal keratinocytes (REK) and de-epidermized dermis. Poster, Annual Meeting of the Controlled Release Society Local Chapter 2007, Halle/Saale, Germany, March 19-20, 2009.

5- J. Kuntsche, **K.S. Ahmed**, A. Fahr, S.S. Funari, P. Garidel. Stratum corneum lipid organization in an epidermal cell culture model (ROC) studied by synchrotron SAXS. Poster, Annual Meeting of the German Pharmaceutical Society (DPhG) 2009, Jena, Germany, September 28 – October 01, 2009.